Department of Precision and Microsystems Engineering

Synthesis of a Long Vertically Aligned Carbon Nanotube Array by Chemical Vapour Deposition

Jeroen Buter

Report no : MNE 2015.023
Coach : Murali Ghatkesar
Professor : Urs Staufer
Specialisation : MNE
Type of report : Final Master Thesis
Date : September 5th, 2015

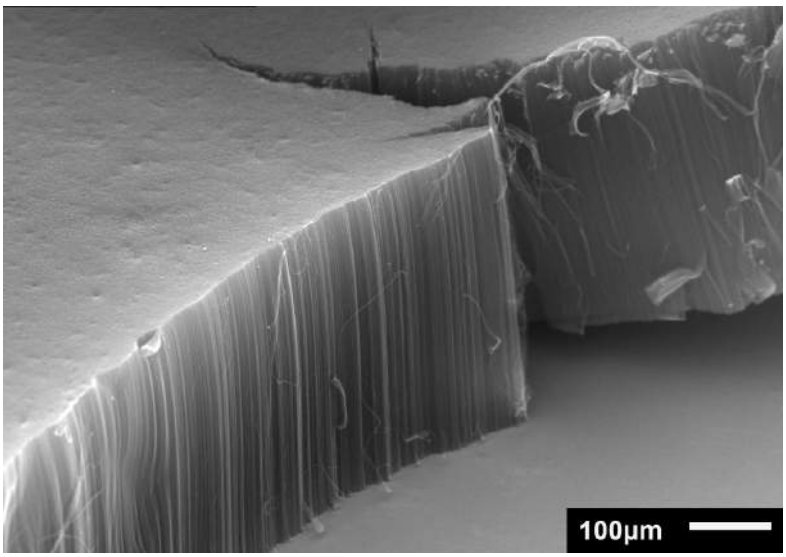

Preface

After one year of hard work, experimenting in the lab, writing and reading at the office or even at home this report could be finished. Of course I could have never completed the thesis without the help of many others. Therefore I would like to take this opportunity to thank those who have made this work possible.

First of all I would like to thank Prof. Dr. Urs Staufer for giving me the opportunity to work in the vastly progressing and exciting field of Carbon Nanotubes. It has been a privilege to work within the group of Micro and Nano Engineering together with motivated and enthusiastic researchers.
Also I would like to thank Dr. Murali Ghatkesar for the guidance provided during this project, the instructions and support given during the experiments in the cleanroom and the discussion we had about the progress and completion of the project.
Furthermore I would like to thank Dr. ir. Sten Vollebregt for helping me with the preparation of the much needed substrates on which CNTs could grow. Also the discussions about phenomena observed during CNT growth were very valuable in completing this project. I want to thank Dr. Minchang Wang for the helpful discussions about the CNT growth procedure, the help with CNT growth in DIMES and in the MNE lab. I would like to thank Dr. Ivan Buijnsters and Prof. Dr. Guido Janssen for the discussions about and help with CVD growth.
When I needed components for the spinning machine, new gas bottles or the CVD oven needed to be adjusted the technical support staff was always there to help. Therefore I would like to thank Rob Luttjeboer, Patrick van Holst and Harry Jansen.
Especially during the first and last months of this project when reading and writing was done, much time was spend in the office. The other students there have helped me to finish this thesis and have some fun along the way. Therefore I would like to thank Rick de Gruiter, Tijn van Omme, Jan-Willem Feitsma, Michiel Dondorp and Adrian Estrada in particular. I would like to thank Gaby Offermans, Corinne duBurck, Marli Guffens and Eveline Matroos of the secretary staff for their support and help during my entire master of PME.
Finally, last but certainly not least, I would like to thank my family and my loving fiancée Kelly van Kooperen for the supporting discussions and for helping me to stay optimally motivated.

Delft, August 2015
Jeroen Buter

Contents

Chapter 1

Introduction

Since the discovery of Carbon Nanotubes (CNTs) in 1991 by Sumio Iijima [1] more and more research has been devoted to their synthesis and possible applications. Carbon Nanotubes consist of a sheet of carbon atoms that is rolled up to create a tube. For the first ten years after their discovery the amount of scientific publications about Carbon Nanotubes increased after each year [2]. The last three years the number of papers about CNTs has stabilized, as can be seen in figure 1.1. The stabilization can mainly be attributed to the emergence of graphene, as also shown in the figure.

There are several reasons for this explosion in publication and patents about CNTs during the first decade. The main reason was the high expectations due to its superior properties. Carbon Nanotubes are about 5 times stiffer and tens of times stronger than steel. Also their electrical and thermal conductivity is about ten times that of copper, a metal generally associated with its good conductivity. These properties of CNTs promise successful applications in multiple fields of research and industry. More detailed information about the properties of CNTs is provided in section 2.3. It is because of these properties that a lot of research is devoted to controlling the growth of Carbon Nanotubes. The second reason for the initial exponential growth of publications with CNTs as topic is a consequence of the first reason. Because of the exceptional properties a large amount of potential applications exist for this novel nanostructure. It is desired to investigate all these possibilities and to improve existing designs. As a result, the other part of the research kick-start is caused by researchers trying to find new applications and to improve on existing systems.

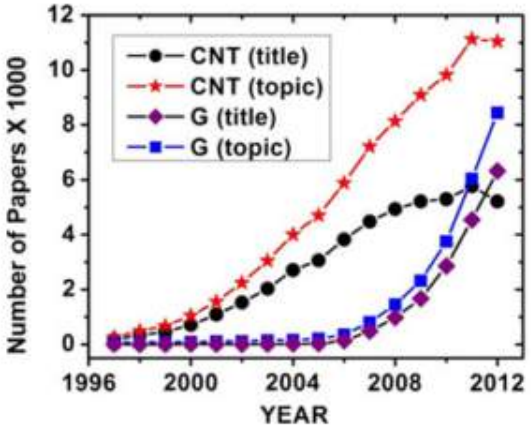

Figure 1.1: The amount of publications containing 'Carbon Nanotubes' (CNT) or 'graphene' (G) in the title or as a topic over the years, from [2].

1.1 Current applications

The synthesis of Carbon Nanotubes is not perfectly controlled yet. The properties of individual tubes still varies widely [3]. Therefore, most of the current applications use them in bulk where the specifications of individual tubes do not matter anymore. As a result, CNTs produced nowadays are mainly produced and used in bulk. Current applications are enhancing the properties of polymers or protecting systems by coating them with a CNT-rich layer [3]. In the first case Carbon Nanotubes are immersed in the still molten polymer. Then the polymer is cast using molds, so that a final shape of the product is created. When the CNTs are used as a coating material the surface underneath can be better protected against corrosion [4], electromagnetic interference [5] or bacteria [6]. It should be noted that more current applications exist, but they are not yet widely adopted in industry.

1.2 Potential applications

Although the current applications are useful already, the future of CNTs might be even brighter. As mentioned before many researchers are working on extending the use of the tubes in everyday applications. So far an extensive list of possible usage of CNTs exist. The main categories of potential applications are structural improvement, electrical circuits, electrical wiring, biomedical and energy storage. To give a glimpse of the possibilities, examples are given of the most important potential applications within the categories. An overview these applications are shown in figure 1.2.

In the field of materials science a lot of effort is made to improve the strength and stiffness of construction materials. Because of their exceptional mechanical properties CNTs are planned to be used as a tough, strong and stiff material. Applications for that material would be in bulletproof vests [7], sports gear or maybe even in a space elevator [8].
Also in electrical engineering CNTs are found to be useful. As was predicted by Gordon E. Moore the amount of transistors on an average integrated circuit doubles each year. Therefore, the amount of interconnects needed to connect all transistors increased dramatically too. Because of their good thermal and electrical conductive properties Carbon Nanotubes might become good candidates for replacing the traditional copper interconnects [9].
Along with the developments in integrated circuits there is a lot of research going on to turn bundles of CNTs into electrical wires. The bundles of CNTs are desired to be twisted into wires as used in devices and larger cables, such as power transmission lines [10] or artificial muscles[11]. This application is still far from commercially viable, since it turns out that transferring the great properties of CNTs to a macroscopic level is a hard task, as will be explained chapter 4.
Other potential applications of CNTs can be found in the field of biomedical engineering.

In fact, in this field the possibilities are broad and diverse. One example of developments in biomedical engineering is using CNTs as scaffold material in bone cell proliferation [12]. Other topics of current research in the field of biomedical engineering is using CNTs to protect DNA from oxidizing [13] or to treat different forms of cancer. For the latter topic the tubes will be designed to deliver the drug at the location of the cancer cells. Also, it is expected that CNTs can be used to detect specific molecules, which might help in detecting cancer in early stages [14].
A last category of research field that are interested in the development of CNTs is energy storage. With the growing amount of sales of electrical cars clever concepts are necessary to store the electrical energy efficiently. Carbon nanotubes are proposed to be used in so called 'super-capacitors' [15]. These capacitors can store more energy per mass or volume than traditional capacitors or batteries. Besides, as opposed to batteries they are able to charge very quickly.

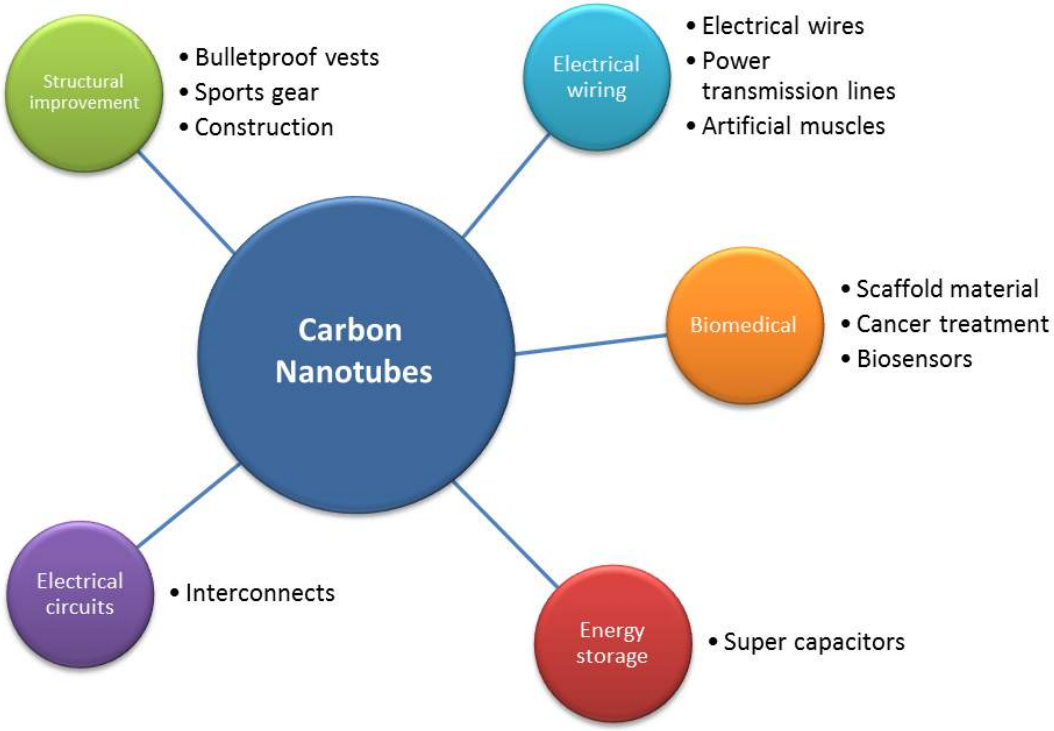

Figure 1.2: Some potential applications of Carbon Nanotubes that are currently extensively studied.

1.3 Goal of this thesis

The goal of this study is to improve employability of CNTs in potential applications, which will be done by contributing to the current knowledge on growing and spinning of CNTs.

This goal is pursued to clear the way for new applications and thereby improvements on current technologies. As mentioned earlier, the list of potential applications is merely meant to give a glimpse of the possibilities that CNTs have to offer. The complete list of all opportunities that come with CNTs is virtually endless. To bring the large potential of CNTs closer to reality two steps should still be taken. First of all, being able to control their growth is of vital importance [16]. Secondly, the properties of individual tubes should be transferred to a macroscopic level. For example, in the field of material science or even in electrical wiring, the excellent strength and conductivity should be available in fibers of several centimeters to meters long.
In general this can be done in two ways. Either the CNTs can be grown to a centimeter long range or they can be spun into a fiber. Because growing CNTs a few centimeters long is difficult, the latter way is chosen to investigate during this thesis. The reason why CNTs will hardly grow longer than a couple of millimeters will be explained in chapter 3.

1.4 Organization of this thesis

This thesis consists, besides the current introduction, of five chapters. Three of which are literature studies to summarize relevant information about specific topics of CNTs. The remaining two chapters will mainly present data found in this study, which will be compared with results from literature.
Chapter 2 will discuss current findings on the structure and properties of Carbon Nanotubes. In chapter 3 the synthesis of Carbon Nanotubes will be described. There are multiple ways CNTs can be grown, all of which will be explained. Chapter 4 will be about the possibilities to spin Carbon Nanotubes into yarn. All three available techniques will be discussed and explained. Chapter 5 contains information about results obtained in this study with respect to the growth of CNTs. In chapter 6 experiments on spinning CNTs are mentioned. The obtained results are compared with results found from literature.
Finally in chapter 7 an overall conclusion of the study is given. Also some recommendations for future work are provided.

References

[1] S. Iijima, "Helical microtubules of graphitic carbon," *Nature*, vol. 354, pp. 56 –58, 1991.

[2] E. Munoz-Sandoval, "Trends in nanoscience, nanotechnology, and carbon nanotubes: a bibliometric approach," *Journal of Nanoparticle Research*, vol. 16, p. 2152, Dec. 2013.

[3] M. D. Volder, S. Tawfick, R. Baughman, and A. Hart, "Carbon nanotubes: present and future commercial applications," *Science*, vol. 535, no. 2013, 2013.

[4] X. Chen, C. Chen, H. Xiao, F. Cheng, G. Zhang, and G. Yi, "Corrosion behavior of carbon nanotubesNi composite coating," *Surface and Coatings Technology*, vol. 191, pp. 351–356, Feb. 2005.

[5] H. M. Kim, K. Kim, C. Y. Lee, J. Joo, S. J. Cho, H. S. Yoon, D. a. Pejakovic, J. W. Yoo, and a. J. Epstein, "Electrical conductivity and electromagnetic interference shielding of multiwalled carbon nanotube composites containing Fe catalyst," *Applied Physics Letters*, vol. 84, no. 4, p. 589, 2004.

[6] A. S. Brady-Estévez, S. Kang, and M. Elimelech, "A single-walled-carbon-nanotube filter for removal of viral and bacterial pathogens.," *Small (Weinheim an der Bergstrasse, Germany)*, vol. 4, pp. 481–4, Apr. 2008.

[7] K. Mylvaganam and L. C. Zhang, "Ballistic resistance capacity of carbon nanotubes," *Nanotechnology*, vol. 18, p. 475701, Nov. 2007.

[8] R. Zhang, Y. Zhang, Q. Zhang, H. Xie, W. Qian, and F. Wei, "Growth of Half-Meter Long Carbon Nanotubes Based on Schultz-Flory Distribution," *ACS nano*, vol. 7, no. 7, pp. 6156–6161, 2013.

[9] A. Naeemi, R. Sarvari, and J. Meindl, "Performance comparison between carbon nanotube and copper interconnects for gigascale integration (GSI)," *IEEE Electron Device Letters*, vol. 26, pp. 84–86, Feb. 2005.

[10] D. Janas, A. P. Herman, S. Boncel, and K. K. Koziol, "Iodine monochloride as a powerful enhancer of electrical conductivity of carbon nanotube wires," *Carbon*, vol. 73, pp. 225–233, July 2014.

[11] N. Sinha and J. T. W. Yeow, "Carbon nanotubes for biomedical applications," *IEEE Transactions on Nanobioscience*, vol. 4, no. 2, pp. 180–195, 2005.

[12] L. P. Zanello, B. Zhao, H. Hu, and R. C. Haddon, "Bone cell proliferation on carbon nanotubes.," *Nano letters*, vol. 6, pp. 562–7, Mar. 2006.

[13] E. J. Petersen, X. Tu, M. Dizdaroglu, M. Zheng, and B. C. Nelson, "Protective roles of single-wall carbon nanotubes in ultrasonication-induced DNA base damage.," *Small (Weinheim an der Bergstrasse, Germany)*, vol. 9, pp. 205–8, Jan. 2013.

[14] S.-r. Ji, C. Liu, B. Zhang, F. Yang, J. Xu, J. Long, C. Jin, D.-l. Fu, Q.-x. Ni, and X.-j. Yu, "Carbon nanotubes in cancer diagnosis and therapy.," *Biochimica et biophysica acta*, vol. 1806, pp. 29–35, Aug. 2010.

[15] M. Kaempgen, C. K. Chan, J. Ma, Y. Cui, and G. Gruner, "Printable thin film supercapacitors using single-walled carbon nanotubes.," *Nano letters*, vol. 9, no. 5, pp. 1872–6, 2009.

[16] R. H. Baughman, "Carbon Nanotubes the Route Toward," *Science*, vol. 297, no. 787, pp. 787–792, 2002.

Chapter 2

Carbon nanotube structures and properties

Abstract

The electrical, mechanical and thermal properties of Carbon Nanotubes are investigated. Their incredibly high conductivity (both electrically as thermally), stiffness and strength is explained by the configuration of a carbon atom and its outer four electrons. The Young's Modulus of a carbon nanotube can easily reach 1000 GPa, while its tensile strength can be 150 GPa. Besides these properties the concepts of chirality, number of walls and structural defects are explained and their influences on electrical conductivity and strength is discussed.

2.1 Introduction

In this study the basic properties of carbon nanotubes will be explained. CNTs can be grown in a lot of different forms and sizes and even in different forms, as discussed in the first section. The second section is about the exceptional electrical, mechanical and thermal abilities of the tubes.

2.2 Carbon Nanotubes structures

Carbon nanotubes are built from single carbon atom layers. The carbon atoms form hexagons which are patterned together to form a sheet. In an unwrapped form this sheet forms the material called graphene. When the graphene is rolled up into a tube a CNT is created, as can be seen in figure 2.1. Both materials are exceptionally strong and well conducting. The reasons why that is the case will be made clear in section 2.3. Although the basic structure of such a tube may seem quite simple, there are a lot of parameters that determine the exact properties of the carbon nanotubes. The most important parameters are: the chirality of the CNTs, the number of walls, the diameter and its quality. The latter is determined by the amount of defects and amorphous carbon on the wall of the CNT. These parameters are in general hard to control during CNT synthesis, as will be explained in the following subsections. But first, to clarify the basic CNT structure the possible bonds of the carbon atom are explained. These subsections are mainly based on the information about CNTs as described in 'Methods for carbon nanotubes synthesis review' by J. Prasek et al. [1] and the book 'Carbon Nanotubes: Science and Applications' by M. Meyyappan [2].

2.2.1 Bonding of carbon atoms

Carbon atoms consist of six electrons in total. Two of those electrons occupy the 1s electron orbital of the atom. The remaining four electrons fill the outer 2s and 2p orbitals. These outer four electrons are available for bonding with another atom, so they function as valence electrons. These four outer electrons are able to fill sp^3, sp^2 or sp orbitals due to appropriate hybridization. The first two of these bonds are shown in figure 2.2.

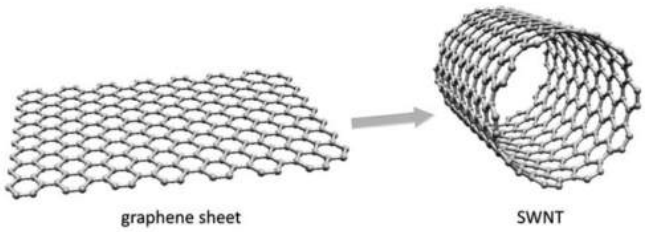

Figure 2.1: Visualization of a graphene sheet and CNTs, from [1].

When one of the two electrons in the 2s orbital is promoted to the p-type orbital a so called sp^3 hybrid is formed. This name is given because there is one electron left in the 2s orbital, while three electrons exist in the 2p orbital. A carbon atom containing this hybrid can form four σ covalent bonds, which will be equally spaced so that a tetrahedral shape will be obtained. The sp^3 bond occurs in the formation of diamond when bonded with other carbon atoms. In case of bonding with hydrogen an alkane hydrocarbon will be created, such as methane or ethane. Properties of this type of bonding are electrically insulation and lead to a high strength material.

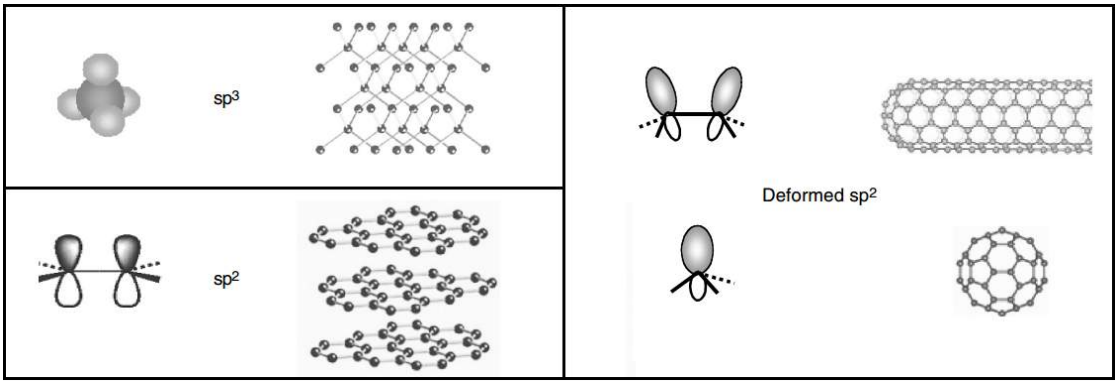

Figure 2.2: Bonding structures of diamond, graphite, nanotubes, and fullerenes. It are the sp^2 bonds which give CNTs and graphene their extraordinary properties. Adapted from [2].

It is also possible that both electrons in the 2s orbital mix with two of the three p-type orbitals. This way three sp^2 configurations will be formed and only one electron will remain in the 2p orbital. The three sp^2 hybrid orbitals are available to from in-plane σ bonds. The 2p orbital electron will form an out-of-plane π bond. The π bond is very weak, although, in principle it could still be covalent. In most cases however, the π bond will be distributed over the three σ bonds and thereby making the material electrical and thermal conductive. Also, the π electron will interact with incoming light, therefore the material will appear black. Because there are three covalent σ available in this configuration, honeycomb (or hexagonal) carbon sheets will typically be formed as

can be found in graphene, CNTs and graphite. Due to reinforcement of the σ bonds by the π bond, the connections with the carbon atom are in general stronger.
Finally, it is possible that the 2s orbital mixes with only one p-type orbital. In that case two sp hybrids are created, while the remaining two electrons are in the 2p orbital. So, there will be two σ bonds and two π bonds. This last configuration is responsible for the molecules containing carbon atoms with only two covalent bonds.

2.2.2 Chirality

The first parameter that can vary from the one CNT to the other is its chirality. First of all it is important to address what chirality actually is. In case of CNTs it can be thought of as the virtual axis on a graphene sheet which the CNT is wrapped around. Figure 2.3 illustrates this phenomenon. The chirality is expressed by two integers (n, m) which represent the ratio between the number of horizontal hexagons and the diagonal ones, respectively. In the figure the example of $(6, 3)$ is given. It can be verified that 6 horizontal and 3 diagonal hexagons can be counted to define the axis of wrapping.
Why is chirality important to consider during a study about carbon nanotubes? The chirality determines whether the CNT wall is metallic or semi-conductive. This means that one of the most important properties of the CNTs, namely whether it is very well conductive or not, is determined by its chiral angle. In case of a chirality where $\frac{n-m}{3}$ is an integer the CNT will be metallic [3]. This is called armchair chirality. Any other configuration will result in a semi-conductive CNT wall. If the integer $m = 0$ and the cirality becomes (n,0), the configuration will be called zigzag chirality. A CNT with zigzag chirality possesses the largest band gap and is therefore the least electrically conducting.
A final useful property of the chirality of a CNT is that the diameter of the tube can be calculated if the two integers are known. To do so the equation $d = \frac{a}{\pi}\sqrt{n^2 + nm + m^2} = 78.3\sqrt{n^2 + nm + m^2}$ can be used. Here $a = 0.246$ nm [4], which is the lattice constant. Physically it means the spacial distance between a unit cell in the lattice and the next unit cell.

2.2.3 Number of walls

To fully define a CNT describing its chirality is insufficient. Another important parameter to consider is the number of walls of the tube. Carbon nanotubes can consist of one or more walls. In literature a distinction is made between Single-Walled Carbon Nanotubes (SWNTs) and Multi-Walled Carbon Nanotubes (MWNTs). Note that the C of carbon is left out of the abbreviation. In some cases also Double-Walled Carbon Nanotubes (DWNTs) and Triple-Walled Carbon Nanotubes (TWNTs) are distinguished.
In principle SWNTs do not differ much from MWNTs, other than the number of walls they have. However, in bulk the difference can be essential for certain applications. These differences will be

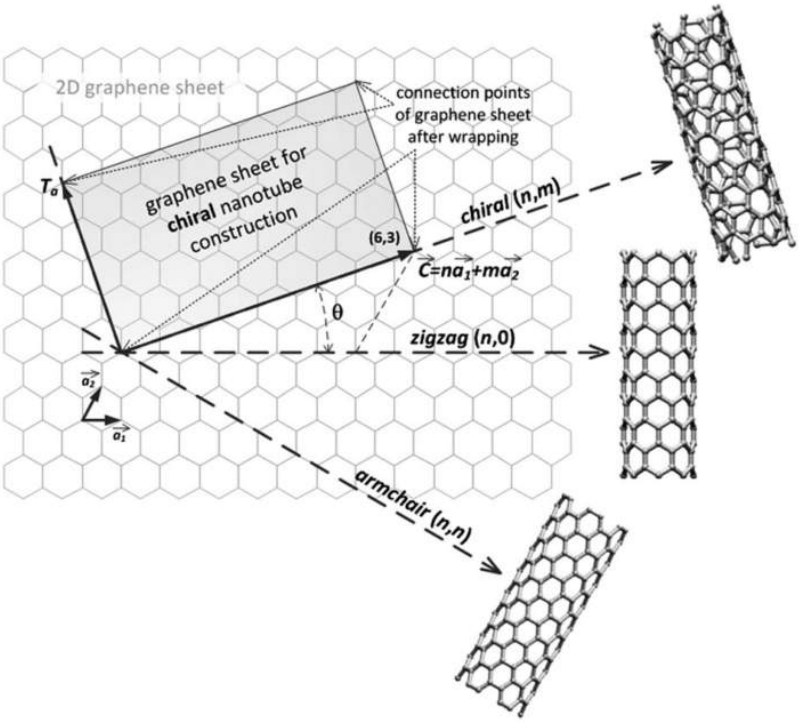

Figure 2.3: Visualization of the chirality of CNTs, from [1].

- MWNTs tend to be more often metallic or at least semi-metallic. On average about two-thirds of the SWNTs will be semi-conductive [5][6]. MWNTs on the other hand, are more likely to be conducting, since only one wall needs to be metallic to be able to transport electrons well.

- Furthermore, it should be noted that the specific strength of MWNTs is lower. Since the walls are not internally connected, the load is not effectively and equally carried over all shells[7]. To a certain extend the same holds for the conductivity [8]. Most of the walls are only adding weight. It can be imagined that in bulk the mechanical and electrical properties are lower for MWNTs when compared with SWNTs. Especially when considered that a MWNT can be thousand times as heavy as a SWNT [9].

- The final large difference is obvious, though important to take note of in this thesis. The diameter of MWNTs is in general a lot larger than is the case for SWNTs. On average the diameter of SWNTs vary between 0.5 and 3 nm, whereas for MWNTs this ranges between 3 and 100 nm [10]. As a consequence, a bundle of SWNTs consist of much more tubes for a specific diameter when compared with a bundle of MWNTs. Since only the outer walls of MWNTs carry the load, the latter bundle will not be as efficient.

When the goal is to spin yarns with a good conductivity and a high strength, it is desired to use SWNTs or DWNTs. As a result, the load will be transferred more efficiently. For better overall conductivity metallic SWNTS are the most desirable, since their diameter is smaller than that of MWNTs. A smaller diameter means more conductive CNTs per cross sectional area of yarn, which enhances the overall conductivity of the yarn.

2.2.4 Defects

Ideally the walls of CNTs consist of a perfect honeycomb structure. In that case the graphene sheet that makes up the wall will contain only perfectly aligned hexagons with at the corners a carbon atom. If this is the case a perfect CNT is formed. In other words: no defects are present. However, it might be the case that the CNT structure is defective. Examples of these defective structures are bent, branched, helical or toroidal carbon nanotubes, as can be seen in figure 2.4. In many cases these structures are associated with topological defects, so that pentagon-heptagon combinations are detectable in the lattice of the carbon nanotube. Furthermore irregularities might be visible such as bamboo structured CNT or a conic tube. In the latter cases the 'tube' might be referred to as a Carbon Nanofiber (CNF).
It is important to note that defects often result a low quality of the CNT. The strength will be significantly reduced, as will the electrical and thermal conductivity. Therefore the amount of defects should be as minimal as possible. Usually this is achieved by growing CNTs at higher temperatures. The drawback is that the growth will be earlier terminated as will become clear in chapter 3.

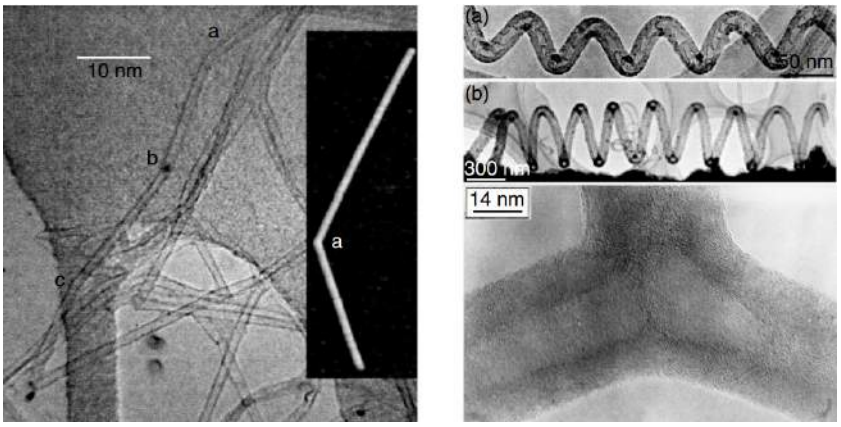

Figure 2.4: Several forms of a defective CNT. A bent, branched and helical CNT. Reprinted from [2].

2.3 Properties of carbon nanotubes

In this section the general properties of carbon nanotubes will be described, as opposed to structural properties as described in the previous section. CNTs show exceptional behavior for their electrical, mechanical and thermal properties.

2.3.1 Electrical

One of the most important reasons that CNTs received this much attention in the scientific community is because of their remarkable electronic properties. From theoretical calculations different insights are obtained on the extraordinary electronic properties of CNTs, SWNTs to be more specific [11], [12], [13]. In one particular model the electronic properties of a graphene sheet are taken as the basis [11]. This model is based on the energy an electron in the lattice has in terms of wavenumbers. The energy of the electron might be interpreted as the band gap as well. By using the wavenumbers of an electron to describe its state in the graphene lattice the energy can be derived as follows.

$$E(k_x, k_y) = \pm\gamma_0\{1 + 4\cos(\frac{\sqrt{3}k_x a}{2})\cos(\frac{k_y a}{2}) + 4\cos^2(\frac{k_y a}{2})\}^{1/2} \tag{2.1}$$

The k_x and k_y are these wave numbers in the x and y direction respectively. Furthermore γ_0 is the nearest-neighbor hopping energy and has a value of about 2.8 eV for graphene lattice [2]. This parameter essentially determines the conductivity. Finally, a is the lattice constant as was seen earlier when calculating the diameter of a certain CNT. The value for the lattice constant is 0.246 nm. With this equation the electrical properties of a graphene sheet can be calculated for different wavenumbers in the x and y directions. The equation is visualized in figure 2.5.

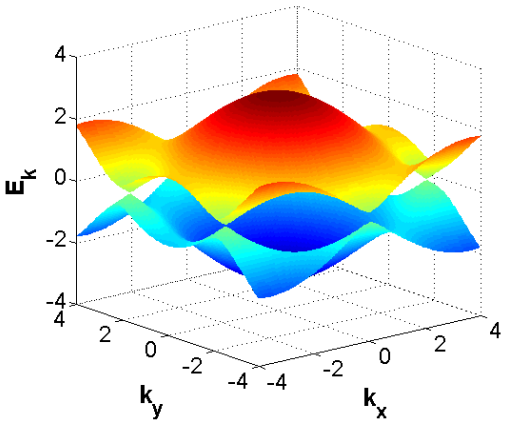

Figure 2.5: Visualization of the dispersion relation linking the wave vector of an electron to its energy. The locations where energy E_k equals zero are called Dirac points.

Now the sheet is rolled up in a certain direction $\mathbf{C}$ to form a nanotube as shown in figure 2.3. Here $\mathbf{C}$ can be expressed as $n\mathbf{a}_1 + m\mathbf{a}_2$. A periodic boundary condition can be imposed along its circumference. The boundary condition will quantize the wavevector $\mathbf{k}$ as $\mathbf{k} \cdot \mathbf{C} = 2\pi q$, where q is an integer. If this is substituted in equation 2.1 a condition for metallic CNTs can be found by setting the equation equal to zero.

Table 2.1: The Young's Modulus, tensile strength and density for several carbon structures. Also steel is mentioned for comparison.

Material	**Young's Modulus (GPa)**	**Tensile strength (GPa)**	**Density (g/cm^3)**
MWNT	1200	150	2.6
SWNT	1054	75	1.3
Graphene	912	2.5	2.6
Steel	208	0.4	7.8

It turns out that the condition for a metallic CNT is $n - m = 3q$ as was mentioned in section 2.2.2 as well.
With this equation it can be argued that, if CNTs grow with a random chirality, one third of the tubes will be metallic and the other two third of the tubes will be semiconductive. It is verified in literature that this is indeed the case [6] [14]. From these observations it can be concluded that in principle CNTs grow with random chirality.

As was seen earlier, CNTs do not always comprise of one wall. In case of multiple walls (MWNTs) or even a rope of tubes, the calculation of conductivity is not as straight forward anymore. Due to intertube coupling a small band gap is induced if the rope consist of metallic tubes. However, when the rope is a mix of two-third semiconductive and one-third metallic CNTs the band gap will be reduced by about 40%.

2.3.2 Mechanical and electromechanical

CNTs are mostly known for their incredible high strength and high stiffness. The high strength of the tubes can be explained by their σ bond, which is the strongest bond existing in nature. Since the entire CNT is build with these bonds it follows that the tube itself possess a magnificent strength. Theoretical studies show that the strength and Young's Modulus of CNTs are comparable to diamond [15]. It should be noted however, that these studies are carried out for perfect carbon structures without compensation for inevitable structural defects. Calculated values for Young's Modulus, tensile strength and densities are shown in table 2.1 for SWNTs, MWNTs, graphene and steel. As pointed out by Meyyappan et al. these theoretical values are in general in good agreement with experimental values, but discrepancies occur due to structural defects. Especially for values of MWNTs a broad range of experimental values is obtained [2]. It is an interesting observation that the stiffness of a SWNT is larger than the in-plane stiffness of a graphene sheet. This is because the strength of the axial component of the σ bonds is increased when the sheet is rolled over to form a seamless cylindrical structure. The Young's modulus of a SWNT can be changed by changing the diameter of the tube. It is found that the elastic modulus is reduced from 1 TPa to 100 GPa by an increase of the CNT diameter from about 3 nm to 20 nm. In general MWNTs are stiffer than SWNTs since the outer shells contribute to the stiffness by coaxial intertube coupling.

Most hard materials allow a maximum strain of 1% before fracture due to excessive propagation of dislocations. In contrast, CNTs can sustain an extraordinary strain of 15% before failure. This feature from CNTs can be explained by the electron bonds as well. As discussed earlier, the outer four electrons of the carbon atom arrange themselves in a deformed sp^2 hybrid bond. Due to these bonds several different deformation modes are possible through which the strain energy can be released. As a consequence of this sp^2 rehybridization the electric properties will change during strain as well. The change is visualized in figure 2.6. During uniaxial strain (either compression or tensile) the band gap for metallic CNTs with chirality (10,10) remain zero. For semiconducting however, CNTs with the other chiral angles the band gap will change as strain is applied. For torsional strain band gaps will change for all chiral angles, except for the CNTs with chirality (19,0) the band gap remains unchanged.

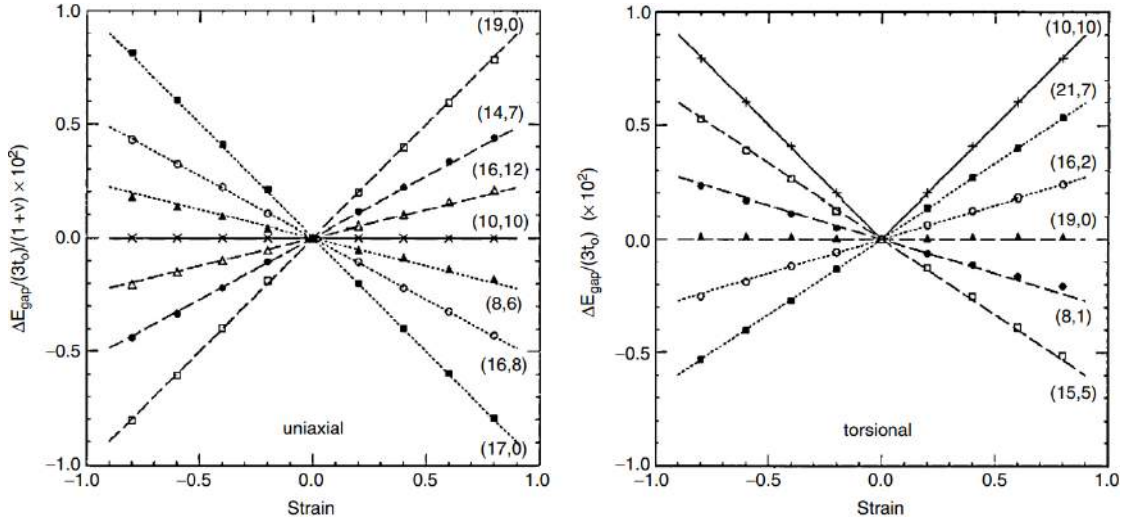

Figure 2.6: The y-axes contain the change in band gap, while the x-axes represents strain. The numbers between parenthesis on the right show the chirality of the according line. The strain in the left figure is for uniaxial strain while the figure on the right is valid for torsional strain. Adapted from [2].

2.3.3 Thermal

On top of the extremely good electrical and mechanical properties, CNTs exhibit outstanding thermal properties as well. Along the tube's axis CNTs are excellent thermal conductors. A thermal conductivity of 3500 $W \cdot m^{-1} \cdot K^{-1}$ has been experimentally verified. However, several calculations suggest a thermal conductivity of SWNTs of 6000 $W \cdot m^{-1} \cdot K^{-1}$ is possible[16]. Compared to copper, a metal known for its good electrical and thermal conductivity, which transmits only 385 $W \cdot m^{-1} \cdot K^{-1}$ the thermal conductivity over the longitudinal axis of CNTs is incredible. Over the cross-sectional axis of a SWNT the conductivity is only 1.64 $W \cdot m^{-1} \cdot K^{-1}$ [17], which is about the same as stone

or moist soil. So across its transversal axis a CNT is actually quite a good thermal insulator. These measured values are justified for temperatures up to 2800 °C in vacuum and 750 °C in air as shown by the study of Thostenson et al. [18].

2.4 Conclusion

In conclusion, CNTs possess multiple outstanding properties. Especially their electrical, mechanical and thermal behavior makes them a material with almost infinite useful applications.
When describing a carbon nanotube one of the most important parameters to mention is its chirality. Chirality can be viewed as the direction of the axis where a graphene sheet is wrapped around. It is expressed as (n,m) where n are the hexagons in the horizontal position and m are the hexagons in the diagonal position as counted from a particular starting point. A chirality of (n,n) is called an 'armchair' configuration and exhibits a metallic electrical conductivity, whereas a chirality of (n,0) is called 'zigzag' chirality and is the least conductive. Any chirality which satisfies $n - m = 3q$ where q is an integer is considered to be metallic.
Furthermore it is important to mention the number of walls when describing a CNT. Multi-Walled Carbon Nanotubes (MWNTs) are stiffer than Single-Walled Carbon Nanotubes (SWNT), but are in general less efficient in transferring a load or electrons. This is the case because only some of the walls will handle the load or are conductive. The other walls will only add weight.
Finally the amount of defects is an important parameter determining the properties of a CNT. A lot of defects will deteriorate its capability of handling high tensile forces. Also the conductivity will be reduced. With the quality of a CNT the amount of defects is meant.
The properties of Carbon Nanotubes are just like those of graphene extraordinary. Although uncertain and still debated the electrical conductivity of a metallic SWNT is in the same order of that of copper [19], while its tensile strength can be as high as 75 GPa. The Young's Modulus of a SWNT is 1054 GPa which is somewhat higher than that of diamond. Finally the thermal conductivity of a CNT has been proven to be at least 3500 $\mathrm{W{\cdot}m^{-1}{\cdot}K^{-1}}$ which is 10 times higher than that of copper.

Now that the basic structures and properties of Carbon Nanotubes are described, the next chapter will discuss how CNT can be grown.

References

[1] J. Prasek and J. Drbohlavova, "Methods for carbon nanotubes synthesis: review," *Journal of Materials*, vol. 21, no. 40, pp. 15872–15884, 2011.

[2] M. Meyyappan, *Carbon Nanotubes: Science and Applications*. Boca Raton: CRC Press LLC, 2004.

[3] X. Lu and Z. Chen, "Curved Pi-Conjugation , Aromaticity , and the Related Chemistry of Small Fullerenes and Single-Walled Carbon Nanotubes," *Chemical Reviews*, vol. 105, no. 10, pp. 3643–3696, 2005.

[4] R. Rao, D. Liptak, T. Cherukuri, B. I. Yakobson, and B. Maruyama, "In situ evidence for chirality-dependent growth rates of individual carbon nanotubes.," *Nature materials*, vol. 11, pp. 213–6, Mar. 2012.

[5] V. Jourdain and C. Bichara, "Current understanding of the growth of carbon nanotubes in catalytic chemical vapour deposition," *Carbon*, vol. 58, pp. 2–39, July 2013.

[6] R. Smalley, Y. Li, and V. Moore, "Single wall carbon nanotube amplification: En route to a type-specific growth mechanism," *Journal of the American Chemical Society*, vol. 128, no. 49, pp. 15824–15829, 2006.

[7] K. Teo and C. Singh, "Catalytic synthesis of carbon nanotubes and nanofibers," *Encyclopedia of Nanoscience and Nanotechnology*, pp. 1 – 22, 2003.

[8] A. Lekawa-Raus, L. Kurzepa, X. Peng, and K. Koziol, "Towards the development of carbon nanotube based wires," *Carbon*, vol. 68, pp. 597–609, 2014.

[9] M. S. Dresselhaus, G. Dresselhaus, and P. Avouris, *Carbon Nanotubes Synthesis, Structure, Properties, and Applications*. Verlag Berlin Heidelberg: Springer Science & Business Media, 2001.

[10] R. H. Baughman, "Carbon Nanotubes the Route Toward," *Science*, vol. 297, no. 787, pp. 787–792, 2002.

[11] R. Saito, M. Fujita, G. Dresselhaus, and M. S. Dresselhaus, "Electronic structure of gaphene tubules based on C60," *Physical Review B*, vol. 46, no. 3, p. 1804, 1992.

[12] J. W. Mintmire, B. I. Dunlap, and C. T. White, "Are fullerene tubules metallic?," *Physical Review Letters*, vol. 68, no. 5, pp. 631–634, 1992.

[13] N. Hamada, S.-i. Sawada, and A. Oshiyama, "New one-dimensional conductors: Graphitic microtubules," *Physical Review Letters*, vol. 68, no. 10, pp. 1579–1581, 1992.

[14] I. Ibrahim, A. Bachmatiuk, and D. Grimm, "Understanding high-yield catalyst-free growth of horizontally aligned single-walled carbon nanotubes nucleated by activated C60 species," *ACS Nano*, vol. 6, no. 12, pp. 10825–10834, 2012.

[15] J. P. Lu, "Elastic properties of carbon nanotubes and nanoropes," *Physical Review Letters*, vol. 79, no. 7, pp. 1297–1300, 1997.

[16] E. Pop, D. Mann, Q. Wang, K. Goodson, and H. Dai, "Thermal Conductance of an Individual Single-Wall Carbon Nanotube above Room Temperature," *Nano Letters*, vol. 6, no. 1, pp. 96–100, 2006.

[17] N. Sinha and J. T. W. Yeow, "Carbon nanotubes for biomedical applications," *IEEE Transactions on Nanobioscience*, vol. 4, no. 2, pp. 180–195, 2005.

[18] E. T. Thostenson, C. Li, and T. W. Chou, "Nanocomposites in context," *Composites Science and Technology*, vol. 65, no. 3-4, pp. 491–516, 2005.

[19] T. W. Ebbesen, H. J. Lezec, H. Hiura, J. W. Bennett, H. F. Ghaemi, and T. Thio, "Electric conductivity of individual carbon nanotubes," *Nature*, vol. 382, pp. 54–56, 1996.

Chapter 3

Carbon nanotube synthesis

Abstract

Three main methods for growing CNTs exist. The synthesis of CNTs was discovered using the arc discharge method, where an electric spark provides the energy for growing CNTs. Later the method of laser ablation was developed. This method can reach gram scale production and is based on a laser providing the required energy for growth. Finally Chemical Vapour Deposition (CVD) was made available for CNT growth as well. Both thermal and plasma enhanced CVD are widely used. Both forms of CVD provide substantial amounts of CNTs and growth can be much better controlled. Also the energy consumption is less for CVD when compared with arc discharge or laser ablation, which makes it more viable for commercialization.
Also the most common and the most relevant growth termination mechanisms are discussed. More specifically the encapsulation of the catalyst particle by amorphous carbon. Also depletion of catalyst can terminate growth and can occur due to catalyst detachment from the substrate, catalyst diffusion into the substrate and Ostwald ripening. Finally, CNT growth can be terminated by strain due to growth termination of neighboring CNTs.

3.1 Introduction

In this chapter the synthesis of carbon nanotubes will be described. The chapter is divided in two parts, the actual growth methods and growth termination mechanisms. The latter part is fundamentally important to the theory behind this study, as will become clear in section 3.3.

3.2 Methods for growing CNTs

A variety of methods to synthesize CNTs are invented. The most important methods are arc discharge, laser ablation and chemical vapour deposition. The latter one is currently used the most and will therefore be described more in depth.

3.2.1 Arc discharge

The first production method that could produce CNTs was the arc discharge method. This method was applied when CNTs were discovered by Iijima [1]. It was also the first to be used for large scale CNT production at an industrial level, as was invented at NEC's Fundamental Research Laboratory [2].
The working principle of the method itself is quite straightforward. Two graphite electrodes are charged with opposite charges, while they are contained in a helium atmosphere. The potential between the electrodes is increased to the point where an arc ignites between them. Due to heat accumulation at the anode CNTs will form from the evaporated carbon coming from the graphite. When this method is applied without any

metal catalysts, the range of diameter of the tubes will be wide. Only MWNTs will form with a minimum of DWNTs. The range of diameters will be narrowed down to only 2 or 3 nm in the presence of catalytic metal nanoparticles [3]. In most cases nickel or cobalt is used as a catalyst. With the use of a catalyst not only is the diameter more controlled, also mostly SWNTs will be formed as opposed to the MWNTs that are formed without the use of a catalyst.

3.2.2 Laser ablation

A major disadvantage of the arc discharge method is the inability to produce CNTs in a larger amount per batch and per unit of time. An alternative was invented in 1995 by the group of R.E. Smalley [4]. This method became known as the laser ablation technique. It was the first method to produce CNTs at a gram scale. Its working principle does not differ much from the arc discharge method. Again a graphite rod of a couple of millimeters is taken. Metal catalyst particles are immersed in the graphite. In most setups the rod is placed in an oven at a temperature of about 1200 °C [4]. Where in case of the arc discharge method the heat was provided by the arc, now the required heat is added by a laser. Temperatures of 1700 °C are reached to locally evaporate the carbon. The general setup used for laser ablation is shown schematically in 3.1
The advantages of these methods (arc discharge and laser ablation) are that they produce high quality CNTs with little defects. However, there are also quite some disadvantages:

- Mass production of CNTs is not possible, since the methodes operate per batch of electrodes.
- High temperature requirements, which make the methods very energy consuming.
- High machinery requirements. Especially for the laser ablation technique the machinery is expensive.
- Little control over diameter of the tubes and the amount of walls. Although the presence of metal catalyst particles provide some certainty about these parameters, they are still not fully controlled and uncertainty remains.

3.2.3 Chemical Vapour Deposition

The third method, Chemical Vapour Deposition (CVD), is currently used the most for the synthesis of CNTs. In industry this was already a familiar method before CNT growth. More specifically, CVD is often used in the semiconductor industry to deposit thin films of a pure material on a substrate. Materials that are deposited using CVD include germanium, thungsten, titanium and several dielectrics. Furthermore CVD is used to form oxides, carbides and nitrides with the substrate surface material. Finally this method can even be used to produce synthetic diamonds or graphene [5].
A lot of variants exist of Chemical Vapor Deposition. In general their working principle is the same. The substrate on which the material should be deposited is placed in an

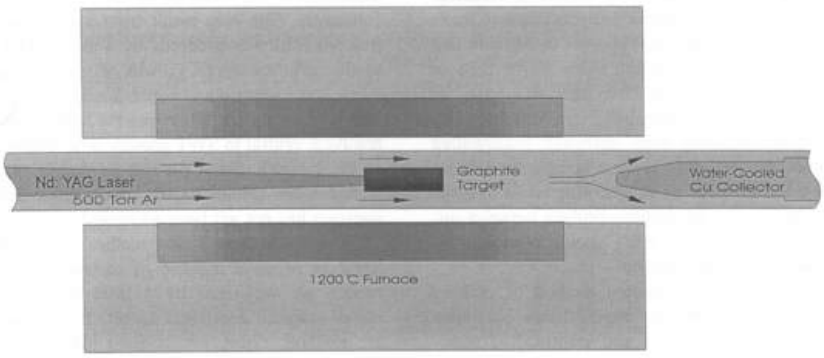

Figure 3.1: Schematic image of the setup as used in the laser ablation method to produce CNTs. Reprinted from Guo et al. [4].

oven. Then the material that is to be deposited is vaporized and blown through the reactor. A low pressure is applied in the oven when operating the system, varying from a couple of millibars to atmospheric pressure. Under the right conditions the vapor will be deposited onto the substrate. These conditions and the exact process will vary from material to material.

When producing CNTs in a CVD reactor the process is essentially the same. As a precursor, which is the carbon containing gas, several options are available. Examples of gases used are acetylene, ethylene, methane, ethane, carbon monoxide or a vaporized alcohol. It is hard to determine which carbon containing precursor is the best. Often the total combination of growth conditions such as catalyst material, temperature, pressure and flow rates is important.
As opposed to the arc discharge method some form of catalyst is required when using CVD to grow carbon nanotubes. In most cases the catalyst is a transition metal, where iron, nickel and cobalt are the most popular ones [3]. In other cases no metal catalyst is used and substitutes are available such as hexagonal silicon-carbides [6], fullerenes [7] or specific scratches on the substrate [8]. The absence of a metal catalyst often induces problems such as lack of structural control or low quality tubes.
A final requirement to grow CNTs in a CVD reactor is that sufficient energy is present to from carbon radicals. Without sufficient energy to separate the carbon atoms from the precursor no radicals will be formed and as a result no carbon is available for CNT growth. The energy is delivered by the heating element of the oven, which should heat the reactor up to at least 400 °C in order to grow CNTs [9]. If lower temperatures are used, from about 120 °C other carbon structures might be formed such as CNFs [10].

3.2.3.1 Commonly used CVD methods

As already mentioned several forms of CVD exist, each with its own additions with respect to the regular thermal CVD. For the growth of CNTs the thermal CVD and Plasma Enhanced Chemical Vapour Deposition (PECVD) are the most commonly used. Other methods that are often used are variants of thermal CVD and PECVD. Examples of these variants are Hot Filament (HF-CVD), Microwave Plasma (MPECVD) and Radio Frequency (RF-PECVD). Since thermal CVD and PECVD are the basic methods for CNT growth they will be discussed in more detail below.

Thermal CVD is the most common type that is used for the synthesis of CNTs. As mentioned above basically all other types of CVD have additional equipment with respect to the basic thermal CVD. The thermal CVD system consist of a quartz tube which is surrounded by a tubular oven. Figure 3.2 shows a schematic view of the thermal CVD oven. The front end of the tube forms the gas inlet, while the back end, also called downstream, is the exhaust. The gas at the inlet of the CVD is called the feedstock and for the growth of CNTs this comprises of a carbon containing gas and a carrier gas. The carrier gas is often an inert gas such as argon or helium. In some cases hydrogen is added to etch away the excess carbon deposited on the walls of the tube, the substrate or the CNTs themselves. For the same purpose vaporized water or oxygen might be added.
Temperatures in the thermal CVD oven may vary from 0 °C to 1200 °C, however, for the growth of CNTs this range is in most cases narrowed down to 600 °C to 900 °C and is dependent on the feedstock that is used. Below these temperatures CNTs will no longer grow because there is not enough energy to form the required carbon radicals. In case of these low temperatures the pressure is in general low, about several millibars. Higher temperatures are associated with higher pressures, which for the growth of CNTs is about atmospheric pressure [11].

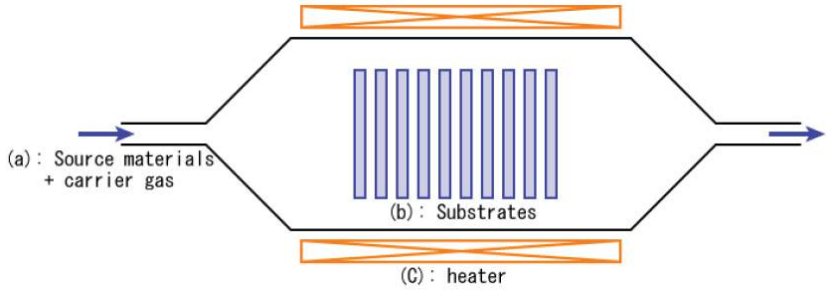

Figure 3.2: Schematic image of a thermal CVD oven. Courtesy of Wikipedia [12].

The last decade research is devoted to the growth of CNTs in a Plasma Enhanced CVD reactor as well. This resulted in a sharp increase in popularity of the method. The advantages of this method that caused this growth in popularity iss discussed later in this section.
PECVD consist of a standard (thermal) CVD system with the ability to create a plasma

on the reaction site. The plasma consists of dissociated feedstock gasses. These gasses are ionized with the use of a strong electric field which is generated by electrodes on the top and bottom of the reactor. As a result the required temperatures to grow CNTs are dropped dramatically. With PECVD CNTs can be grown at much lower temperatures, with a minimum of about 120 °C [10]. It follows that PECVD is used mainly in the semiconductor industry, since higher temperatures are to be avoided when producing chips. High temperatures are not tolerated at certain production processes in this industry and besides, the chips might become damaged. Another advantage of growing CNTs with PECVD is that the direction of the plasma can be used as an alignment tool. In case of thermal CVD the tubes can grow upward due to a crowding effect, which means that the CNTs push each other upward with the help of Van der Waals Forces. However, when plasma is applied, free standing nanotubes can be created in the direction of the plasma. When CNTs are grown together there is a higher tendency to create a well aligned forest in the presence of plasma, whereas without a tangled spaghetti-like forest might be created.

3.2.3.2 Advantages of CVD

The use of Chemical Vapour Deposition for growing CNTs offers some advantages over the use of laser ablation or arc discharge. These advantages can be listed as follows:

- The most important advantage is that CNT growth can be a lot better controlled when using CVD. By carefully choosing the catalyst particles the thickness of the tubes can be more or less estimated. Besides, the number of walls is greatly affected by the size of the catalyst particles. The size of these particles can be influenced by picking a certain thickness of the catalyst layer [13]. Besides the diameter and number of walls, the length of the CNTs can be defined to a certain extend by varying the growth time.

- With CVD CNTs are grown on a substrate. Therefore CNTs might grow in a vertically aligned forest, which opens up possibilities for other applications. These forests can be used for spinning, super capacitors and structural improvements, whereas individual CNTs cannot.

- With CVD it is possible to grow CNTs on a larger scale. In fact, CNTs can be grown continuously [14]. It can be imagined that this feature is required to grow CNTs at an commercial quantities.

- The energy consumption of CVD is a lot lower, since the required temperatures are a lot lower, as concluded earlier as well. For scaling CNT growth to an industrial level the energy consumption should be minimized.

3.3 Growth termination mechanisms

The length of CNTs is important for many different applications, for example for the spinning of a wire. Many groups have tried to grow long CNTs. However, a distinction should be made between individual grown CNTs and CNTs grown in a forest. By applying the kite-mechanism, where the catalyst particle stays on top of an individual CNT and floats along with the gases, CNTs can be grown of over half a meter long [15][16]. However, when grown in a forest CNTs can be grown up to 'only' 12.4 mm [17]. It should be noted that 'long' CNTs grown in a forest is not well defined, since growth slows down gradually. When a forest grows several hundred microns the first ten minutes it is said to be long [18].
Since length of CNTs is important for many applications, research has been devoted to the understanding of the maximum reachable length in a certain process. The mechanism responsible for the stagnation of CNT growth is called the growth termination mechanism, or termination mechanism in short. In this section the most common termination mechanisms will be discussed and it will be explained why and when they occur.

3.3.1 Encapsulation by amorphous carbon

Encapsulation of the catalyst by amorphous carbon (a-c) is assumed to be one of the most common causes for growth termination[19]. In some cases it is also referred to as catalyst poisoning.
With this growth termination mechanism it is assumed that an excess of carbon radicals are present in the CVD oven. Due to saturation of the catalyst particles with carbon these radicals cannot diffuse into the catalyst material to form a CNT. Instead they accumulate at the surface of these catalyst particles. This graphitic shell will then block the supply of the fresh carbon containing gas, with the consequence that no new radicals will reach the surface of the catalyst particles. It follows that there will be no carbon present to continue the growth of the carbon nanotube [20]. An impression of this termination process is shown in figure 3.3.

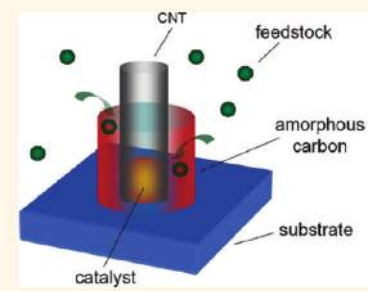

Figure 3.3: Schematic image of a catalyst particle encapsulated by amorphous carbon. Reprinted from Schunemann et al. [19].

For some substrates denser and taller forest can be grown than on others and originally the encapsulation of the catalyst layer by amorphous carbon was discovered in a search for reasons why some substrates perform better than others. When looking to the substrate with high-resolution TEM after the growth process Li et al. discovered that the catalyst particles without a CNT were encapsulated with a graphitic shell [21]. After this study it became widely associated with catalyst inactiv-

ity, the encapsulation of catalyst particles by amorphous carbon appeared as a reason of the termination of the growth process. Proof that the shell of amorphous carbon was formed during the CVD process instead of during the cooling stage thereafter, remained experimentally hard to obtain [22].
It is because of this lack of evidence that this termination mechanism was still debated in various scientific circles. Eventually it turned out that a substrate with a layer of amorphous carbon on top of it, was not able to produce CNTs during the CVD process [19]. This indicates that the layer of a-c is formed during the growth process and not during the cooling stage. Furthermore, careful analyses of Stadermann et al. led to the conclusion that growth cessation can indeed be caused by amorphous carbon accumulating on the surface of the catalyst [20].

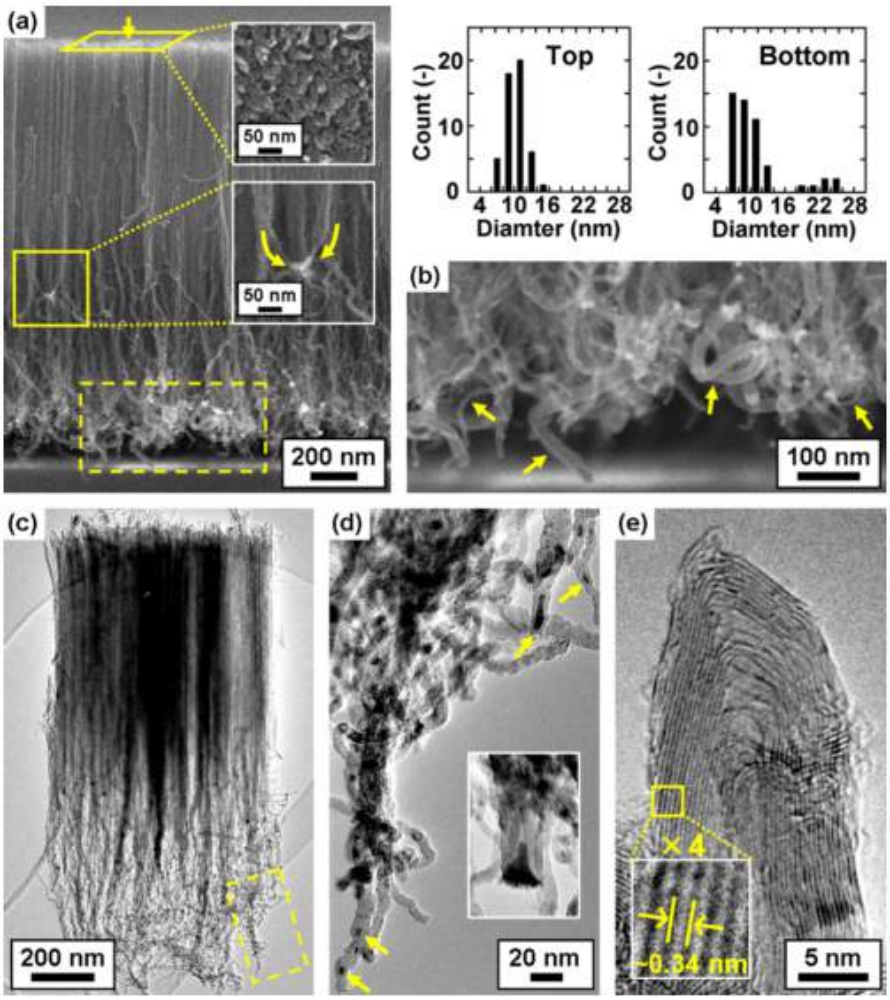

Figure 3.4: Figure d) shows a TEM image from catalyst containing CNT forest. The black dots within the CNTs are the catalyst material (iron). This proves the catalyst detachment during growth. Reprinted from [23].

3.3.2 Catalyst detachment

The catalyst layer is an extremely important part in the growth of CNTs. In combination with the annealing time a lot of the CNT parameters will be determined. For example the density of CNTs in the forest is one of those parameters, as well as the diameter of the CNTs and the quality (number of defects) [22]. While this catalyst is so important, it is also very delicate. There are several different mechanisms that can cause the catalyst to deplete, namely the detachment of the catalyst, Ostwald ripening or diffusion into the substrate. In this subparagraph the detachment of the catalyst will be discussed.

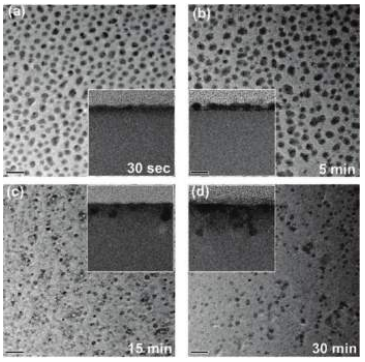

Figure 3.5: This figure shows how diffusion takes place during the growth process. The scalebar of the outer figures is 20nm, while the inner figures contain a scalebar of 10nm. Reprinted from Kim et al. [24].

The detachment of catalyst material is extensively described by Sugime et al. [23]. In this study the goal was to observe the CNT growth kinetics and growth mechanisms. When looking at the morphology of the forest after the growth process it turned out the bottom part of the CNTs contained a lot of defects and irregularities. Closer inspection with TEM led to the discovery of catalyst material in the CNTs themselves. It turned out that the catalyst particles are slowly crumbling into the CNTs as the CNTs grow. This happens because the metal catalyst is hypothesized to be liquid as described in the section 3.3.4. The consequence will be that the catalyst particle shrinks in size and no longer matches the diameter of the CNT that is growing on top of it. This will terminate the growth. Besides, the CNTs are more and more contaminated with catalyst material which will promote the formation of defects. The detachment of catalyst material and accumulation thereof in CNTs is shown in figure 3.4.

3.3.3 Catalyst diffusion into the substrate

Another form of catalyst depletion is when the it diffuses into the substrate. Because of the elevated temperatures during the CNT growth process, the energy added to the substrate is high enough to enable diffusion.

It can be imagined that little catalyst particles remain suitable for growing CNTs if half of them has diffused into the layer underneath, as shown in figure 3.5. It applies here as well that the catalyst particles shrink, in this particular case due to partial diffusion. Also in this case the difference in diameter of the catalyst particle and its CNT becomes too large to sustain growth.

A diffusion barrier, as its name suggests, is to a certain extend capable to prevent

diffusion of the catalyst layer. In most cases this barrier is a thin layer of only tens of nanometers thick. A lot of research has been devoted to finding even better diffusion barriers, as is illustrated in 3.5 as well. A very common diffusion barrier is alumina (Al_2O_3) with a thickness varying between 10 and 20 nm. Other suitable materials for a diffusion barrier seems to be silicon dioxide (SO_2), titanium nitride (TiN), silicon nitride (SiN_x) and ITO [25].

3.3.4 Ostwald ripening

Theories on Ostwald ripening are extensively described by P.W. Voorhees (1985) [26]. The following explanation for the term Ostwald ripening is very relevant for CNT growth initiation and termination:

> In general, any first-order phase transformation process results in a twophase mixture composed of a dispersed second phase in a matrix. However, as a result of the large surface area present, the mixture is not initially in thermodynamic equilibrium. The total energy of the two-phase system can be decreased via an increase in the size scale of the second phase and thus a decrease in total interfacial area. Such a process is termed Ostwald ripening or coarsening. (p. 231)

This phenomenon also occurs when growing CNTs at elevated temperatures. As explained earlier, most CNT growth processes are enabled by a catalyst layer of only a few nanometers thick. During the process the oven will heat up the substrates, which in turn will reach high temperatures as well. As pointed out by Jourdain et al.[22], at the scale of nanoparticles the melting points are significantly depressed as indicated by the following equation:

$$T_{\mathrm{m}}(r) = T_{\mathrm{m}}^{\mathrm{bulk}} \left(1 - \frac{4\sigma_{\mathrm{sl}}}{H_{\mathrm{f}}\rho r} \right) \tag{3.1}$$

Here $T_{\mathrm{m}}(r)$ and $T_{\mathrm{m}}^{\mathrm{bulk}}$ are the particle and bulk melting points, respectively, σ_{sl} is the surface tension at the solid-liquid interface, H_{f} is the bulk latent heat of substance per volume unit. In other words, H_{f} is the change in entropy when a specific amount of substance melts. Finally ρ and r is the density and radius of the particle, respectively. With this equation in mind it is reasonable to assume a liquid state of the catalyst layer during the growth process, as calculated by Shibuta et al. [27].
As a consequence the catalyst particles become highly mobile. Furthermore it is important to realize that the equilibrium vapor pressure is lower for larger particles. A lower vapor pressure is associated with a higher stability of the material. It follows that it is thermodynamically favored to have larger particles, which is why the nanoparticles have the tendency to cluster together.
Ostwald ripening forms an extremely important phenomenon during CNT growth. It is due to this coarsening that the original smooth catalyst layer is torn apart and forms nanoparticles, which in turn are required to transform the carbon atoms in the atmosphere into carbon nanotubes. An annealing time too short will mean that the smooth

catalyst layer is not ripped apart enough, but on the other hand: an annealing time too long results in large clusters of catalyst material. In both of those two cases CNTs will not be able to be formed. That is why the right annealing time is critical.
However, Ostwald ripening can also be a cause of growth termination. Even when the catalyst particles are formed and growth is initiated, coarsening will continue to occur. The result is shown in figure 3.6. Like with other forms of catalyst depletion, the catalyst particles will no longer fit the CNTs. Therefore it will terminate the growth process.

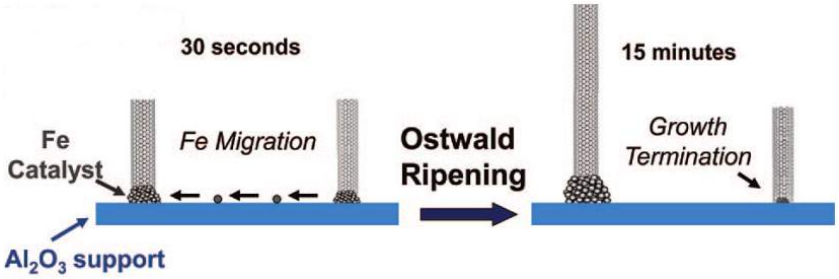

Figure 3.6: Figure of Ostwald ripening causing termination of the CNT growth process. Reprinted from Amama et al. [28].

3.3.5 Strain within the forest

The final growth termination mechanism discussed here is specifically focused on CNT forests as a whole. If it was only for the termination mechanisms discussed so far it would be hard to explain why extremely long carbon nanotubes of 55 cm are reached when growing them individually, while the longest CNTs grown in an array are 'only' 7 mm, as mentioned earlier. In order to explain these differences in final length of individual tubes versus CNTs in an array, research has been devoted to termination due to strain in a forest. It is thought that CNTs in a forest become entangled with each other and at some point the growth of a CNT will terminate due to one of the above mentioned termination mechanisms. Since this CNT is entangled with other CNTs it has to be pulled loose from the substrate and lifted along with its neighboring CNTs. It follows that it is more energy intensive to grow for the surrounding CNTs. It can be the case that this additional energy barrier is too high to continue growth, thereby terminating the process. This eventually causes all CNTs in the forest to stop growing.

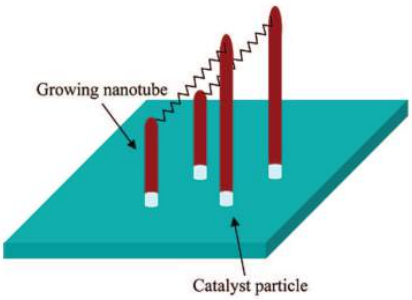

Figure 3.7: Here the principle of the model for strain in a CNT forest is shown. The CNTs are interconnected with springs to model entanglement. Reprinted from Han et al. [29].

A clear insight in this termination mechanism is provided by the model of Han et al. [29]. The entanglement is modeled by a spring attached to the end of the CNTs, as is shown in figure 3.7. Every tube has its own growth rate assigned based on a fixed number plus a very small random variation. Once the height difference between the tips of two neighboring CNTs becomes to large, the growth rate will be set to zero. From this model it can be deduced that even variations in growth rate will disturb growth overall. Therefore, when the carbon containing precursor does not diffuse equally enough into the catalyst particles, the growth process might be substantially slowed down. This in term will neighboring and entangled CNTs slow down as well.

3.4 Conclusion

With this study it can be concluded that the CVD growth is favorable over other CNT synthesis methods. The main reasons being that CVD growth prefers formation of CNTs over other carbon structures, better control over tube diameter and wall number, better control over CNT morphology and this way of growing is less energy consuming. Besides, CNTs can be grown on a large scale by using CVD.
Furthermore it can be concluded that CNTs grown in forests are unlikely to reach lengths above several millimeters. This is due to strain in the forest, which is caused by neighboring CNTs that have stopped growing. The terminated CNTs have to be pulled up and should be broken loose from the substrate in order to continue growth of the other CNTs. Growth is initially likely to be caused by either catalyst depletion or amorphous carbon on the catalyst blocking the supply of fresh radicals needed for growth.

References

[1] S. Iijima, "Helical microtubules of graphitic carbon," *Nature*, vol. 354, pp. 56 –58, 1991.

[2] T. Ebbesen and P. Ajayan, "Large-scale synthesis of carbon nanotubes," *Nature*, vol. 358, no. 6383, pp. 220–222, 1992.

[3] J. Prasek and J. Drbohlavova, "Methods for carbon nanotubes synthesis: review," *Journal of Materials*, vol. 21, no. 40, pp. 15872–15884, 2011.

[4] T. Guo, P. Nikolaev, A. Thess, D. Colbert, and R. Smalley, "Catalytic growth of single-walled nanotubes by laser vaporization," *Elsevier*, vol. 243, no. 1-2, pp. 49–54, 1995.

[5] R. S. Balmer, J. R. Brandon, S. L. Clewes, H. K. Dhillon, J. M. Dodson, I. Friel, P. N. Inglis, T. D. Madgwick, M. L. Markham, T. P. Mollart, N. Perkins, G. a. Scarsbrook, D. J. Twitchen, a. J. Whitehead, J. J. Wilman, and S. M. Woollard, "Chemical vapour deposition synthetic diamond: materials, technology and applications.," *Journal of physics. Condensed matter : an Institute of Physics journal*, vol. 21, p. 364221, Sept. 2009.

[6] V. Derycke, R. Martel, and M. Radosavljevic, "Catalyst-free growth of ordered single-walled carbon nanotube networks," *Nano Letters*, vol. 2, no. 10, pp. 1043–1046, 2002.

[7] I. Ibrahim, A. Bachmatiuk, and D. Grimm, "Understanding high-yield catalyst-free growth of horizontally aligned single-walled carbon nanotubes nucleated by activated C60 species," *ACS Nano*, vol. 6, no. 12, pp. 10825–10834, 2012.

[8] B. Liu, W. Ren, L. Gao, S. Li, and S. Pei, "Metal-catalyst-free growth of single-walled carbon nanotubes," *Journal of the American Chemical Society*, vol. 131, no. 6, pp. 2082–2083, 2009.

[9] Y. Yamazaki, N. Sakuma, M. Katagiri, M. Suzuki, T. Sakai, S. Sato, M. Nihei, and Y. Awano, "High-quality carbon nanotube growth at low temperature by pulse-excited remote plasma chemical vapor deposition," *Applied Physics Express*, vol. 1, no. 3, pp. 0340041–0340043, 2008.

[10] S. Hofmann, C. Ducati, J. Robertson, and B. Kleinsorge, "Low-temperature growth of carbon nanotubes by plasma-enhanced chemical vapor deposition," *Applied Physics Letters*, vol. 83, no. 1, pp. 135–137, 2003.

[11] P. T. a. Reilly and W. B. Whitten, "The role of free radical condensates in the production of carbon nanotubes during the hydrocarbon CVD process," *Carbon*, vol. 44, no. 9, pp. 1653–1660, 2006.

[12] "Wikipedia - Chemical Vapor Deposition," 2015.

[13] K. Liu, Y. Sun, L. Chen, C. Feng, X. Feng, K. Jiang, Y. Zhao, and S. Fan, "Controlled growth of super-aligned carbon nanotube arrays for spinning continuous unidirectional sheets with tunable physical properties," *Nano Letters*, vol. 8, no. 2, pp. 700–705, 2008.

[14] X. Lepró, M. Lima, and R. Baughman, "Spinnable carbon nanotube forests grown on thin, flexible metallic substrates," *Carbon*, vol. 48, pp. 3621–3627, Oct. 2010.

[15] S. Huang, M. Woodson, R. Smalley, J. Liu, D. U. V, and N. Carolina, "Growth Mechanism of Oriented Long Single Walled Carbon Nanotubes Using Fast-Heating Chemical Vapor Deposition Process," *Nano Letters*, vol. 4, no. 6, pp. 1025–1028, 2004.

[16] R. Zhang, Y. Zhang, Q. Zhang, H. Xie, W. Qian, and F. Wei, "Growth of Half-Meter Long Carbon Nanotubes Based on Schultz-Flory Distribution," *ACS nano*, vol. 7, no. 7, pp. 6156–6161, 2013.

[17] W. Cho, M. Schulz, and V. Shanov, "Kinetics of Growing Centimeter Long Carbon Nanotube Arrays," *Intech*, pp. 223–237, 2013.

[18] X. Zhang, Q. Li, Y. Tu, Y. Li, J. Y. Coulter, L. Zheng, Y. Zhao, Q. Jia, D. E. Peterson, and Y. Zhu, "Strong carbon-nanotube fibers spun from long carbon-nanotube arrays.," *Small*, vol. 3, pp. 244–248, Feb. 2007.

[19] C. Schunemann and F. Schaffel, "Catalyst poisoning by amorphous carbon during carbon nanotube growth: fact or fiction?," *ACS Nano*, vol. 5, no. 11, pp. 8928–8934, 2011.

[20] M. Stadermann, S. Sherlock, and J. In, "Mechanism and kinetics of growth termination in controlled chemical vapor deposition growth of multiwall carbon nanotube arrays," *Nano Letters*, vol. 9, no. 2, pp. 738–744, 2009.

[21] Y. Li, W. Kim, Y. Zhang, M. Rolandi, D. Wang, and H. Dai, "Growth of single-walled carbon nanotubes from discrete catalytic nanoparticles of various sizes," *Journal of Physical Chemistry B*, vol. 105, no. 46, pp. 11424–11431, 2001.

[22] V. Jourdain and C. Bichara, "Current understanding of the growth of carbon nanotubes in catalytic chemical vapour deposition," *Carbon*, vol. 58, pp. 2–39, July 2013.

[23] H. Sugime and S. Esconjauregui, "Growth kinetics and growth mechanism of ultra-high mass density carbon nanotube forests on conductive Ti/Cu supports," *ACS applied materials & interfaces*, vol. 6, pp. 15440–15447, 2014.

[24] S. Kim and C. Pint, "Evolution in catalyst morphology leads to carbon nanotube growth termination," *The Journal of Physical Chemistry Letters*, vol. 1, no. 6, pp. 918–922, 2010.

[25] J. Garcia-Cespedes and S. Thomasson, "Efficient diffusion barrier layers for the catalytic growth of carbon nanotubes on copper substrates," *Carbon*, vol. 47, no. 3, pp. 613–621, 2009.

[26] M. Division, "The Theory of Ostwald Ripening," *Journal of Statistical Physics*, vol. 38, no. 1, pp. 231–252, 1985.

[27] Y. Shibuta and S. Maruyama, "A molecular dynamics study of the effect of a substrate on catalytic metal clusters in nucleation process of single-walled carbon nanotubes," *Chemical Physics Letters*, vol. 437, no. 4-6, pp. 218–223, 2007.

[28] P. B. Amama, C. L. Pint, L. McJilton, S. M. Kim, E. a. Stach, P. T. Murray, R. H. Hauge, and B. Maruyama, "Role of water in super growth of single-walled carbon nanotube carpets.," *Nano letters*, vol. 9, no. 1, pp. 44–49, 2009.

[29] J.-h. Han, R. A. Graff, B. Welch, C. P. Marsh, R. Franks, and M. S. Strano, "A Mechanochemical Model of Growth Termination in Vertical Carbon Nanotube Forests," *Acs Nano*, vol. 2, no. 1, pp. 53–60, 2008.

Chapter 4

CNT yarn spinning techniques

Abstract

In this study the three methods for spinning CNT yarn is discussed. These methods are dry spinning, wet spinning and directs spinning. The most important advantage of dry spinning over the other two methods is the ability to fine-tune structural appearances of the CNTs, such as height, diameter and number of walls. Because of this a high quality yarn can be spun. A disadvantage of the wet spinning technique is that the resulting yarn is impregnated with polymer reducing its electrical conductivity. The main disadvantage of direct spinning is that a modified CVD system is required, making this method less accessible.

4.1 Introduction

Although Carbon Nanotubes (CNTs) possess extraordinary mechanical, electrical and thermal properties it remains difficult to take advantage of these qualities at a macroscopic level. One solution researchers have come up with is to spin CNTs in a yarn. Currently three methods of spinning Carbon Nanotubes into yarn are developed. The method for spinning yarn that is used the most is dry spinning. Most research conducted about spinning CNTs has been devoted to this particular process. Dry spinning is based on pulling CNTs out a forest and due to a combined twisting and pulling motion creating a yarn. The other two methods for spinning CNTs into yarn are wet spinning and direct spinning. Wet spinning is carried out by dispersing CNTs in a liquid. By dispersing this CNT saturated liquid in a specific other liquid a gel of CNTs can be formed, which can be spun. The latter method, direct spinning, is based on spinning a CNT aerogel that is created with Chemical Vapor Deposition as soon as it comes out of the oven. In this study these three methods are discussed and compared.

4.2 Methods of spinning a CNT yarn

In each of the subsection below a one of the three spinning methods is described. The working principle of the method will be explained and properties of the resulting yarn is mentioned. Finally the advantages and disadvantages of each method are stated.

4.2.1 Dry spinning

The method of dry spinning was mentioned for the first time in a study by Jiang et al. [1]. The method was actually discovered by accident, after an attempt of pulling out a bundle of CNTs. A bundle typically consist of ten to hundred CNTs. Instead of a free standing bundle a wire of about 30 cm was obtained.
The reason that a wire could be created has to do with the degree of alignment of the CNT array. A wire tends to form only when the forest is sufficiently spinnable. This means that the bundles are structurally ordered and not fully entangled. In order to be

spinnable the bundles within the forest should stick together by Van der Waals forces and some mild entanglements with neighboring bundles at the bottom and the top of the forest.

As indicated in figure 4.1 the CNT bundles are pulled from the substrate and follow one by one as long as the end knots at the top and bottom of the forest are strong enough to overcome the force required to pull a bundle from the substrate [2].

A super aligned CNT array with the correct morphology for spinning can be identified by its low level of tortuousness, which is shown in figure 4.2. According to Huynh et al. [3] there is no clear difference in the density of both forests and both forests come down to about $3 * 10^{10}$ CNTs/cm^2.

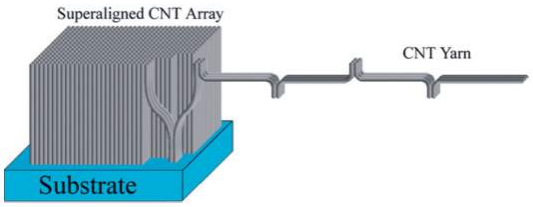

Figure 4.1: Schematic image of a model that explains the yarn formation from a CNT forest. Reprinted from Zhang et al. [2].

Intuitively it might seem illogical to prefer the super aligned forests. It might be reasoned that for a forest containing more entanglement it will be easier to pull the next bundle of CNTs along with the originally pulled bundle. However, in practice it is clearly proven that better aligned forests are easier spinnable. This is the case because the spinning procedure requires a constant bundle by bundle roll off from the forest. When a bundle of CNTs of the highly entangled and tortuous forests are pulled away, they immediately tend to grab a large amount of bundles along as well. This results in a large chunk of CNT bundles clustered together and not able to roll off to form a ribbon, web or yarn.

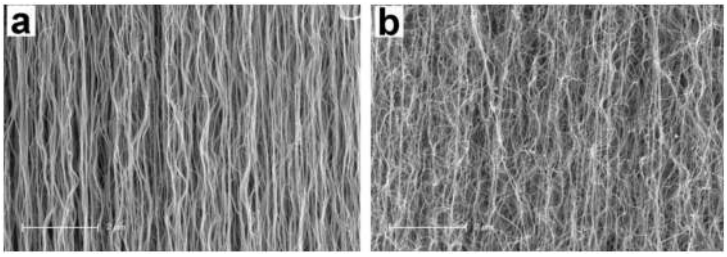

Figure 4.2: Figure 4.2a shows the morphology of a highly spinnable CNT array, while figure 4.2b shows a forest which is not spinnable at all. The clear difference is the lower level of tortuousness in the case of the spinnable forest. Reprinted from Huynh et al. [3].

According to several papers the initiation of the spinning process could be done simply by using a pair of sharp tweezers [4][5][6][3]. At first the initial web, the triangle which connects CNT bundles over the entire front of the array, is formed. When this web is

formed the process will look like as is shown in figure 4.3. The end of the web is twisted together and attached to a spindle on a rail. This spindle will start to rotate and thereby twisting the initial yarn. Simultaneously the yarn will be pulled, either by moving the spindle backwards or by winding the yarn around a pulley. A clear video of the initiation of the spinning process is provided in the supplementary data of a paper by Ghemes et al. [6].

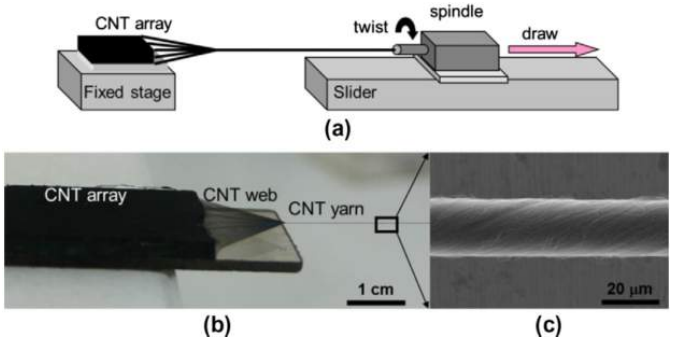

Figure 4.3: After the formation of the initial web the process of spinning CNTs from an array will look like shown here. Reprinted from Ghemes et al. [6].

One of the advantages of this method over other CNT spinning methods is that this method does not require the use of chemicals. Also the growth process and CNT spinning process are decoupled, which means that in principle a regular CVD oven can be used without modifications. Furthermore, the CNTs that are used can be modified quite a lot as long as the forest as a whole remains spinnable. For example the diameter and number of walls of the CNTs can be adjusted, but also a variation of forest height is allowed within this spinning process.
The main disadvantage is that this process requires a quite specific morphology of the forest. Besides, the initiation of the spinning process is not always easy, since the formation of the web is quite tedious. However, as long as a spinnable forest can be obtained this process is preferred over other methods. In principle there are a lot of proven ways to create a spinnable forest on different substrates. This is exemplified by table 4.1 where an overview is shown of different substrates used in different studies.
Besides the substrates mentioned in table 4.1, two interesting and somewhat alternative cases of growing a spinnable CNT forest exist. The first one is described by Inoue et al. where iron chloride ($FeCl_2$) is inserted into the CVD oven as a catalyst precursor along with the acetylene gas, which serves as a carbon precursor. It is interesting to notice that this combination will form CNT forests on quartz or SiO_2 substrates [9]. Another interesting substrate of growing a spinnable CNT forest is used by Lepro et al. [10]. Here a commercial stainless steel foil of about 50 micron is used as a substrate. Alumina (Al_2O_3) or silicon oxide (SiO_x) is used as a diffusion barrier layer and finally a catalyst layer of 2 nm Fe is deposited. Because the substrate is essentially a foil it opened up possibilities to have a continuously turning conveyor belt growing CNTs on the one side and spinning on the other, so infinitely long yarn could be spun as shown in figure 4.4.

Table 4.1: An overview of substrates used for the growth of spinnable forests. The first column shows the author of the particular paper, while the second and third columns contain the diffusion barrier material and thickness, respectively. The fourth and fifth column provides information on the catalyst material and thickness, respectively.

Authors Authors	**Barrier material**	**Barrier thickness (nm)**	**Catalyst material**	**Catalyst thickness (nm)**
Jayasinghe et al. [4]	Al_2O_3	10	Fe	2
Zhang et al. [5]	Al_2O_3	10	Fe	1
Zheng et al. [7]	Al_2O_3	10	Fe	0.8
Huynh et al. [3]	SiO_2	50	Fe	2
Gilvaei et al. [8]	-	-	Fe	4

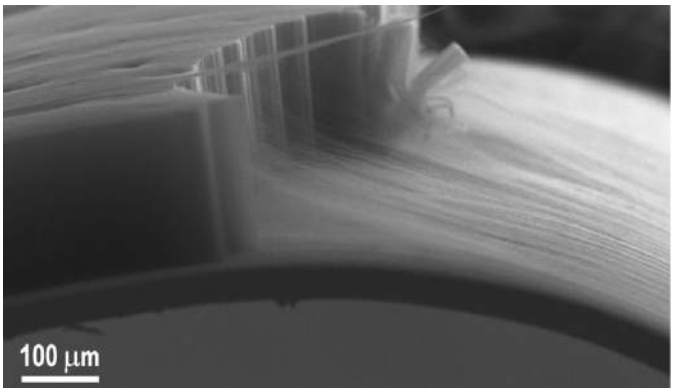

Figure 4.4: The flexible substrate made from stainless steel foil proves to be suitable for spinnable CNT growth. Reprinted from Lepro et al. [10].

With this method of spinning quite strong yarns can be produced compared to the other CNT spinning methods, as indicated in figure 4.5. This is mainly the case because the length of the CNTs can be varied over quite a broad range with this method, as was mentioned earlier as one of the advantages of dry spinning. The longer the CNTs in the forest (and thus in the yarn) are, the more the strength of the yarn resembles the strength of individual tubes. This correlation between forest height and yarn strength is already investigated by several groups. Vilatela et al. has made a chart containing information about the yarn strength as reported in literature versus their according forest length from which they are spun, as is shown in figure 4.5.
In literature there are about a dozen cases where CNT yarns are spun on which tensile tests are conducted. According to Miao [12] the best result up to 2013 was obtained by Li et al. who reached a tensile strength of 3.3 GPa [13].

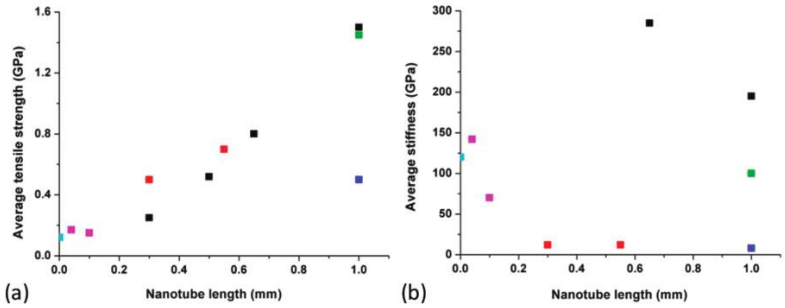

Figure 4.5: (a) Yarn strength and (b) stiffness versus forest length as reported in literature. The data are for yarn spun from dry spinning (black: DWNTs and MWNTs; red: MWNTs; and blue: MWNTs), direct spinning (green: mostly DWNTs) and wet spinning (pink: MWNTs; light blue: SWNTs). Reprinted from Vilatela et al. [11].

4.2.1.1 Improvements on dry spinning

Several groups have tried (and succeeded) to improve the strength, stiffness or conductivity of CNT yarn spun by dry spinning. The spinning process itself is improved by optimizing the amount of twist and tension during spinning [14]. To further improve the yarn additions to the spinning process can be implemented. There are three proven additions to a regular spinning process which lead to a stronger yarn:

- The first way to improve the strength is by doping the yarn into a volatile liquid after it is being spun. Due to the liquid the yarn will be contract and the density of CNT bundles per cross sectional area increases. Having a reduced diameter of the yarn, its strength increases. Furthermore a slight increase in strength will be induced due to increased Van der Waals forces. In most cases ethanol is used as a volatile liquid. After doping the yarn will be dried so that the liquid evaporates. The increased density and Van der Waals forces remain.

- Secondly, in line with the previous addition, the yarn might be impregnated with a polymer. When for example polyvinyl alcohol (PVA) is used the CNTs get bonded together, though with the relatively weak π bonds. By impregnating an electrically conductive polymer, the electrical conductivity of the yarn can be improved.

- Finally it is possible to improve the strength of a CNT yarn by pressurizing the yarn. This is basically the mechanical form of increasing the density by a liquid. As illustrated by Wang et al. and Zhong et al. the strength can be improved up to ten times by rolling the yarn [15] [16].

4.2.2 Wet spinning

Wet spinning, also referred to as co-agulation spinning, existed before the method was implemented to spin a CNT yarn. The method is used for making Kevlar, acrylic, and poly(acrylonitrile) (PAN) fibers [14]. Therefore it is no surprise that this method was the first to be used to spin a CNT yarn. In 2000 Vigolo et al. succeeded to implement the wet spinning technique to form a CNT yarn [18]. The method that is used can be explained with the help of figure 4.6. For this particular process of wet spinning single walled CNTs, produced with the arc-discharge method, were used. The SWNTs were dispersed in an aqueous solution containing sodium dodecyl sulfate (SDS) using an ultrasonic bath. When a homogeneous dispersion was obtained, the suspension was injected in a co-flowing stream of polymer solution containing 5 wt% polyvinylalcohol (PVA). This was done by using a syringe needle with a diameter of 0.5 mm at a rate of 10 to 100 ml per hour. PVA is presumed to replace some SDS molecules on the walls of the CNTs and since PVA, unlike SDS, does not provide an efficient stabilization against van der Waals attractions the CNTs will start to contract. This way a CNT gel is formed which can be collected and pulled out of the PVA solution. When properly washed, dried and spun a pure CNT yarn is formed.

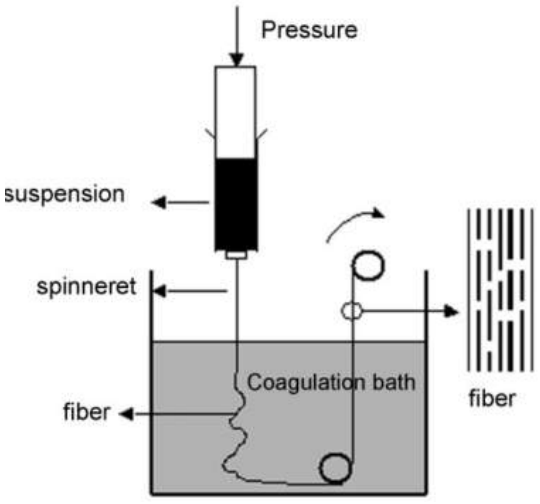

Figure 4.6: Schematic image of a typical setup as used for the wet spinning process. Reprinted from Zhang et al. [17].

Once discovered this method is adjusted by using different chemicals as well. Thereby the process could be made easier, faster or more accessible. Also the quality of the yarn could be improved by changing the chemicals that are used.
Dalton et al. noticed that the spinning process invented by Vigolo et al. was rather slow (about 1 cm per minute) and the yarns where short (only 10 cm). Furthermore it is mentioned that the gel created when the suspension is injected into the VPA is weak and hard to handle [19]. Therefore some adjustments are made to obtain a process that is easier to handle and resulting in a stronger (1.8 GPa) yarn with a Young's Modulus of 80 GPa [20]. The main adjustments are the use of Lithium Dodecyl Sulfate (LDS) as the surfactant instead of SDS and the method for injecting is different. With the modified method the suspension is injected in the center of a cylinder in which a co-flowing stream of VPA flows. The final yarn consist for about 60% in weight of SWNTs and has an

average diameter of 50 μm. The other 40% of the weight consist of VPA which has the function of keeping the CNTs together by Van Der Waals forces. Besides, the VPA chains are responsible for an highly efficient load transfer over the yarn, which enhances the mechanical properties.
Because VPA is embedded in the CNT yarn its thermal and electrical conductivity is not high, especially not when compared to the conductivity of individual CNTs. To solve that problem another noteworthy study about CNT wet spinning is done by Ericson et al. [21]. The process is said to be industrially viable. The first step is dispersing 8 wt% of SWNTs in 102% sulfuric acid (2 wt% excess SO_3). Even the smallest amount of moist into the suspension could cause phase separation and disrupt the homogeneity. After sufficient mixing the suspension is injected into a bath of diethyl ether, 5 wt% aqueous sulfuric acid or water to form the yarn. In case of the diethyl ether coagulation bath the resulting yarn dried quickly and all diethyl ether evaporated, leaving a yarn from only CNTs. With these surfactant and coagulation liquid a yarn of about 30 meter could be obtained with a diameter of 50 μ. The Young's Modulus is about 120 GPa and tensile strength is around 116 MPa. The ether coagulated yarn possess a low electrical resistivity of $2 \cdot 10^{-6}$ Ωm, while the polymer containing yarn by Vigolo et al. has a resistivity of 10^{-3} Ωm.
An important disadvantage of the previous method is the use of the sulfuric acid. It can be dangerous to work with and regular industrial equipment might be damaged with prolonged contact time of the acid. Therefore a method by Zhang et al. [17] is proposed where no acid is used. Instead ethylene glycol is used as medium to form a liquid crystalline dispersion with. The homogeneous suspension was injected into a diethyl ether bath using a syringe needle of 130 μm in diameter. Upon entering the ether bath, the ethylene glycol rapidly diffuses out of the extruded nanotube fiber into the ether bath. Simultaneously the ether is back-diffusing into the fiber, resulting in a ether swollen yarn. As for the study of Ericson et al., the ether as well as remaining glycol was evaporated by heating the yarn up to 280 °C. The Young's Modulus from the yarn from MWNTs was 69$\pm$41 GPa. The resistivity was measured to be $1.25 \cdot 10^{-4}$ Ωm.

Advantages of wet spinning are that it is relatively easy and allows a wider range of CNT morphology when compared to dry spinning. Besides, not much additional equipment is needed for the spinning process itself. A drawback would be that the resulting yarn is often impregnated with polymers, reducing its conductivity and possible its tensile strength as well. Longer CNTs tend to be difficult to disperse homogeneously and as can be seen in figure 4.5 this results in general to a poor quality yarn.

4.2.3 Direct spinning

Both aforementioned methods, dry spinning and wet spinning, relied on post processing methods after the growth of CNTs. The principle of direct spinning is based on CNT growth and spinning simultaneously. The method is first mentioned by Zhu et al. [22], where a vertically placed tubular CVD oven is used. Hydrogen functions as a carrier

gas during the growth process. Furthermore a solution of n-hexane with a specific composition of 0.018 g/ml ferrocene and 4 wt% thiophene is pyrolyzed in the oven. The ferrocene functions as catalyst particles and the carbon atoms are supplied by the hexane. This way CNTs grow while falling downwards and clustering together. This method will form strands of about 20 cm long and about 0.3 mm in diameter. Smaller yarns of about 50 μm in diameter can be obtained by peeling them off from the strands. The properties of the resulting yarns are excellent with a strength of 1 GPa, a Young's Modulus of 100 GPa and a resistivity between 5 and $7 \cdot 10^{-6}$ Ωm. The process of forming the 20 cm long strands is shown in figure 4.7a.
Improvements on this process are made by Li et al [23]. Instead of forming strands CNT bundles are actively pulled out of the oven as they grow. The vertical oven where a clustered so called 'sock' or aerogel of CNTs is formed. The sock will be formed slowly and moves towards the open end of the tube. Without manual correction the sock will stick onto the wall and form a membrane across the tube once the cool (500 °C) open part is reached. However, instead of letting the membrane form, the aerogel is drawn by a mechanical winder with a same speed at which the CNTs are formed. The process is schematically shown in figure 4.7b. Although the mechanical properties of the resulting yarn are comparable with what was reached by Zhu et al., an extraordinary low resistivity of $1.2 \cdot 10^{-6}$ Ωm is reached.

Although the quality of the yarn measured by its strength, stiffness and conductivity are relatively high as reached with direct spinning, a drawback could be that a modified CVD oven is required. Furthermore, the process parameters are hard to tune. For example, increasing the growth time is impossible without changing the gas flows since the aerogel will reach the end of the tube as it is carried by the gas. Therefore it would be difficult to improve on this method by improving the length or quality of the grown CNTs.

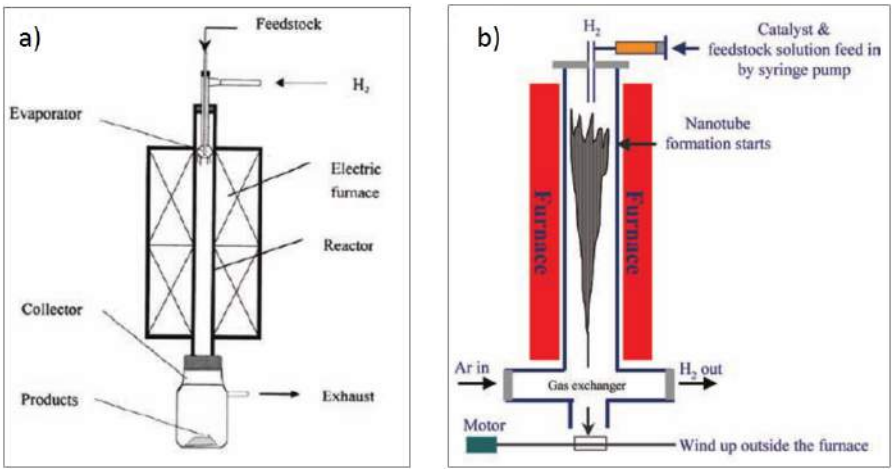

Figure 4.7: a) shows a schematic illustration of the system as used by Zhu et al. to form 20 cm long CNT strands. Figure from [14]. b) shows an illustration of direct spinning from aerogel as described by Li et al. Reprinted from Motta et al. [24].

4.3 Conclusion

It is found that the method of dry spinning is the most accessible since basic materials can be used. For the direct spinning method the CVD oven should be adapted, making the method less favored by research groups with CNT growth experience in a particular system. Furthermore, the method of wet spinning requires the use of chemicals, while for dry spinning only a pair of tweezers are necessary. Another important disadvantage of wet spinning is that the resulting yarn will be contaminated with the chemicals, reducing its electrical properties.
In terms of the mechanical properties of the resulting yarns dry spinning is favored as well, since the highest tensile strength is reached with this method. The reason a high quality yarn can be spun with dry spinning is that the CNTs can be tunes during the growth process. In general the worst mechanical properties are obtained with wet spinning.

References

[1] K. Jiang, Q. Li, and S. Fan, "Nanotechnology: spinning continuous carbon nanotube yarns.," *Nature*, vol. 419, no. 6909, p. 801, 2002.

[2] X. Zhang, K. Jiang, C. Feng, P. Liu, L. Zhang, J. Kong, T. Zhang, Q. Li, and S. Fan, "Spinning and processing continuous yarns from 4-inch wafer scale super-aligned carbon nanotube arrays," *Advanced Materials*, vol. 18, pp. 1505–1510, 2006.

[3] C. P. Huynh and S. C. Hawkins, "Understanding the synthesis of directly spinnable carbon nanotube forests," *Carbon*, vol. 48, no. 4, pp. 1105–1115, 2010.

[4] C. Jayasinghe, "Spinning yarn from long carbon nanotube arrays," *Journal of Materials Research*, vol. 26, no. 5, pp. 645–651, 2011.

[5] X. Zhang, Q. Li, Y. Tu, Y. Li, J. Y. Coulter, L. Zheng, Y. Zhao, Q. Jia, D. E. Peterson, and Y. Zhu, "Strong carbon-nanotube fibers spun from long carbon-nanotube arrays.," *Small*, vol. 3, pp. 244–248, Feb. 2007.

[6] A. Ghemes, Y. Minami, and J. Muramatsu, "Fabrication and mechanical properties of carbon nanotube yarns spun from ultra-long multi-walled carbon nanotube arrays," *Carbon*, vol. 50, no. 12, pp. 4579–4587, 2012.

[7] L. Zheng, G. Sun, and Z. Zhan, "Tuning Array Morphology for High-Strength Carbon-Nanotube Fibers," *Small*, vol. 6, no. 1, pp. 132–137, 2010.

[8] A. F. Gilvaei, K. Hirahara, and Y. Nakayama, "In-situ study of the carbon nanotube yarn drawing process," *Carbon*, vol. 49, pp. 4928–4935, Nov. 2011.

[9] Y. Inoue, K. Kakihata, Y. Hirono, T. Horie, A. Ishida, and H. Mimura, "One-step grown aligned bulk carbon nanotubes by chloride mediated chemical vapor deposition," *Applied Physics Letters*, vol. 92, no. 21, 2008.

[10] X. Lepró, M. Lima, and R. Baughman, "Spinnable carbon nanotube forests grown on thin, flexible metallic substrates," *Carbon*, vol. 48, pp. 3621–3627, Oct. 2010.

[11] J. J. Vilatela, J. A. Elliott, and A. H. Windle, "A Model for the Strength of Yarn-like Carbon Nanotube Fibers," *ACS Nano*, vol. 5, no. 3, pp. 1921–1927, 2011.

[12] M. Miao, "Yarn spun from carbon nanotube forests: Production, structure, properties and applications," *Particuology*, vol. 11, no. 4, pp. 378–393, 2013.

[13] Q. Li, X. Zhang, and R. DePaula, "Sustained growth of ultralong carbon nanotube arrays for fiber spinning," *Advanced Materials*, vol. 18, no. 23, pp. 3160–3163, 2006.

[14] W. Lu, M. Zu, J.-H. Byun, B.-S. Kim, and T.-W. Chou, "State of the art of carbon nanotube fibers: opportunities and challenges.," *Advanced materials*, vol. 24, pp. 1805–1833, Apr. 2012.

[15] J. Wang, X. Luo, T. Wu, and Y. Chen, "High-strength carbon nanotube fibre-like ribbon with high ductility and high electrical conductivity," *Nature communications*, pp. 1–8, 2014.

[16] X.-H. Zhong, Y.-L. Li, J.-M. Feng, Y.-R. Kang, and S.-S. Han, "Nanoscale Fabrication of a multifunctional carbon nanotube cotton yarn by the direct chemical vapor deposition spinning process," *Nanoscale*, vol. 4, pp. 5614–5618, 2012.

[17] S. Zhang, K. K. K. Koziol, I. a. Kinloch, and A. H. Windle, "Macroscopic fibers of well-aligned carbon nanotubes by wet spinning," *Small*, vol. 4, no. 8, pp. 1217–1222, 2008.

[18] B. Vigolo, a. Pénicaud, C. Coulon, C. Sauder, R. Pailler, C. Journet, P. Bernier, and P. Poulin, "Macroscopic fibers and ribbons of oriented carbon nanotubes.," *Science (New York, N.Y.)*, vol. 290, no. 5495, pp. 1331–1334, 2000.

[19] A. B. Dalton, S. Collins, J. Razal, E. Munoz, V. H. Ebron, B. G. Kim, J. N. Coleman, J. P. Ferraris, and R. H. Baughman, "Continuous carbon nanotube composite fibers: properties, potential applications, and problems," *Journal of Materials Chemistry*, vol. 14, no. 1, pp. 1–3, 2004.

[20] A. B. Dalton, S. Collins, J. M. Razal, and V. Howard, "Super-tough carbon-nanotube fibres," *Nature communications*, vol. 423, p. 703, 2003.

[21] L. M. Ericson, H. Fan, H. Peng, V. A. Davis, W. Zhou, J. Sulpizio, Y. Wang, R. Booker, J. Vavro, C. Guthy, A. N. G. Parra-vasquez, M. J. Kim, S. Ramesh, R. K. Saini, C. Kittrell, G. Lavin, H. Schmidt, W. W. Adams, W. E. Billups, M. Pasquali, W.-f. Hwang, R. H. Hauge, J. E. Fischer, and R. E. Smalley, "Macroscopic , Neat , Single-Walled Carbon Nanotube Fibers," *Science*, vol. 305, pp. 1447–1451, 2004.

[22] H. W. Zhu, C. L. Xu, D. H. Wu, B. Q. Wei, R. Vajtai, and P. M. Ajayan, "Direct synthesis of long single-walled carbon nanotube strands.," *Science*, vol. 296, no. 5569, pp. 884–886, 2002.

[23] Y. Li, I. Kinloch, and A. Windle, "Direct spinning of carbon nanotube fibers from chemical vapor deposition synthesis," *Science*, vol. 276, no. 2004, 2004.

[24] M. Motta, A. Moisala, I. a. Kinloch, and A. H. Windle, "High performance fibres from 'dog bone' carbon nanotubes," *Advanced Materials*, vol. 19, no. 21, pp. 3721–3726, 2007.

Chapter 5

Systematic study of CVD oven conditions for high quality CNT forest growth

Abstract

It is found that growing CNTs can yield results of bad quality or non-reproducible results when unfamiliar with the process. In this study CNT arrays are grown in a tubular CVD oven and errors leading to undesired results are identified. It is found that the errors can be divided into three groups, namely system, condition or operation errors. System errors are easily verified and consist of leakages, limited purity of gases, inadequate recipes or turbulence in the system. In contrast, condition errors are hard to detect but can severely affect the quality of the arrays. Humidity in the oven, contamination during cleaning and no preheating of the oven belong in this category. Finally, results are also affected if operation errors exist. It is discussed to what extent variation in gas flows, sample location in oven and variation in annealing time can deteriorate results. Finally, due to differences between individual substrates, the CNT forest height and quality will differ even if all other errors are removed.

5.1 Introduction

Nowadays countless research groups have succeeded in growing Carbon Nanotubes, both as individual tubes and as forests. Therefore it seems that the growth of CNTs is very well controlled and easy to imitate by research groups new to the field. However, if a regular tubular Chemical Vapor Deposition (CVD) oven is used there can be some pitfalls. In literature little can be found about bad quality or non-reproducible results when growing CNTs in a tubular CVD oven or the use of CVD in general. Neither is information about disturbing factors ruining CNT growth available.
As found in this study the results of growing CNTs can be variable and non-reproducible if an improper procedure is used or no attention is paid to the operating conditions of the CVD oven. Varying results can even be the case when the exact same amount of gas flows are used throughout the growth process, as indicated by figure 5.1. This study investigates why these differences occur and how high quality and reproducible CNT forests can be grown when new to the field of CNT growth.

5.2 Materials and methods

The oven used for this study is shown schematically in figure 5.2. The oven is used at atmospheric pressure and the precursor gases used for the growth of CNTs are argon, hydrogen and ethylene. The gases are supplied by Linde with a purity of 99.9% for the hydrogen and argon, while the ethylene (C_2H_4) has a purity of 99.5%. Unless stated otherwise the growth recipe used throughout the study consist of 400 sccm argon, 400 sccm hydrogen and 200 sccm ethylene. A full description of the growth procedure is written in the supplementary materials. Also aspects on safety during CNT growth are mentioned in the supplementary materials. The growth temperature was 750 °C while the growth time was always kept at 10 minutes. Furthermore, before the actual growth

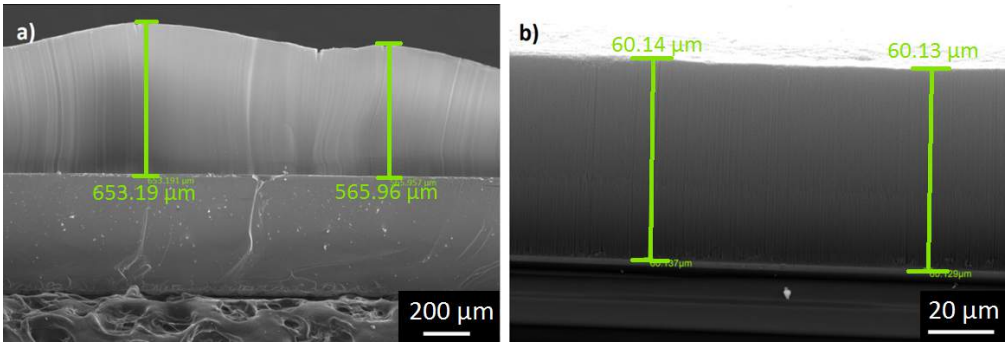

Figure 5.1: Side view of forests that are grown using the same gas flows and times during their growth processes. However, the results differ substantially with the CNT forest of a) having a maximum height of about 650 micron, whereas the forests of b) is only about 60 micron tall.

step the oven was flushed with 600 sccm argon for the first 5 minutes while heating up. Then the oven was flushed with 400 sccm hydrogen, while the temperature continue to ramp up to the final temperature. It took the oven about 8 minutes to reach 750 °C. A clear overview of the gases and temperatures during the entire growth process is shown in figure 5.3.

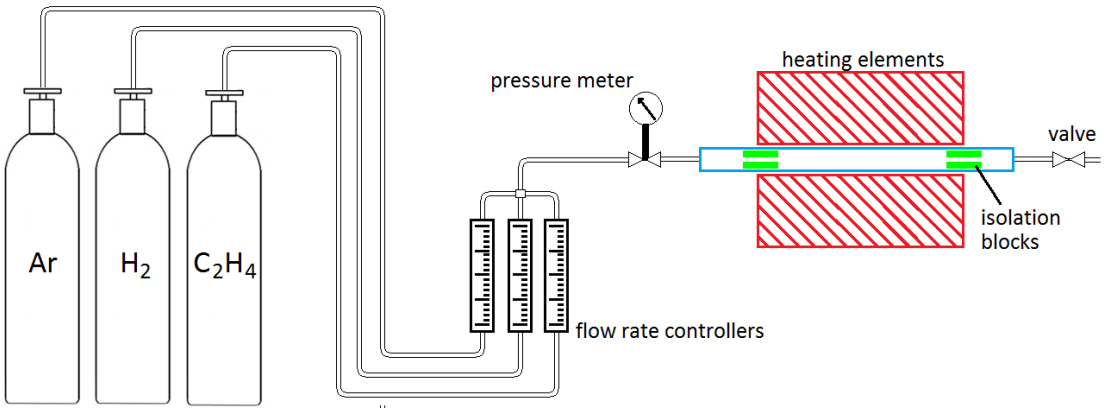

Figure 5.2: A schematic figure of the CVD oven that is used for CNT growth throughout this study.

The growth of the CNT forests was done on substrates of silicon wafer on which 10 nm alumina (Al_2O_3) is sputtered. For the catalyst layer on top of the diffusion barrier three thicknesses were used that were put in the oven simultaneously for all conducted experiments. The thicknesses of the Fe catalyst layers were 1 nm, 2 nm and 5 nm. These layers were evaporated onto the surface of the alumina. All substrates used for CNT growth where cut into pieces of about 0.5 by 0.5 cm.

Stage	Gases	Rate (sccm)
1	Argon	600
2	Hydrogen	400
3	Argon	400
	Hydrogen	400
	Ethylene	200
4	Argon	600

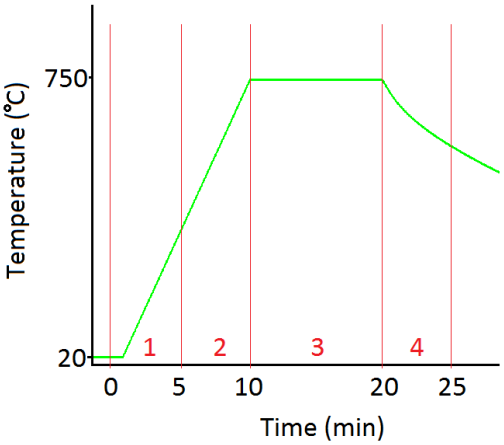

Figure 5.3: The table on the left provides an overview of the gas flow rates during the different stages of the growth process. The figure on the right shows the temperature and duration of each stage. The red numbers represent the particular stage. Stage 1 is preflushing with argon and stage 2 is removing oxides from the substrate with hydrogen. Stage 3 is the actual growth step and the final step is post-flushing with argon.

5.3 Results and discussion

In order to find the most important parameters that could potentially lead to non-reproducible results or short forests of bad quality, a list with possible disturbing factors was initially suggested. Within this study these factors were verified by carrying out different experiments. Some parameters that were initially suspected of potentially causing results to be unsatisfactory turned out to be harmless, while other parameters are indeed found to prevent the growth of a high-quality tall forest. For convenience table 5.1 provides an overview of possible disturbances and is divided in three types of errors. Errors in the CVD system itself are mentioned in the left column, errors that depend on specific conditions of the oven in the column in the center and the right column contains errors that could harm CNT growth during operation of the oven. When problems in reproducibility of CNT growth occur, it is recommended to first run some simple tests to rule out any errors within the system. Operation errors can be avoided simply by keeping all controllable parameters such as gas flows and sample location in the oven the same. It is advisable to look carefully to the condition dependent errors, as these are hard to notice but can have a severe impact on the results.

Table 5.1: The parameters in the left column can be considered first when no reproducible and/or desired results can be obtained as they are easy to verify. The column in the middle shows the condition dependent errors which can affect the results the most severely and are hard to notice. The right column contains the operation errors which are easily prevented with careful operation of the CVD oven.

System errors	**Condition errors**	**Operation errors**
Leakages	Humidity in the oven	Variation in gas flows
Limited purity gases	Contamination of cleaning	Growth location in oven
Inadequate recipe	No preheating of oven	Variation in annealing time
Turbulence in system		

5.3.1 System errors

When only short forests were grown with largely defective CNTs, some simple checks were done to ensure no contaminants enter the system during growth. Besides the possibility of entering contaminants and although improbable, turbulent gas flows might have prevented the growth of high quality CNT forests. These possible disturbances could be verified easily, so before other types of errors were investigated these tests were performed to ensure that the system was in principle capable of growing CNTs. Temperature and pressure were directly measured and kept constant during growth.

- The first check to verify the state of the system was checking for any leakages. This was done by increasing the gauge pressure in the oven tube to 50 kPa. After 48 hours the pressure meter did not show any visual difference. It could therefore be assumed that no leakages are present in the system.

- Furthermore it was verified of the impurity of the gases were not substantially high. The purity provided originally was 99.5% for all three gases. A study by In indicates that higher levels of purity are even undesirable, as a small amount of water particles is needed for the growth of CNT forests [1]. Furthermore, the gas bottles were delivered and installed at the beginning of the study, so it is presumed purity is still as ordered.

- Although it has been found that multiple recipes (combinations of specific gas mixtures, timing and temperatures) are capable of growing CNTs any random combination is not likely to yield CNT growth. It should therefore be ensured that a viable growth recipe is being operated. However, such a recipe is different for each type of oven, diameter of the oven tube and gases that are used. Therefore no general statements can be made, but an overview of viable recipes from different research groups is shown in the supplementary materials. For this study a recipe for CNT array growth was found gradually after several experiments and adjustments to gas flow rates, as shown in figure 5.4.

- As a final check before looking into condition dependent or operation errors the flow condition was verified. Turbulence has to be avoided in the CVD oven to obtain repeatable results. Since the flow during the CNT growth process is a mixture of several gases, calculating the Reynolds number is difficult. If the entire flow is assumed to be the least viscous gas, hydrogen in this case, a Reynolds number of about 50 can be calculated, as shown in the supplementary Materials. For the calculation of an actual gas mixture is referred to [2].

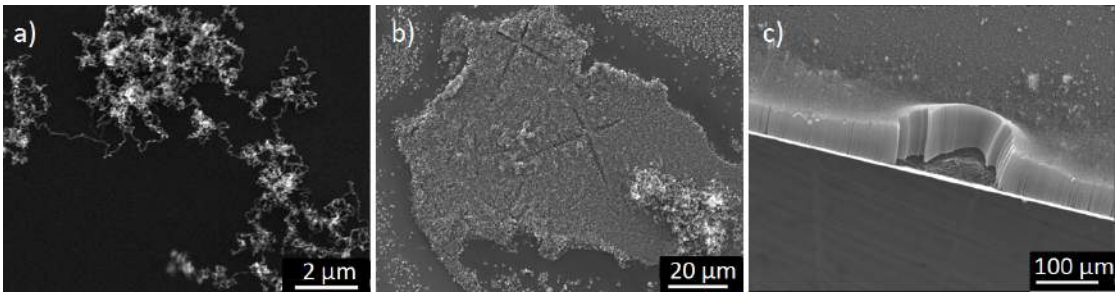

Figure 5.4: This figure contains the progress made towards a viable recipe in chronological order. Figure a) is grown using 50 sccm C_2H_4, 400 sccm H_2 and 800 sccm Ar, whereas b) was grown using 100 sccm C_2H_4, 400 sccm H_2 and 400 sccm Ar and c) had gas flows of 150 sccm C_2H_4, 400 sccm H_2 and 400 sccm Ar.

5.3.2 Condition errors

Although the recipe was kept exactly the same and system errors were ruled out, it was found that results still varied. Three parameters could be identified which caused severe reductions in quality of resulting forests. These parameters together, humidity, contamination of and preheating, determine the condition of the inside of the oven. Also, they are closely linked to one another. For example by preheating the oven before starting the CNT growth processes not only is humidity in the oven largely reduced, but virtually any form of contamination is burned as well. Preheating the oven was done by ramping up the oven to 750 °C with the tube filled with a mixture of argon and hydrogen. At 750 degrees the oven is flushed with argon for 5 minutes and then cooled down to below 500 °C. After cooling down the samples were loaded into the oven and the growth procedure was initiated.

A decline in quality of the results might be caused by uncontrolled humidity in the oven. It is well known that a small amount of water vapor can improve growth results [3] [4] [5] [6]. Typical values for the amount of water used during growth are 150 ppm. However, air at atmospheric pressure and room temperature typically contains about 10-20 grams water per kg air, which comes down to 10.000 to 20.000 ppm. This is a factor 100 higher than typical values used for water assisted CNT growth. It comes to no surprise that this high amount of water vapor holds back proper growth. Therefore the humidity in

the oven should be reduced prior to growing CNTs. This can either be done by excessive flushing of Argon or by simply preheating the oven in combination with moderately flushing. The effects of preheating the oven is discussed later.

The second condition error is the contamination induced by cleaning. This error might be unexpected and paradoxical. It was found that after cleaning the tube of the oven every first attempt of growing a CNT forest failed when not properly preheated. Typically no CNTs grew at all, with the exception of some very locally grown ones. Incidentally short forests grew with typical lengths in the order of 20 microns. However, the second time growing better results were obtained again without preheating the oven prior to the CNT growth. The differences are shown in figure 5.5. The reason that in general the first run does not yield any noteworthy results might be due to two different factors. First, after cleaning, dust particles of the cleaning tissue and moisture from the air might attach to the inside wall of the tube. Second, the gas inlet and outlet piping are exposed to air during cleaning which might humidify and contaminate the piping. More information about the cleaning procedure is provided in the supplementary materials.

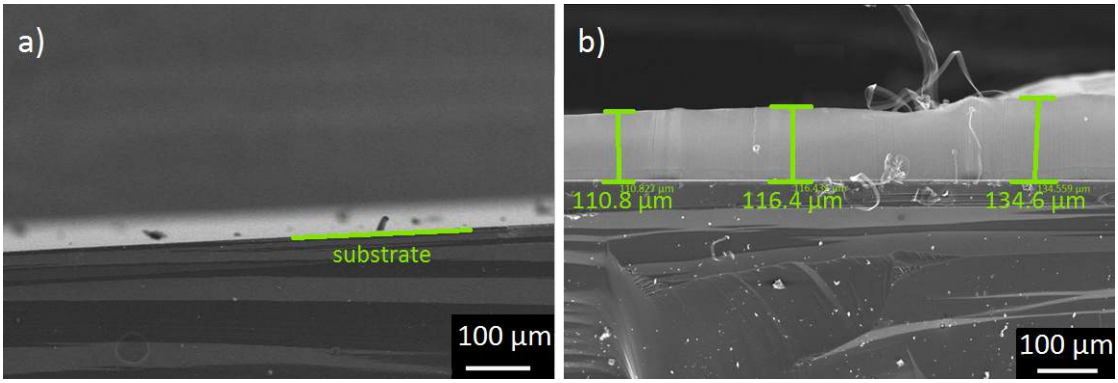

Figure 5.5: In general a clear difference exists between forests grown directly after cleaning the oven as shown in a) or after three uses when cleaned as shown in b). Both pictures are taken from the side of the sample. The left sample did not grow a CNT forest, whereas the right sample produced a CNT forest with a height of about 120 microns.

The final factor that prevents the reproducible growth of a tall CNT forest is whether or not the oven is preheated. It has become clear that humidity or contaminants can severely disturb forest growth. One way of removing these factors effectively is by preheating the oven. As mentioned earlier the oven is ramped up to 750 degrees under a moderate flow of hydrogen or argon. At this temperature water molecules are evaporated and thereby removed from the walls of the tube. Besides, contaminating particles like dust are likely to be decomposed and swept away with the gas flow.

Although the removal of water molecules is reason enough to preheat the oven, there seems to be another effect of preheating that enhances CNT growth. It was found that

the wall of the tube did not accumulate any amorphous carbon (a-c) when preheated, while without preheating enough a-c was accumulated that the tube had become black and opaque after only a few growth experiments. It is presumed that the quartz tube takes a longer time to heat up and is still cold during CNT growth if not properly preheated. The carbon radicals will therefore condense onto and stick to the relatively cold wall. As a consequence there are less carbon radicals available for CNT growth thereby stagnating the process. The importance of preheating the oven is probably best illustrated by figure 5.6 where a forest of about 300 microns is grown directly after cleaning the oven and preheating step. Compared to earlier results after cleaning the oven without preheating as shown in figure 5.5a the results with preheating are clearly more desirable.

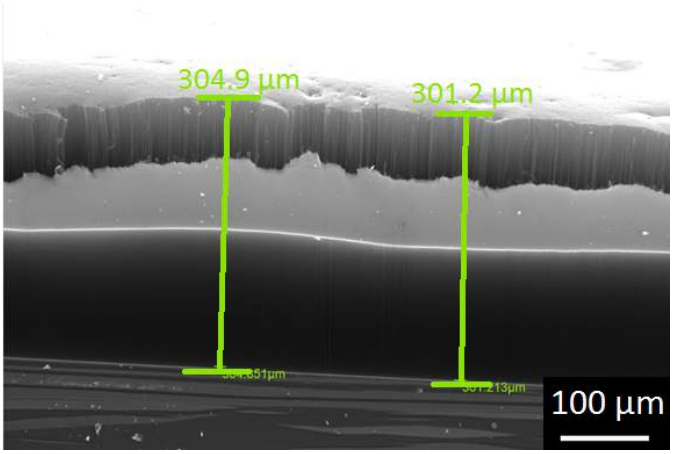

Figure 5.6: A CNT forest is grown directly after cleaning the oven and a preheating step. The forest is about 300 microns high.

5.3.3 Operation error

The next three parameters are well within the control of the operator of the CVD oven. However, if not carefully monitored during an experiment results might vary even if the parameters earlier mentioned in this paper are kept the same. In principle these operation errors will not occur. Therefore they are merely discussed to provide insight in their degree of influence on final results such as forest height and CNT quality.
The first parameter may not prevent the growth of a CNT forest altogether but will most certainly influence the forest height that will be achieved is the location of the substrate in the oven. On the front of the quartz tube the gases will still need to reach the required temperature and depending on flow rates and type of inlet the gas flows still need to get settled. In contrast, downstream at the end of the tube the gases are settled and at the same temperature as the oven. So depending on the location of the substrate it will be exposed to another amount of carbon radicals in different flow conditions. It should therefore be noted that placing the substrate on the utmost front of the oven

will most likely not result in a CNT forest, since the carbon containing precursor is not reactive. This is shown in figure 5.7 where the difference of CNT forests grown on different locations in the tube is visualized. It is clearly visible that, although the substrate is covered with CNTs, no real forest grew on the front of the oven tube. In the center of the tube forests start to appear. Nucleation of CNT forests has initiated at multiple location but these sites have not agglomerated into a smooth forest. At the back of the oven, however, the CNT forest start to take shape. From the figure it can be concluded that the most ideal spot to grow is in the back of the oven. The reason is presumably the more constant conditions due to settling and heating of the gas, which will result in a more constant supply of carbon radicals.

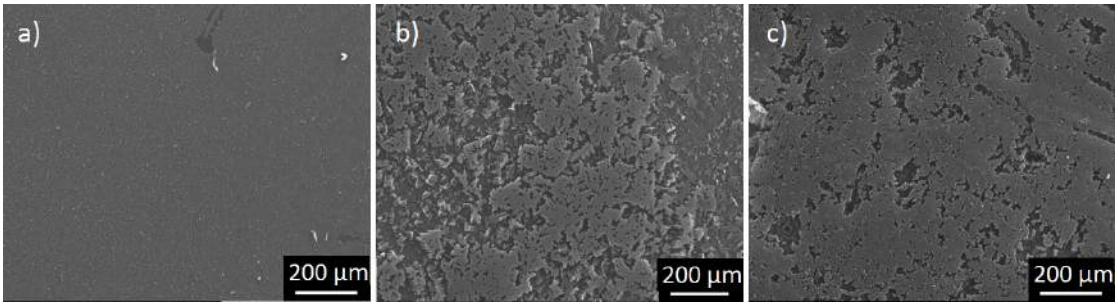

Figure 5.7: Top view from different forests grown on different locations of the tube. The forest of a) is placed 4 cm into heated part, the forest in b) is grown in the center and c) at 4 cm from the back of the heated part of the oven tube.

As for the location of the substrate in the oven, the annealing time of the samples will not be varied on purpose if repeatable results are desired. However, it is found that even relatively small changes in annealing time could potentially prevent the growth of a CNT array. The annealing time is defined in this study as the time between stage 2 and stage 3 of figure 5.3. The temperature is at 750 °C and the gas flow consist of 400 sccm hydrogen. As is shown in figure 5.8 an annealing time of only 5 minutes caused the CNT forest to grow on the 5 nm Fe catalyst layer instead of on the 2 nm Fe layer. It can be seen that the longer the annealing time, the better a CNT forest grows on thicker catalyst layers. It seems that even for the regular case (upper row), without annealing time and only heating up to 750 °C, is too much to grow a forest on the 1 nm Fe catalyst layer. When the annealing time is elongated by 5 minutes a CNT array no longer grows on the 2 nm as well. This phenomenon can be explained by the dynamics of the catalyst layer at elevated temperatures. Because the layer is so thin, Ostwald ripening will tear the layer apart at sufficient high temperatures. Initially small islands, also called catalyst particles or quantum dots, will form. As the temperatures remain high enough these catalyst particles will cluster together to eventually form clusters incapable of sustaining CNT growth.
Both results, with or without annealing time, where verified at least five times and in all cases results were in agreement with figure 5.8. However, it should be noted that the effect of annealing was not visible when grown at a temperature of 650 °C using the

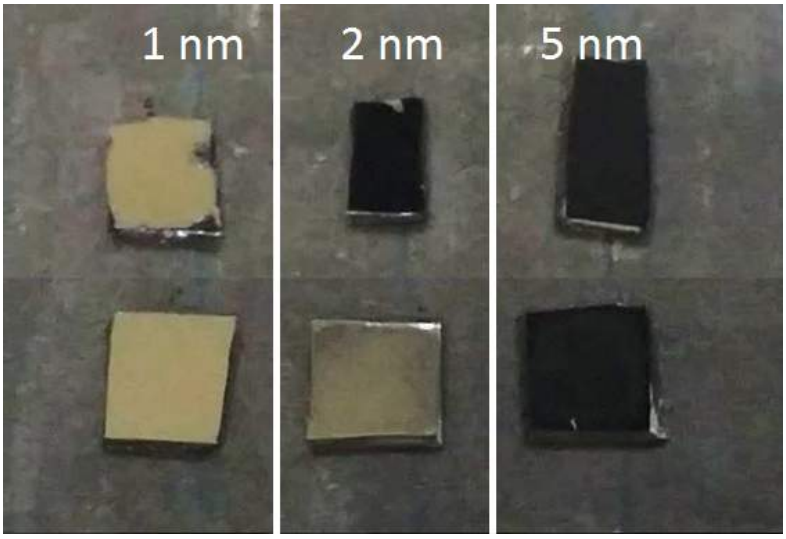

Figure 5.8: Photograph of the top view of samples grown with different annealing times. The upper row is grown without annealing time, while the samples on the bottom row are grown with an annealing time of 5 minutes. The numbers above indicate the according thickness of the Fe catalyst layer. The samples are about 0.5 by 0.5 cm.

AIXTRON Black Magic PECVD system. Samples where first annealed at 750 °C for at least five minutes, while others were grown without annealing time. When these samples were then grown in the AIXTRON Black Magic PECVD system, no clear differences were visible as is shown in figure 5.9. According to the results of figure 5.8, no forest or substantial shorter forest should have grown on the substrate of figure 5.9b. The differences between the procedures of both figures is growth recipe and the fact that the results of 5.9 were cooled between annealing and growth. In conclusion the differences in results are due to the lower growth temperature in the AIXTRON Black Magic PECVD system or due to the cool down of the samples between annealing and growth.

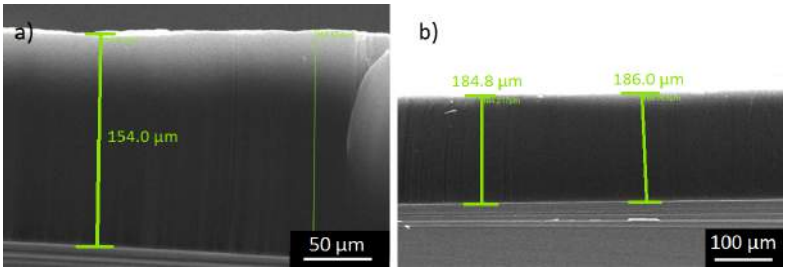

Figure 5.9: Figure 5.9a shows the side view of a forest grown on 2 nm without annealing, while figure 5.9b is the side view of a forest grown on 2 nm after 4 minutes annealing. Forest lengths are about 160 microns and 185 microns, respectively.

As a final remark on possible varying results after CNT growth, it was found that it could be difficult to keep the flow rates constant. The use of variable area flow meters is accurate as long as they are operated in conditions (the temperature and pressure) they are calibrated for. Furthermore they should be operated around at least the regime where the float stays in the center of the total range. In that case the error in percentages of the total flow rate is relatively small.

5.3.4 Differences between samples

Even if all errors for bad results are solved or prevented and the growth procedure is handled exactly the same, the results between the one growth experiment and the other will still be different. Results will not vary from no growth at all to a high quality long forest, but differences in forest height will be well visible. The cause for this non-reproducibility is differences between individual substrates. This cause does not fit in table 5.1 as it is not an error that can be prevented in any way. Still it is worthwhile mentioning, since variation in results from experiment to experiment will occur because of this.

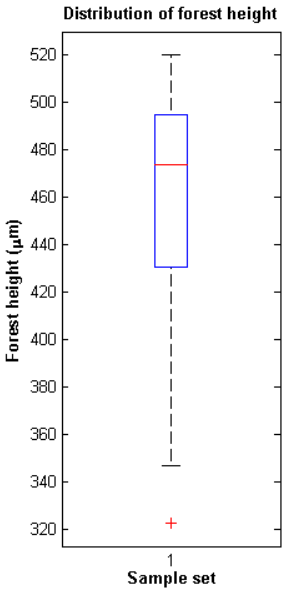

Figure 5.10: Simplified representation of the distribution of forests height over the 24 different samples shown in a boxplot.

When the substrates are prepared and alumina is sputtered on the silicon the thickness will not always be the same. In our case this is even more relevant for the catalyst Fe layer, which reaches an approximate thickness of 1 nm in a matter of seconds. Therefore it is difficult to prepare a substrate with the exact same thickness all over the wafer. To indicate the effect a different thickness of diffusion barrier can have, figure 5.11 shows a forest grown on a sample with two alumina thicknesses. The difference in thickness is done here on purpose and will not nearly be as explicit when a smooth layer is intended, but the small variations that are present over the whole wafer will affect the forest height to a certain extend. Furthermore, not every sample will be exactly as clean as another. Finally minor scratches might be present on samples, which could deteriorate the forest growth to a certain level. To show the effect multiple substrates are placed in the AIXTRON Black Magic PECVD system simultaneously and forest of about the same height are grown. Differences in forest height can only be due to differences of substrates, since the growth conditions are the same over the entire sample holder. To give an impression of the distribution in forest height of the 24 samples a boxplot is shown in figure 5.10.

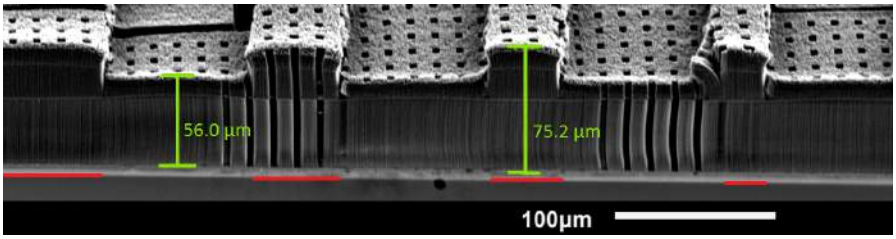

Figure 5.11: The parts of the substrate indicated with red contain a 20 nm alumina layer, whereas the other parts are only equipped with a 10 nm diffusion barrier. It is clearly visible that this difference in alumina layer results in a difference in forest height. The holes in the forest are due to patterning of the Fe catalyst layer.

5.3.5 Quality of reliably grown CNT arrays

When keeping the CNT growth procedure free from the controllable errors described above, high quality forest could be grown repeatedly. The forest is said to be of high quality when the CNT contain a low amount of defects, which corresponds to straight bundles, and there should be little or no amorphous carbon on the wall of the nanotubes. Both are investigated to verify the quality of the array. The side from a typical forest is shown in figure 5.12a. It can be clearly seen that straight CNT bundles have formed. Almost no curved bundles can be identified and the side of the array contain only few irregularities. The straightness of the bundles indicates a low amount of defects, which in turn suggests suitable growth conditions.

The other indicator for the quality of the CNT forest is amorphous carbon on the sidewall of individual CNTs. This indicator can only be quantitatively verified using TEM. Figure 5.12 b) shows such an image. The edges of the CNTs are clearly visible and show almost no amorphous carbon. With these results it can be concluded that the forest is of high quality.

5.4 Conclusion

In conclusion, problems that can occur during the growth of vertically aligned CNT arrays can be categorized in three types of errors. The first type of errors involves the system itself and consist of leakages, limited purity of gases that are used, inadequate growth recipe, or turbulence in the system. It is found that leakages are easy to detect by pressurizing the oven. It is unlikely that a limited purity of the gases reduce the quality of the results. On the contrary, some amount of impurity is even proved to enhance CNT growth. It is also improbable that turbulence occurs in the system, yet it might be useful to keep in mind when results are of insufficient quality. If the recipe is in principle capable of growing CNTs, the system itself is suitable of high quality forest growth.
The next type of error involves condition errors, which are hard to detect. Both humidity and any other forms of contamination can be reduced if not removed by preheating the

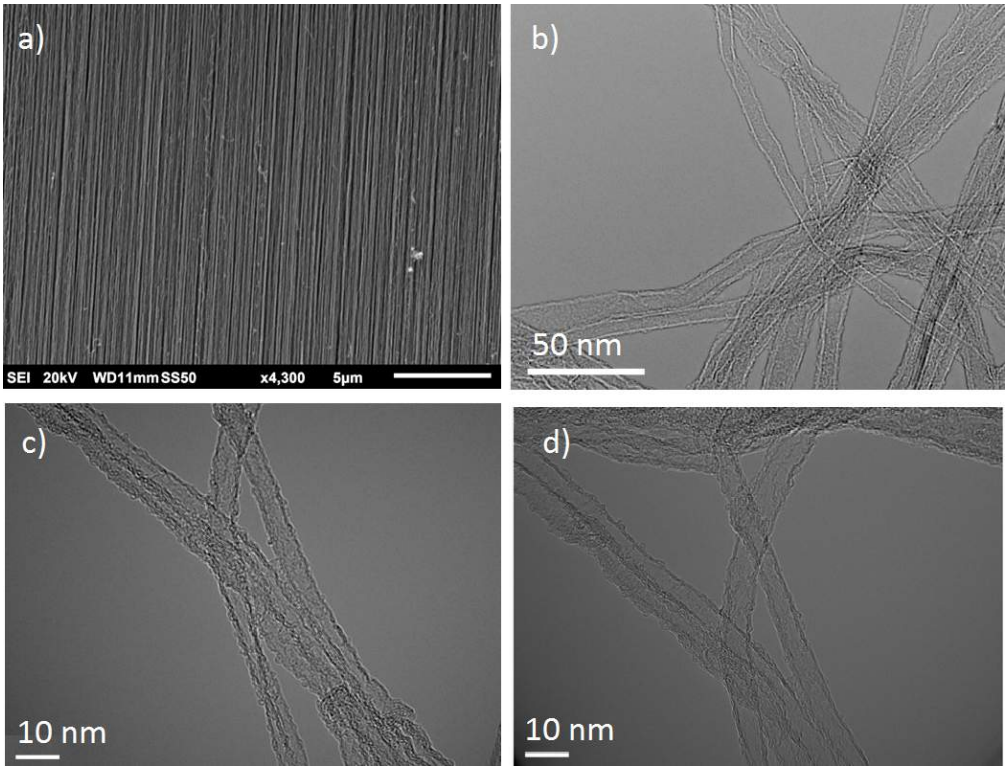

Figure 5.12: Figure a) shows the side of a typical forest as grown without controllable errors. Figure b) shows a TEM image of the sidewalls of several CNTs. The bottom two TEM images show CNTs grown with the AIXTRON for comparison. It can be seen that the quality does not differ much.

system. Another advantage of preheating is the reduction in accumulating amorphous carbon on the side wall of the oven.
The final type of error concerns constant operating parameters. It is found that especially the substrate location should remain constant and preferably in the back of the oven. Reduction in forest quality or reproducibility might be caused by variation in gas flows or annealing time, but to what extent depends on the amount of variation.
Once reproducible results were obtained a high quality of the CNT arrays could be confirmed. The tubes were straight, which indicates a low amount of defects. Also the amount of amorphous carbon on the sidewalls was low.

References

[1] J. B. In, "Electronic Thesis and Dissertations Reliable Growth of Vertically Aligned Carbon Nanotube Arrays by Chemical Vapor Deposition and In-situ Measurement of Fundamental Growth Kinetics in Oxygen-free Conditions By Jung Bin In A dissertation submitted in parti," *UC Berkeley Electronic Theses and Dissertations*, 2011.

[2] C. R. Wilke, "A Viscosity Equation for Gas Mixtures," *The Journal of Chemical Physics*, vol. 18, no. 4, p. 517, 1950.

[3] K. Hata, D. Futaba, K. Mizuno, and T. Namai, "Water-assisted highly efficient synthesis of impurity-free single-walled carbon nanotubes," *Science*, vol. 306, pp. 1362–1364, 2004.

[4] P. B. Amama, C. L. Pint, L. McJilton, S. M. Kim, E. a. Stach, P. T. Murray, R. H. Hauge, and B. Maruyama, "Role of water in super growth of single-walled carbon nanotube carpets.," *Nano letters*, vol. 9, no. 1, pp. 44–49, 2009.

[5] D. N. Futaba, K. Hata, T. Yamada, K. Mizuno, M. Yumura, and S. Iijima, "Kinetics of Water-Assisted Single-Walled Carbon Nanotube Synthesis Revealed by a Time-Evolution Analysis," *Physical Review Lettersq*, vol. 95, no. 56104, pp. 1–4, 2005.

[6] S. Chakrabarti, T. Nagasaka, Y. Yoshikawa, L. Pan, and Y. Nakayama, "Growth of super long aligned brush-like carbon nanotubes," *Japanese Journal of Applied Physics, Part 2: Letters*, vol. 45, no. 28, pp. 720–722, 2006.

Supplementary material

Cleaning the oven

Especially without proper preheating of the oven a large amount of amorphous carbon condensed on the quartz tube during growth. This amorphous carbon causes undesired, but interesting results as shown later on in these supplementary materials. After four experiments of growing CNTs the tube had become fully opaque due to the black deposits, as can be seen in figure 5.13. To prevent possible contamination or changing growth conditions during follow-up experiments the tube had to be cleaned.

Figure 5.13: The quartz tube after four growth experiments. Carbon deposits have turned the tube black and opaque.

The cleaning of the oven was first tried with only isopropanol, since this could not leave any residue. However, this turned out to be inadequate and a polishing paste had to be used as well. The paste that was used is called Pikal Paste for Metal Polishing.
The procedure for cleaning was first to wrap two cylindrical foams with a diameter of 6 cm and a length of 10 cm in dust-free tissues. One of the foams was soaked with isopropanol and the other was covered with the paste. They were put in the quartz tube along with its longitudinal axis. By pressing the foams together and moving them back and forth in the tube a readily quick cleaning procedure was exercised. When the tube was visually clean again, it was once more cleaned with a fresh tissue and isopropanol to remove any remaining paste or contaminants.

As discussed earlier, good growth results were hard to obtain after cleaning the oven. It was therefore verified if the polishing paste was properly removed with the post-cleaning with isopropanol. To do so two pieces of silicon where covered with the paste, while one of the two was cleaned with isopropanol. Using SEM no remainders of the paste could be noted on the cleaned piece of silicon. Also from an EDX analysis it could be concluded that all polishing paste will be removed from the surface after cleaning with isopropanol, as shown in table 5.2. This proves that any less-optimal results after cleaning the oven comes from contaminants in the air such as dust and/or humidity from the ambient environment. As discussed earlier, after proper preheating of the oven, good results could be obtained even directly after cleaning.

Table 5.2: EDX results from a sample covered with polishing paste.

Element	Mass (%)	Atom (%)
Si	1.82	0.85
Al	7.11	3.48
O	15.78	13.01
C	75.29	82.66
Total	100.00	100.00

Table 5.3: EDX results of a silicon sample first covered with paste and then cleaned with isopropanol.

Element	Mass (%)	Atom (%)
Si	100.00	100.00
Total	100.00	100.00

Table 5.4: Different recipes as used by different research groups. The carrier gas is not specified, since some groups use helium, while others prefer to use argon or nitrogen.

Group reference	Tube ⌀ (cm)	Temp (°C)	Carrier gas (sccm)	H_2 (sccm)	C_2H_4 (sccm)	Water (ppm)
Yasuda et al. [1]	2.54	750	900	0	100	0
Chakarabarti et al. [2]	2.54	750	105	80	15	350
Delzeit et al. [3]	2.54	750	0	0	1000	0
Lepro et al. [4]	7.2	760	700	200	100	0
Zhu et al. [5]	5.08	740	650	50	150	0
Li et al. [6]	2.54	750	94	6	100	0
Zhang et al. [7]	2.54	750	132	8	30	0
Luo et al. [8]	4.7	750	300	150	50	0

Recipes by literature

Ever since the discovery of CNTs a vast amount of CVD growth recipes are used. The specific parameters such as gases and their flowrates, temperature and pressure that are required for optimal growth are heavily dependent on the CVD system. Since almost every research group has a different CVD system, all groups have there own preferred growth recipe. In table 5.4 an overview is provided of several research groups with their particular growth recipe. Many recipes using acetylene, ethylene, methane or other carbon containing precursors do exist, but the focus is here on ethylene recipes since this gas is used in this study. The recipes as shown in the table vary widely, so it is hard to find a basis for newcomers to the field of CNT growth. It is also noticeable that only one recipe uses water vapor. This is much more common for recipes using acetylene and is supposed to etch away amorphous carbon during the growth process. Furthermore it should be noted that every group has its own way of heating up prior to growth. Some groups use a pure hydrogen environment, while others use a pure argon flow during heat up. This differences has an particular influence on the growth and final forest morphology as well. Except for the recipe by Delzeit et al. all groups use a sample of silicon wafer plus 10 nm Al_2O_3 and 1 nm Fe.

References

[1] S. Yasuda, D. N. Futaba, T. Yamada, J. Satou, A. Shibuya, H. Takai, K. Arakawa, M. Yumura and K. Hata. Improved and large area single-walled carbon nanotube forest growth by controlling the gas flow direction. *ACS Nano*, 3(12):4164-4170, 2009

[2] S. Chakrabarti, T. Nagasaka, Y. Yoshikawa, L. Pan and Y. Nakayama. Growth of super long aligned brush-like carbon nanotubes. *Japanese Journal of Applied Physics*, 45(28):720-722, 2006

[3] L. Delzeit, C. V. Nguyen, B. Chen, R. Stevens, A. Cassell, J. Han and M. Meyyappan. Multiwalled Carbon Nanotubes by Chemical Vapor Deposition using multilayered metal catalysts. *The Journal of Physical Chemistry B*, 106(22):5629-5635, 2002

[4] X. Lepró, M. D. Lima and R. H. Baughman. Spinnable carbon nanotube forests grown on thin, flexible metallic substrates. *Carbon*, 48(12):3621-3627, 2010

[5] C. Zhu, C. Cheng, Y. H. He, L. Wang, T. L. Wong, K. K. Fung and N. Wang. A self-entanglement mechanism for continuous pulling of carbon nanotube yarns. *Carbon*, 49(15):4996-5001, 2011

[6] Q. W. Li, X. F. Zhang and R.F DePaula. Sustained growth of ultralong carbon nanotube arrays for fiber spinning. *Advanced Materials*, 18(23):3160-3163, 2006

[7] Y. Zhang, G. Zou, S. K. Doorn, H. Htoon, L. Stan, M. E. Hawley, C. J. Sheehan, Y. Zhu and Q. Jia. Tailoring the morphology of Carbon Nanotube Arrays: from spinnable forests to undulating foams. *ACS nano*, 3(8):2157-2162, 2009

[8] Y. Luo, X. Wang, M. He, X. Li and H. Chen. Synthesis of high-quality carbon nanotube arrays without the assistance of water. *Journal of Nanomaterials*, Volume 2012, Article ID 542582, 5 pages, 2012

Calculation of Reynolds number

As mentioned earlier the Reynolds number of the flow during CNT growth can hardly be calculated analytically. The reason is that the flow consist of different gases. Besides, the gases are heated up to 750 °C within the first centimeters of entering the oven. This changes the flow substantially due to expansion of the gases. Yet, a simple estimation of the Reynolds number is made using the equation:

$$\mathrm{Re} = \frac{\rho V D}{\mu} \tag{5.1}$$

Where ρ is the density of hydrogen (0.09 kg/m^3). The density of hydrogen is taken, because it yields the least favorable properties of the three gases that are used. The velocity V of the gas calculated by dividing the cross-sectional area of the tube ($A = \pi \cdot r^2 = \pi \cdot 0.0225^2 = 1.59 \cdot 10^{-3}$) over the total flow of 1000 sccm (which equals $1.67 \cdot 10^{-5}$ m^3/s). The velocity of the gases then becomes $1.05 \cdot 10^{-2}$ m/s. The diameter D equals $0.045 \cdot 10^{-2}$ m and finally the dynamic viscosity of hydrogen is $8.4 \cdot 10^{-6}$ Pa·s. In that case the Reynolds number can be calculated to be 55.24, which is far below the transition limit of about 2300 where the flow becomes turbulent. So even when the gas is fully heated up to 750 °C and its volume becomes three times as large the Reynolds number is still not even close to the transition of becoming turbulent. It is can therefore be presumed that the flow remains laminar.

Explanation of growth procedure

Below an explanation of the entire growth procedure is provided. The method includes the preheating step, which seems to be necessary for obtaining desirable and reproducable results. A picture of the oven that was used is shown in figure 5.14a. It can be seen that the oven has buttons on the left which are used to program a heating schedule. The red and green buttons on the right are stop and continue of heating elements, respectively. Figure 5.15 shows the variable area flow meters used to verify the flow through the oven. Figure 5.14b shows a gas bottle. It consists of the bottle itself, an intermediate piece where pressures are measured and the outlet. The metal knob on the right should be opened to allow gas to the intermediate part and the small plastic knob should be opened to allow gas to flow out towards the system. The knob in the center controls the pressure at which the gas is flowing out of the intermediate part towards the oven. This pressure is shown in the left meter. **It is always kept just above zero**, to reduce the risk of high pressures in the oven when the exhaust lines become clogged for some reason. The right pressure meter shows how much gas is still left in the bottle. One bar (0.1 MPa) in a bottle of 5 liter corresponds to 5 liters of gas.

Figure 5.14: At the left a photograph of the CVD oven is shown. The photograph on the right shows one of the gas bottles (hydrogen) that was used.

Figure 5.15: A photograph of the variable area flow meters used in this study.

It is advisable to close the right valve of the oven every time there is no gas flowing to prevent back flow of exhaust gases. The preheating of the oven can be accomplished as follows:

1. Open the gas bottles. This is done by turning the metal knob on the right and the small plastic knob on the left two or three turns anti-clockwise.
2. Connect the oven to the grid by plugging it in the socket.
3. Make sure the ceramic blocks are just inside the oven and their ends align with the ends of the oven. The samples should not yet be placed in the oven.
4. Press the green button of the oven to enable the heating elements.
5. Start heating up the oven by holding the lowest button on the left for a couple of seconds.
6. Make sure the valves of the oven tube are opened.
7. Once the oven reaches 200 °C start flushing with argon (600 sccm) for 5 minutes. On the flow meter this corresponds to 4.99 dT/dF.
8. Once the oven reaches 750 °C flush again for 5 minutes with argon and the same flow rate.
9. Finally, press the red button to switch off the heaters and let the oven cool down to 500 °C. It is normal that the tube becomes somewhat fogged. If that happens, keep flushing argon with a gentle 400 sccm flow rate (3.33 dT/dF).

Once the oven is cooled down enough (to about 500 °C) it can be opened to let the samples in. In order to do so, first all flow meters should be closed. A ventilation and air-filter system should be pointed at the right end of the oven tube before opening it.

Once the oven is opened the ceramic block can be removed, but since it is still hot it should not be touched with bare hands. The left ceramic (the far end) should be pushed 1.5 to 2 cm backwards (towards the gas inlet) with the metal rod. Now the samples can be loaded on a boat of quartz glass. Finally the previously removed ceramic block can be placed back and should protrude 1.5 to 2 cm just as the other block. Once the oven is closed again and the ventilation system is pulled back the growth process can start.

1. First flush with argon again with a flow rate of 600 sccm for 5 minutes. The temperature can be kept around 480 degrees but not any higher by switching between the green and red button.

2. After flushing with argon a 5 minute flush with hydrogen is needed. A flow rate of 400 sccm (11.76 dT/dF) is sufficient.

3. After flushing for 10 minutes in total the oven can be heated up to 750 °C again.

4. Just before reaching this temperature the growth gases can be allowed inside the oven. The mixture contains 400 sccm (3.33 dT/dF) argon, 400 sccm (11.76 dT/dF) hydrogen and 200 sccm (2.4 dT/dF) ethylene.

5. Once 10 minutes of growth has been passed the oven can be shut down by pressing the red button and holding the stop button on the left for a couple of seconds. The gas flows should be shut down as well, except for argon. The argon can be used to flush with for 5 minutes and a flow rate of 600 sccm (4.99 dT/dF).

6. After cooling down to a safe temperature at least below 500 °C the samples could be retrieved by the same way as they were put in. 500 °C is the limit here since it is the auto-ignition temperature of hydrogen. Although the hydrogen should be gone by the last flushing step, it is better to avoid any risk.

Safety issues during CNT growth

Of course safety is an imperative aspect of CNT growth. Two safety issues arose when growing CNTs during this study, which might be relevant for other groups to take notice of. The first issue is due to unidentified vapors being formed during the growth process. The fog could be seen at the cool end of the oven and it was mostly formed when the oven was not properly preheated. Since it is unclear what substances are present in the fog, toxic vapors might have been formed as well. When the oven was opened after the growth procedure a penetrative odor could be smelled. It does not need much explanation that this could potentially be hazardous for the human body. To circumvent this risk a ventilation system was installed that could be aimed at the open part of the oven. This system sucks up the air and filters it using a active carbon filter. The chosen solution is thought to be effective since the odor can no longer be smelled.

The second issue involves the use of hydrogen at elevated temperatures. Hydrogen has an auto-ignition temperature of 500 degrees Celsius and the growth procedure requires a temperature of at least 750 °C. As long as no air, oxygen to be more specific, is inside the oven there is no problem. However, by flushing with argon prior to growth the air in the oven is only diluted. To a certain extend it is uncertain when the amount of oxygen is low enough to avoid the risk of explosion. It is found that 5 minutes of flushing with 600 sccm will remove enough oxygen. However, this will be dependent on the volume of the oven as well.

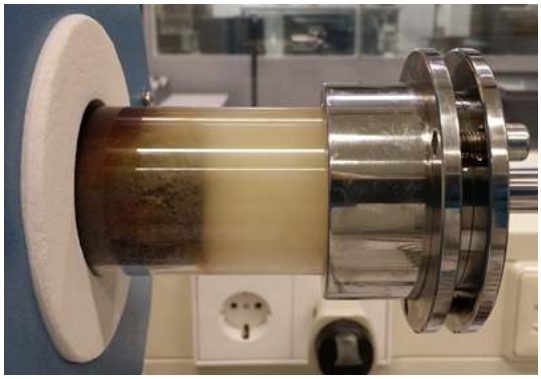

Figure 5.16: During CNT growth a fog become visible due to condensing carbon radicals forming unspecified vapors.

Both issues are the best solved by using a vacuum pump with a filter. The pump could be used to remove and filter any unknown vapors at the end of the growth process as well as any hydrogen left in the oven. Consequently the oven could be opened safely. The same is true for vacuum the oven tube prior to heating up the oven. Once it is ensured that oxygen is removed the hydrogen can be added safely, even at elevated temperatures.

Other interesting results that were obtained.

During this study more results were obtained that might be worthwhile mentioning. The first is indicated by the SEM figure shown in figure 5.17. Here two stacks of CNTs were grown on top of each other. This phenomenon typically occurred when the oven was not cleaned and a lot of amorphous carbon was deposited on its sidewall. It is therefore theorized that the first layer formed during the heat up stage while the oven was being flushed with hydrogen. The a-c from the sidewall is partially removed and carried along with the hydrogen. As a result carbon radicals are created before actual CNT growth resulting in the first stack. In that case the second stack is grown during the actual growth stage.

Another interesting result is when the growth flow rates are changed during CNT growth. The first five minutes of the growth stage a flow of 600 sccm argon, 250 sccm hydrogen and 150 sccm ethylene was used, while the latter five minutes the regular flow rates of 400 sccm argon, 400 sccm hydrogen and 200 sccm ethylene was applied. A clear separation of forest morphology can be seen at about half of the total height of the forest. Since it is forest growth on an alumina substrate a base-growth mechanism can be assumed. Consequently the upper part of the forest is likely to be caused by the first recipe, resulting in a less wavy forest.

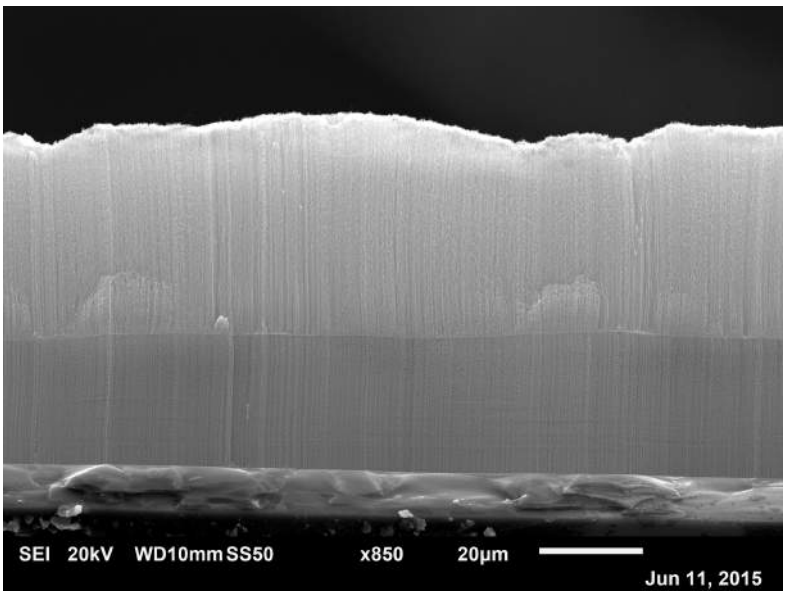

Figure 5.17: Side view of two stacked layers of CNTs grown on top of each other. This effect is due to an oven tube with vast amounts of amorphous carbon that gets released during anneal process. The bottom layer grows when the actual growth process has started.

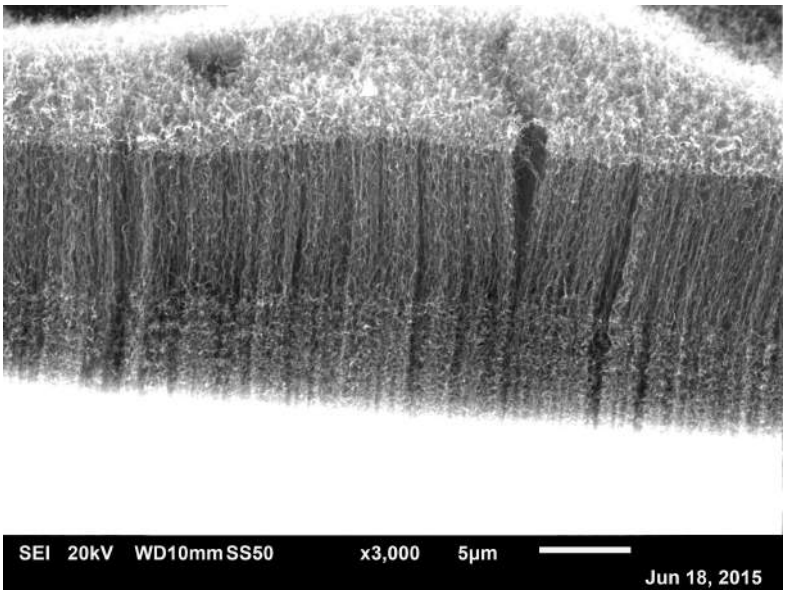

Figure 5.18: Two different recipes are used. After five minutes changed to the other. The difference is clearly visible in the morphology of the forest.

Chapter 6

Investigation of morphological requirements for spinnable CNT forests

Abstract

Several potential reasons for low spinnability of a CNT array are investigated. It is found that spinnability is not affected by the substrate-forest interaction. The spinnability of a free-standing forest is compared with the spinnability of a substrate-bound forest and it turned out that there is no noticeable difference between both cases. From studies by other groups it is clear that forest height does not influence spinnability within a certain range either. It is concluded that interaction between CNTs within the forest is a key factor. The low spinnability of forests synthesized in this study is likely to be caused by a lack of interconnecting bundles. The specific morphology with these interconnecting bundles can be obtained on a broad variety of substrates, as shown by several different studies. It has been found that the amount of interconnects can be more or less controlled by a change in growth recipe.

6.1 Introduction

Since the dimensions of Carbon Nanotubes (CNTs) are extremely small with diameters of several nanometers, the possible applications of individual tubes are limited. The length of CNTs can be grown into millimeter range [1][2][3][4] up to even 7 mm [5], which is enough for most envisaged applications such as chip interconnects, coatings, composites and supercapacitors [6]. However, other applications desire the excellent mechanical, electrical or thermal properties over a longer range than several millimeters, such as electrical wires, power transfer lines or structural enhancements [7]. For those applications a macroscopic product with the properties of individual CNTs is needed. One evident way to reach this is by spinning the individual CNTs into a yarn. This can either be done by dry spinning [8][9][10][11], wet spinning [12][13][14][15] or direct spinning [16][17]. These studies come a long way in developing purposeful CNT yarns for aforementioned applications. However, strength and conductivity of the yarns is not nearly as good as of individual CNTs.
The goal of this study was to reproduce and improve upon results reached by groups working with the dry spinning method of CNT yarn. In this study it has proven to be difficult to obtain a fully spinnable CNT forest. Therefore this study will focus on the responsible mechanisms that could lead to these forests. Recommendations to replicate earlier accomplishments on spinning will be discussed, to provide clear directions for future efforts of growing a spinnable forest.

6.2 Materials and methods

The basis for the substrate used in this study was a silicon wafer. A 10 nm thick diffusion barrier layer of alumina (Al_2O_3) is sputtered onto the wafer. The catalyst material to grow the CNT arrays on is iron, which is deposited on top of the Al_2O_3 by evaporation. Unless otherwise stated the thickness of the catalyst layer is 1 nm, but thicknesses of 2

Table 6.1: An indication of the level of spinnability, which is a subjective property. Table from [9]

Rating	**Observation**
0	Forest forms clean face when broken
1	CNTs partly dragged out of the forest front
2	CNTs form short tufts or strings when spun
3	Web breaks easily even at low speeds (1 m/min)
4	Splitting web, spinnable at moderate speed (10 m/min)
5	Dense web, spinnable at high speed (¿20 m/min)

nm or 5 nm Fe were sometimes tried as well.
Two systems were used for CNT growth. The first system used was the tubular CVD oven. In this case the oven was heated up to 750 °C while flowing hydrogen with 400 sccm. The gases used for growth consisted of 400 sccm argon, 400 sccm hydrogen and 200 sccm ethylene. More information about the growth procedure can be found in 5.
The other system for CNT growth was the AIXTRON Black Magic PECVD system, hereafter referred to as the AIXTRON. In this case typical gas flow rates during growth were 200 sccm N_2, 700 sccm H_2 and 50 sccm C2H4, while the growth temperature was set to 650 °C. Before adding the acetylene the samples were annealed for 4 minutes at 500 °C in an hydrogen environment. During operation the CVD system was at a low pressure of 80 mbar.
The pulling of the yarns was done manually with tweezers. The substrate was secured on the table of a stereoscope. With a magnification of about 5 times the forest was clearly visible and CNT bundles could be grabbed. Besides dry spinning, wet spinning was tried as well, as described in the supplementary materials.

6.3 Results and discussion

During this study spinnability was judged for various CNT forests. Spinnability itself is a subjective property and cannot be quantitatively measured. To be able to express a level of spinnability several rating systems are defined. One of the most convenient and the most explicit formulated systems is declared by Huynh et al., who defined spinnability on a scale from 1 to 5 [9]. The different levels of spinnability are clearly distinguished from one another and are easily verified by gently pulling the CNT bundles. This rating table is shown at table 6.1 and provides an overview of the different values for spinnability.
Spinnability was verified for forests with a height of 300 μm and also for forests with a height of 500 μm. Furthermore a distinction was made between forests grown on 1 nm Fe catalyst layer or 2 nm catalyst layer. However, none of the grown forests could be rated 4 or higher, since a stable web could not be formed. The typical value for spinnability of the tested forests is rated to be 2, since only small wires could be pulled out from the forest as shown in figure 6.1. In some cases small initial webs could be formed, but

they snapped if pulled any further, as can be seen in figure 6.2. In the supplementary materials some of these wires that could be pulled are shown. In general the shorter forests were better spinnable than the longer forests. The thickness of the catalyst layer was hard to correlate with spinnability. The tubulur CVD produced better spinnable forests on 2nm Fe, while forests grown in the AIXTRON were better spinnable when grown on 1 nm Fe. However, since no forest was concluded to be spinnable, the question became why that is the case. The four possible causes that were investigated are forest-substrate connection, forest height, amorphous carbon on the top and forest morphology.

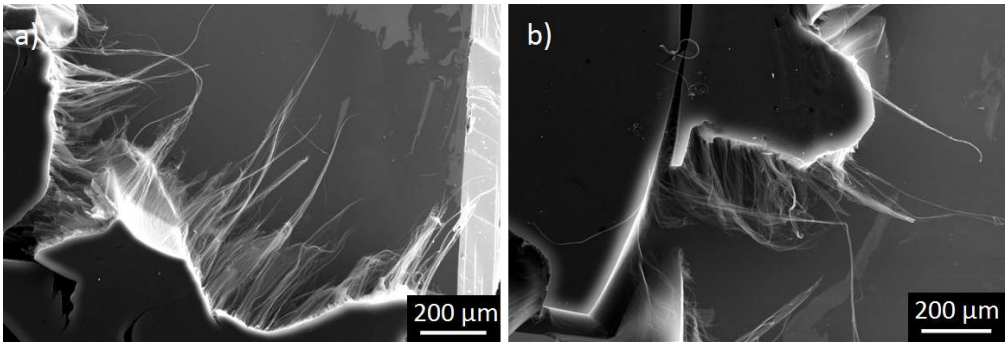

Figure 6.1: A top view from two forests and their edges after a chunk of CNT bundles are dragged away. The strings are clearly visible, but initiated webs are still absent.

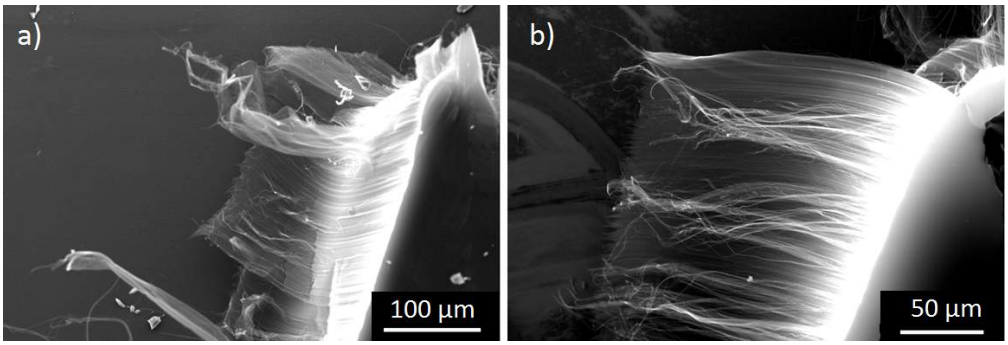

Figure 6.2: In contrast to figure 6.1 here initiated webs are clearly visible. These forests are closer to full spinnability, but the web still splits after being pulled by tweezers.

6.3.1 Causes of low spinnability

It is theorized that the connection between the CNTs and the substrate can be too strong. Therefore a continuous spinning process can not be initiated. The connection between the forest and its substrate could not be quantitatively determined during this study, but it was found that a gently pushed forest easily came off the substrate without

any microscopically visible damage. In such cases the forest would become a freestanding entity. The first study to mention dry spun CNT yarn also used a free standing forest with one edge taped to a substrate [18]. This was imitated to verify whether a forest-substrate connection or not would make a difference in spinnability, as shown in figure 6.3. Even in this position the forest was not spinnable. In fact, no difference could be noted between the forest attached to the substrate or standing freely; both produced small strings, but no initial webs. It can therefore be concluded that the forest is not attached too strongly to the substrate. The lack of spinnability is most likely due to an incorrect forest height, too much amorphous carbon and/or a non-suitable morphology.

According to different studies found in literature a spinnable forest is not bound by a narrow range of heights. Jiang et al. pulled a continuous yarn from a forest with a length of 100 μm high [18]. The spinnable forest of Lepró et al. reached a height of 160 μm [8], while the height of the forests of Sears et al. was 350 μm [19]. Furthermore a spinnable range of 300-600 μm for forest height is given by Jayasinghe et al. [10] and Huynh et al concludes that forests up to 900 μm are spinnable [9]. Finally, Li et al. goes even further by claiming a forest spinnability between 500 and 1500 μm [4]. Since both forest of 300 μm and 500 μm are tested for spinnability it can be presumed that forest height does not form the problem either. Furthermore it is found that the shorter forests were not particularly more spinnable than the longer forests that were synthesized. In some cases both could produce only strings and in other cases initial webs could be formed for both the shorter and the longer forests. It can be concluded that height is not likely to be limited factor in spinnability in the current case where the heights vary between 300 and 500 microns.

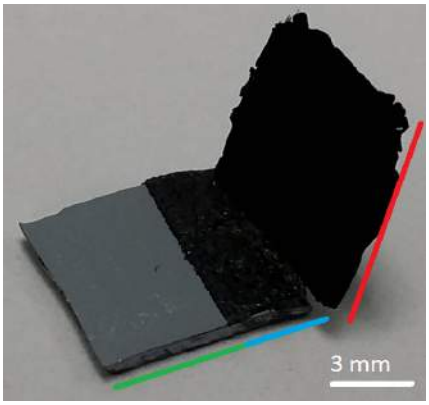

Figure 6.3: When gently pushed to an edge the whole forest broke loose from the substrate. It was then taped to the substrate to fix it standing upwards. The red line indicates the edge of the forest, the green line the edge of the substrate and the blue line goes along the tape.

As found by Li et al. the amount of amorphous carbon in the CNT forest does affect its spinnability [4]. The amorphous carbon can be seen by the naked eye by looking at the shade of the forest. When no amorphous carbon is present the forest appears to be perfectly black. The term popular term VANTA-black is derived from Vertically Aligned Carbon NanoTube Array (VANTA where the C is left out). In contrast, if the top of the forest appears to be grayish or even shiny the amounts of a-c are high. In the latter case, a shiny top, it is likely that graphite causes this color. However, this is

just as bad for spinnability since it makes the forest brittle and hard to rip apart evenly. Three forests with different amounts of a-c/graphite are shown in figure 6.4. Besides changing the shade, the a-c makes the forest more brittle which can be detected by using tweezers. A gentle push on the top of the forest will reveal how soft the forest is and thus the amount of a-c is indicated. The decrease in spinnability due to a-c is confirmed by other groups as well [9][20]. It is found that forests grown in the tubular CVD oven are always somewhat grayish, indicating the presence of amorphous carbon within or on top of the forest. In contrast, the AIXTRON produces the VANTA-black forests without amorphous carbon. Yet, the spinnability of all these forests do not differ greatly and are rated a 1 or 2 depending on the individual sample.

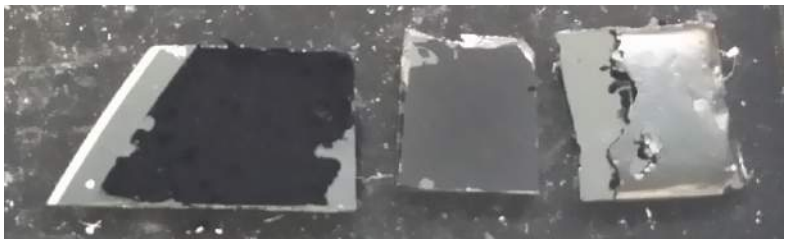

Figure 6.4: Photograph of three forests. The left forest is pure black and contains low amounts of a-c. The central forest is grayish and contains medium amounts of a-c, while the forest on the right shows a shiny top most likely due to a thin graphite layer.

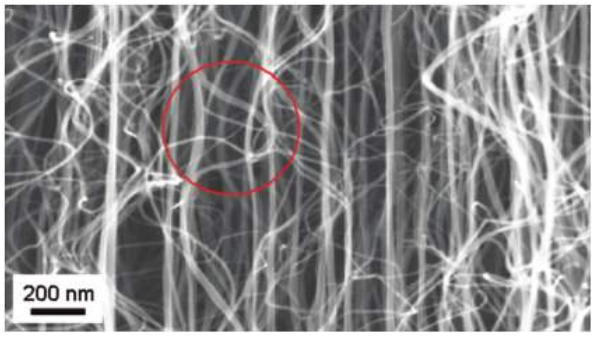

Figure 6.5: Interconnecting bundles are clearly visible in this figure. They are one of the requirements to obtain a spinnable forest. Reprinted from [21]

The morphology of the forest seems to be a critical factor in determining the spinnability. Various studies claim that a spinnable forest should be well aligned, sometimes called superaligned. A higher level of alignment is associated with a higher level of spinnability [22][23][9][24]. This can be explained by the most extreme case of misalignment, where CNTs are fully entangled with a large amount of surrounding CNTs. As a result, the CNT bundles cannot be pulled away gradually. A whole chunk of surrounding CNTs will be broken out of the array and a relatively clean edge will be left. Misaligned, curved and tortuous forests are widely acknowledged to be unspinnable. On the other extreme of alignment CNTs are perfectly parallel. When a CNT bundle is pulled under these circumstances it will not carry any other bundles since there is no strong connection of entanglement. This makes it very

easy for the bundle to come loose from the substrate. However, it can be imagined that there should be a proper connection between the parallel bundles, otherwise only one bundle is removed and no yarn could be spun. As modeled by Kuznetsov et al. [25] and experimentally proven by Zhu et al. [21] this connection is formed by so called interconnecting bundles. As their name indicate these bundles connect the vertically aligned CNT bundles by entanglement. This entanglement is much stronger than the Van der Waals forces by which CNTs are normally stuck together. As pointed out by Zhu et al. these entanglements will tighten up once a bundle is pulled out of the forest. The entanglements will form knots and thereby keeping multiple CNT bundles together so that a yarn can be spun.
Figure 6.6 shows the morphology of several different highly spinnable forests from different groups. They all show interconnecting bundles as well as the right alignment.

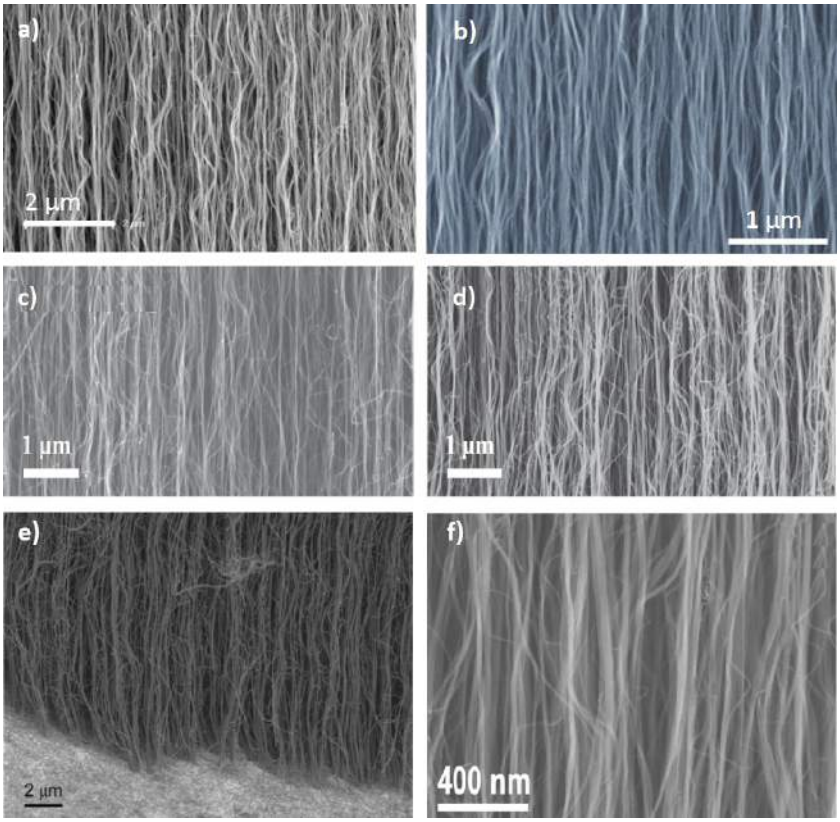

Figure 6.6: Highly spinnable forests from literature. Figure a) is adapted from [9], figure b) from [26], figure c) and d) from [27], figure e) from [11] and figure f) from [8]

However, when these forests are compared with the CNT forests grown in this study a some clear differences can be seen. The left and right images of figure 6.7 shows the side view of the forests grown with the AIXTRON and the tubular CVD system, respectively. The forest on the left shows a well aligned top of the forest. However, at the lower end of

the forest more curved bundles are visible. Since the forest is grown on alumina, which results in a strong bond with iron catalyst, a base growth mechanism can be assumed. In that case the curves at the bottom can be associated with more defects in the CNTs due to less ideal growth conditions [28]. This in turn can be explained by the gradual accumulation of amorphous carbon on the catalyst particles during the growth process. The a-c blocks the supply of enough radicals and therefore more defects in CNT walls will be invoked.
In the right column of figure 6.7 a forest is shown that is well aligned from the bottom to the top. It appears that proper growth and catalyst conditions are present during the entire growth stage. This can be derived from the straight CNT bundles all over the cross section of the array. The recipe used for the tubular CVD system contained a larger hydrogen flow than the recipe of the AIXTRON and it is hypothesized that this caused more etching of the catalyst particles as is also found by Zhang et al. [29]. Therefore the particles might remain free of amorphous carbon coating, which in turn keeps the amount of defects in CNTs low. Finally it is noted that the left forest of figure 6.7 is grown in 15 minutes, while the right forest only needed 10 minutes to reach its height of 450 μm. The lower growth rate of the left forest is in agreement with its higher degree of curliness in comparison to the right forest, as indicated by Yamada et al. as well [2]. The spinnability of both forest was about equal and was rated a one or two. Small strings or initial webs could be pulled and a continuous spinning process could not be sustained.

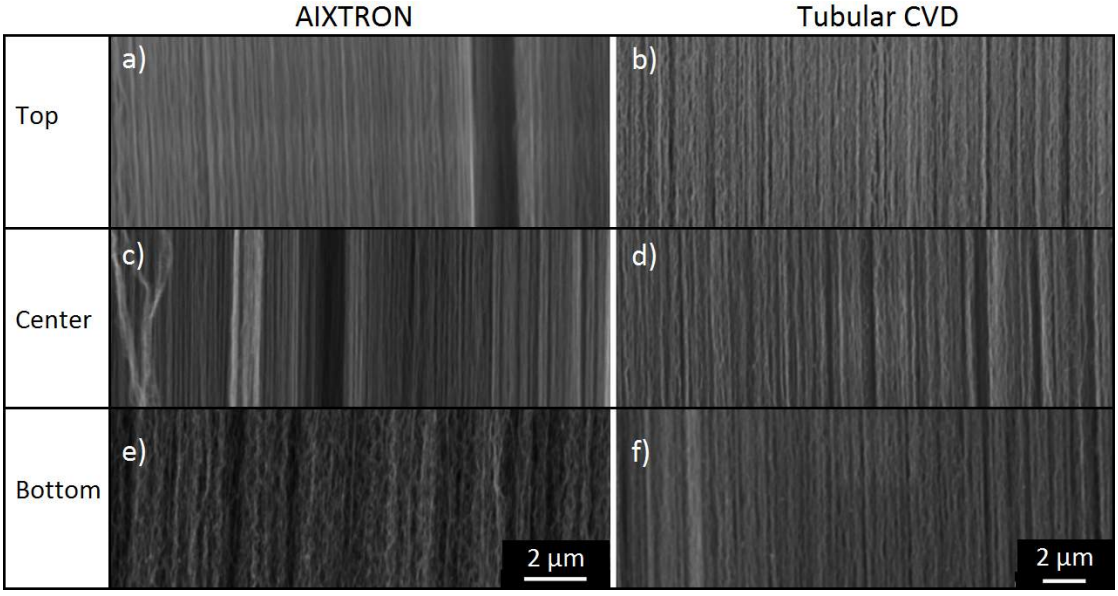

Figure 6.7: Figure a), c) and e) show the top, center and bottom morphology of a 470 μm high forest, respectively. This forest is grown with the AIXTRON. Figure b), d) and f) show the top, center and bottom morphology of a 450 μm high forest as grown with the tubular CVD.

In summary, from the clarification of the four causes for low spinnability it can be presumed that the low spinnability is not due to strong forest/substrate interactions or inappropriate heights of the forests. It seems likely the the low spinnability of the forest grown with the AIXTRON on the left of figure 6.7 is because of its lack of connecting CNT bundles and possibly because of the low level of alignment at its bottom as well. Although the forest on the right of figure 6.7 is fully aligned it has no interconnecting bundles and appear to be gray at the top. The a-c causes the forest to be brittle and as a result hard to spun.

6.3.2 Efforts to improve spinnability

Since connecting bundles are required to grow spinnable CNT arrays, the final question becomes how to grow a forest that contains these connecting CNT bundles? It seems that catalyst thickness is not a critical factor in growing intertwined CNT bundles, since Zheng et al. [20], Zhang et al. [30]and Jayasinghe et al [10] all used different iron catalyst thicknesses of 0.8, 1 and 2 nm respectively on a 10 nm thick alumina layer. Gilvaei et al. used even a 4 nm Fe catalyst layer, but directly on silicon [23]. The fact that spinnable forests with this specific morphology were grown on these different substrates, proves that the catalyst thickness is not the key factor.

If the composition of the substrate is not of importance, the influence of the CNT array morphology must come from the growth process. According to Gilvaei et al. the difference between a spinnable forest and non-spinnable forests is their pretreatment before growth. In a study by Zhang et al. it is shown that a particular pretreatment substantially affects forest morphology and spinnability [31]. Without any annealing time spinnable forests were grown, but with an annealing time of 10 or 60 minutes the CNT arrays turned out to be no longer spinnable. Spinnability was also affected by the gas mixture entering the oven during temperature ramp up. This is confirmed by Zheng et al. who reports that a carrier gas with 2% hydrogen results in the best spinnable forest, while no hydrogen at all is only barely spinnable [20].
To verify the influence of heating up the oven with different gases several experiments were carried out. Prior to the actual growth the tubular CVD oven was heated up to the 750 °C in different environments. The environments that were tried consisted of 100% argon, 50% argon and 50% hydrogen, 25 % argon and 75% hydrogen and finally also 100% hydrogen. It turned out that for all except the 100% hydrogen environment no CNT forests could be grown on the 1 nm and 2 nm catalyst layers. A relatively thin forest of 100 microns did grow on the samples with 5 nm iron catalyst. This thin forest was very wavy and curly as well. So from these results it seems only hydrogen is allowed during the heat up stage.
Since the spinnability could not be changed by changing the composition of the gas mixture experiments with different growth recipes were conducted as well. Figure 6.8 shows two forests grown with different recipes. More specifically forest of figure 6.8a was grown with 400 sccm argon, 600 sccm hydrogen and 300 sccm ethylene. The forest on

the right of figure 6.8 was grown under a flow of 600 sccm argon, 600 sccm hydrogen and 300 sccm ethylene. It can be seen that more interconnecting bundles are formed with respect to the regular grown forest of figure 6.7. It remains unclear why the increase in flow rate with respect to the original recipe of 400 sccm argon, 400 sccm hydrogen and 200 sccm ethylene leads to an increase in interconnecting bundles. It is theorized that the amount of interconnecting bundles is strongly correlated to the amount of carbon radicals being available locally. By having the right combination of total flow and amount of carbon precursor there are just enough carbon radicals available to grow an aligned CNT forest. However, at some instances CNTs become defective due to a shortage of available radicals. These CNTs will bend and form interconnecting CNTs. Although more interconnecting bundles were formed with the higher flow rates, a lot more amorphous carbon or graphite was formed as well. This was observed by the brittle grayish layer on top of the forest. Yet their spinnability was quite good and could be rated a two or three.

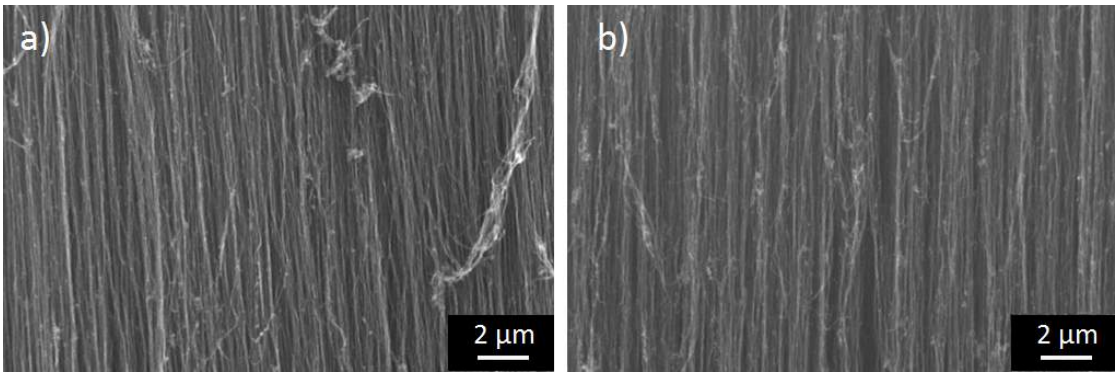

Figure 6.8: Forests with different morphology could be obtained by changing the gases and flow rates during the growth stage.

Unfortunately no fully spinnable forest could obtained during this study. However, with the careful analyses of the creation of interconnecting CNT bundles and the formation of an amorphous carbon layer on top of the forest, directions can be provided for the growth of a spinnable forest. It is expected that an increase in interconnecting bundles and a decrease of amorphous carbon on the top of the forest will lead to spinnable forest. Therefore, it is recommended for future work to keep changing the recipe parameters. Besides, experiments with a controlled water bubbler might lead to the etching of the amorphous carbon top layer [32].

6.4 Conclusion

It has been found that spinnability of a forest might be hard to obtain. It can be concluded that spinnability is not likely to be affected by substrate-forest interaction forces. This was verified by comparing spinnability of a free standing forest with a forest attached to the substrate. In both cases only wires of a few millimeters could be drawn, which indicates non-optimal spinnability. Furthermore, a wide range of forest heights is potentially allowed to still have spinnable forests. More relevant for spinnability seems to be the amount of amorphous carbon inside the forest, which is indicated by a shade of gray. Also a minimum amount of interconnecting CNT bundles should be present in the forest. The amount of interconnecting bundles that are formed is found to be dependent on the growth recipe. Heating up the samples in an environment containing some argon yielded no CNT forest growth, while heating up in hydrogen enabled the growth CNTs.

References

[1] Y. Inoue, K. Kakihata, Y. Hirono, T. Horie, A. Ishida, and H. Mimura, "One-step grown aligned bulk carbon nanotubes by chloride mediated chemical vapor deposition," *Applied Physics Letters*, vol. 92, no. 21, 2008.

[2] T. Yamada, T. Namai, K. Hata, D. N. Futaba, K. Mizuno, J. Fan, M. Yudasaka, M. Yumura, and S. Iijima, "Size-selective growth of double-walled carbon nanotube forests from engineered iron catalysts.," *Nature nanotechnology*, vol. 1, no. 2, pp. 131–136, 2006.

[3] E. R. Meshot and a. J. Hart, "Abrupt self-termination of vertically aligned carbon nanotube growth," *Applied Physics Letters*, vol. 92, no. 11, p. 113107, 2008.

[4] Q. Li, X. Zhang, and R. DePaula, "Sustained growth of ultralong carbon nanotube arrays for fiber spinning," *Advanced Materials*, vol. 18, no. 23, pp. 3160–3163, 2006.

[5] S. Chakrabarti, T. Nagasaka, Y. Yoshikawa, L. Pan, and Y. Nakayama, "Growth of super long aligned brush-like carbon nanotubes," *Japanese Journal of Applied Physics, Part 2: Letters*, vol. 45, no. 28, pp. 720–722, 2006.

[6] M. D. Volder, S. Tawfick, R. Baughman, and A. Hart, "Carbon nanotubes: present and future commercial applications," *Science*, vol. 535, no. 2013, 2013.

[7] W. Lu, M. Zu, J.-H. Byun, B.-S. Kim, and T.-W. Chou, "State of the art of carbon nanotube fibers: opportunities and challenges.," *Advanced materials*, vol. 24, pp. 1805–1833, Apr. 2012.

[8] X. Lepró, M. Lima, and R. Baughman, "Spinnable carbon nanotube forests grown on thin, flexible metallic substrates," *Carbon*, vol. 48, pp. 3621–3627, Oct. 2010.

[9] C. P. Huynh and S. C. Hawkins, "Understanding the synthesis of directly spinnable carbon nanotube forests," *Carbon*, vol. 48, no. 4, pp. 1105–1115, 2010.

[10] C. Jayasinghe, "Spinning yarn from long carbon nanotube arrays," *Journal of Materials Research*, vol. 26, no. 5, pp. 645–651, 2011.

[11] A. Ghemes, Y. Minami, and J. Muramatsu, "Fabrication and mechanical properties of carbon nanotube yarns spun from ultra-long multi-walled carbon nanotube arrays," *Carbon*, vol. 50, no. 12, pp. 4579–4587, 2012.

[12] B. Vigolo, a. Pénicaud, C. Coulon, C. Sauder, R. Pailler, C. Journet, P. Bernier, and P. Poulin, "Macroscopic fibers and ribbons of oriented carbon nanotubes.," *Science (New York, N.Y.)*, vol. 290, no. 5495, pp. 1331–1334, 2000.

[13] A. B. Dalton, S. Collins, J. Razal, E. Munoz, V. H. Ebron, B. G. Kim, J. N. Coleman, J. P. Ferraris, and R. H. Baughman, "Continuous carbon nanotube composite fibers: properties, potential applications, and problems," *Journal of Materials Chemistry*, vol. 14, no. 1, pp. 1–3, 2004.

[14] L. M. Ericson, H. Fan, H. Peng, V. A. Davis, W. Zhou, J. Sulpizio, Y. Wang, R. Booker, J. Vavro, C. Guthy, A. N. G. Parra-vasquez, M. J. Kim, S. Ramesh, R. K. Saini, C. Kittrell, G. Lavin, H. Schmidt, W. W. Adams, W. E. Billups, M. Pasquali, W.-f. Hwang, R. H. Hauge, J. E. Fischer, and R. E. Smalley, "Macroscopic , Neat , Single-Walled Carbon Nanotube Fibers," *Science*, vol. 305, pp. 1447–1451, 2004.

[15] S. Zhang, K. K. K. Koziol, I. a. Kinloch, and A. H. Windle, "Macroscopic fibers of well-aligned carbon nanotubes by wet spinning," *Small*, vol. 4, no. 8, pp. 1217–1222, 2008.

[16] H. W. Zhu, C. L. Xu, D. H. Wu, B. Q. Wei, R. Vajtai, and P. M. Ajayan, "Direct synthesis of long single-walled carbon nanotube strands.," *Science*, vol. 296, no. 5569, pp. 884–886, 2002.

[17] Y. Li, I. Kinloch, and A. Windle, "Direct spinning of carbon nanotube fibers from chemical vapor deposition synthesis," *Science*, vol. 276, no. 2004, 2004.

[18] K. Jiang, Q. Li, and S. Fan, "Nanotechnology: spinning continuous carbon nanotube yarns.," *Nature*, vol. 419, no. 6909, p. 801, 2002.

[19] K. Sears, C. Skourtis, K. Atkinson, N. Finn, and W. Humphries, "Focused ion beam milling of carbon nanotube yarns to study the relationship between structure and strength," *Carbon*, vol. 48, pp. 4450–4456, Dec. 2010.

[20] L. Zheng, G. Sun, and Z. Zhan, "Tuning Array Morphology for High-Strength Carbon-Nanotube Fibers," *Small*, vol. 6, no. 1, pp. 132–137, 2010.

[21] C. Zhu, C. Cheng, Y. H. He, L. Wang, T. L. Wong, K. K. Fung, and N. Wang, "A self-entanglement mechanism for continuous pulling of carbon nanotube yarns," *Carbon*, vol. 49, no. 15, pp. 4996–5001, 2011.

[22] X. Zhang, K. Jiang, C. Feng, P. Liu, L. Zhang, J. Kong, T. Zhang, Q. Li, and S. Fan, "Spinning and processing continuous yarns from 4-inch wafer scale super-aligned carbon nanotube arrays," *Advanced Materials*, vol. 18, pp. 1505–1510, 2006.

[23] A. F. Gilvaei, K. Hirahara, and Y. Nakayama, "In-situ study of the carbon nanotube yarn drawing process," *Carbon*, vol. 49, pp. 4928–4935, Nov. 2011.

[24] M. Miao, "Yarn spun from carbon nanotube forests: Production, structure, properties and applications," *Particuology*, vol. 11, no. 4, pp. 378–393, 2013.

[25] A. a. Kuznetsov, A. F. Fonseca, R. H. Baughman, and A. a. Zakhidov, "Structural model for dry-drawing of sheets and yarns from carbon nanotube forests," *ACS Nano*, vol. 5, no. 2, pp. 985–993, 2011.

[26] T. Iijima, H. Oshima, Y. Hayashi, and U. Bhimrao, "In-situ observation of carbon nanotube fiber spinning from vertically aligned carbon nanotube forest," *Diamond & Related Materials*, vol. 24, pp. 158–160, 2012.

[27] D. Jung, J. H. Kim, K. H. Lee, L. J. Overzet, and G. S. Lee, "Effects of pre-annealing of Fe catalysts on growth of spin-capable carbon nanotubes," *Diamond and Related Materials*, vol. 38, no. 2, pp. 87–92, 2013.

[28] A. Cassell and J. Raymakers, "Large scale CVD synthesis of single-walled carbon nanotubes," *The Journal of Physical Chemistry B*, vol. 103, pp. 6484–6492, 1999.

[29] H. Zhang, G. Cao, Z. Wang, Y. Yang, Z. Shi, and Z. Gu, "Influence of Hydrogen Pretreatment Condition on the Morphology of Fe / Al 2 O 3 Catalyst Film and Growth of Millimeter-Long Carbon Nanotube Array," pp. 4524–4530, 2008.

[30] X. Zhang, Q. Li, Y. Tu, Y. Li, J. Y. Coulter, L. Zheng, Y. Zhao, Q. Jia, D. E. Peterson, and Y. Zhu, "Strong carbon-nanotube fibers spun from long carbon-nanotube arrays.," *Small*, vol. 3, pp. 244–248, Feb. 2007.

[31] Y. Zhang, G. Zou, S. K. Doorn, H. Htoon, L. Stan, M. E. Hawley, C. J. Sheehan, Y. Zhu, and Q. Jia, "Tailoring the Morphology of Carbon Nanotube Arrays : From Spinnable Forests to Undulating Foams," *ACS nano*, vol. 3, no. 8, pp. 2157–2162, 2009.

[32] P. B. Amama, C. L. Pint, L. McJilton, S. M. Kim, E. a. Stach, P. T. Murray, R. H. Hauge, and B. Maruyama, "Role of water in super growth of single-walled carbon nanotube carpets.," *Nano letters*, vol. 9, no. 1, pp. 44–49, 2009.

Supplementary material

Results on pulling the forests

Although no continuous spinning process could be initiated from the forests with low spinnability, small wires could be pulled. The wire is shown in figure 6.9. Also, to see the structure of the wire a more zoomed in image is shown in figure 6.10. It can be seen that the wire is about two millimeters long and both ends are connected to chunks of CNTs. The chunk initially grabbed with tweezers to start pulling the wire. When this length was reached the right chunk was grabbed from the forest to keep the wire intact. The wire is not twisted and relatively thin. It can therefore be seen in figure 6.10 that the wire contains loose CNT bundles along its side.

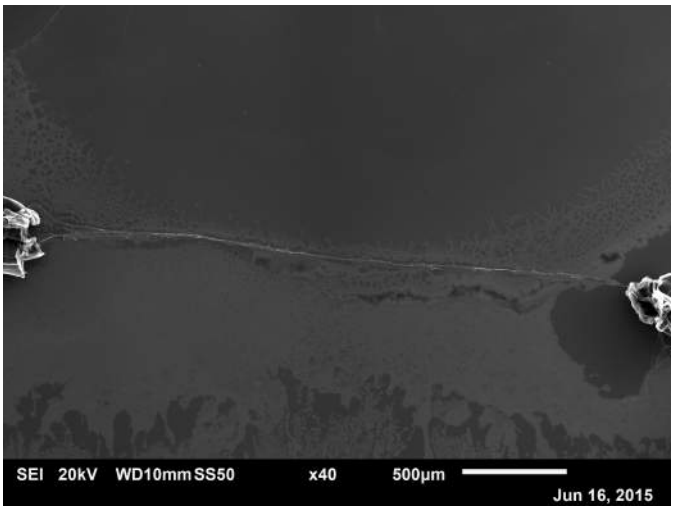

Figure 6.9: String pulled from CNT forest. Both ends consist of CNT chunks.

Measuring resistance

The resistance of the wires pulled from the forest could be effectively measured. This was accomplished by depositing two droplets of conductive silver paste on a clean substrate. The centers of the droplets were spaced apart with the same length of the CNT wire that was to be measured. While the paste was still wet the end chunks of the wire could be placed on top of the droplets. The connection was well established since both end chunks partially sunk in the paste. However, as can be seen from figure 6.11, since the wire is not spun its thickness and density was not uniform along its longitudinal axis. This makes the calculation of resistivity merely an estimation.

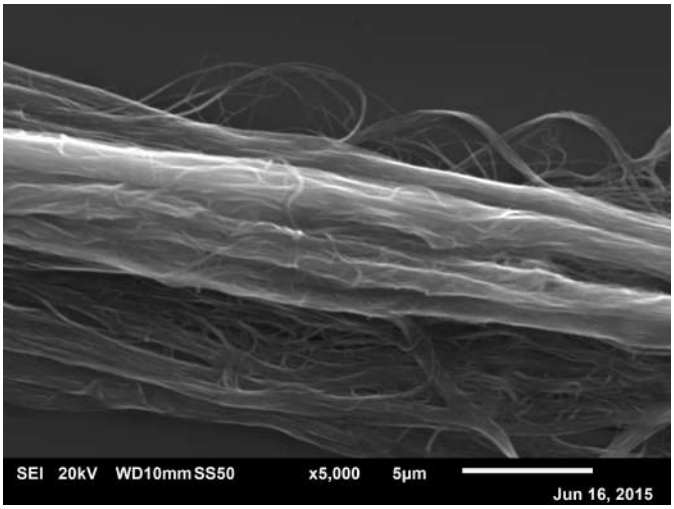

Figure 6.10: Zoom in of the CNT string.

Wet spinning

When a CNT yarn could not be obtained by dry spinning, wet spinning was tried as well. In case of wet spinning, as described in chapter 4, CNTs are dispersed in a liquid A which is in turn dispersed in a liquid B. Liquid A will dissolve in liquid B and since liquid B contracts the CHTs together the remaining CNTs will form of a sort of gel. This gel can be pulled and twisted and liquid B will evaporate so that a dense and pure yarn is the result. The experiment conducted to create a yarn by wet spinning is based on the process described by Zhang et al. [1]. For liquid A ethylene glycol is used, while for liquid B diethyl ether is used. The CNTs where grown using the tubular CVD with the standard recipe. The lengths of the CNTs where about 100 micron. An amount of about 5 wt% CNTs is mixed with the ethylene glycol. During sonication the mixture of CNTs and ethylene glycol is supposed to become a homologous dispersion. However, the chunks of CNTs remained clustered together as can be seen on the left of figure 6.12.

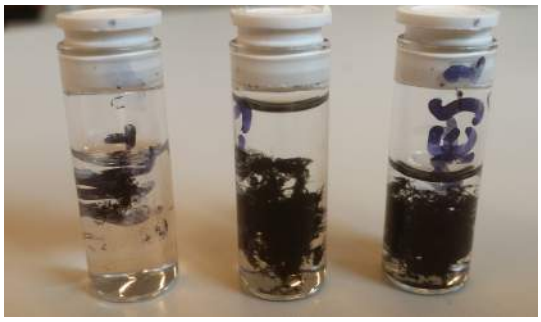

Figure 6.12: Three dispersions CNTs in ethylene glycol (left) and in ethanol (center and right). The CNT chunks remained clustered together and could not be dispersed homogeneously by sonication.

Since dispersing in ehtylene glycol did not lead to the desired results, it was tried to disperse the CNTs in ethanol, which is more commonly used. As can be seen from the center and right tube of figure 6.12

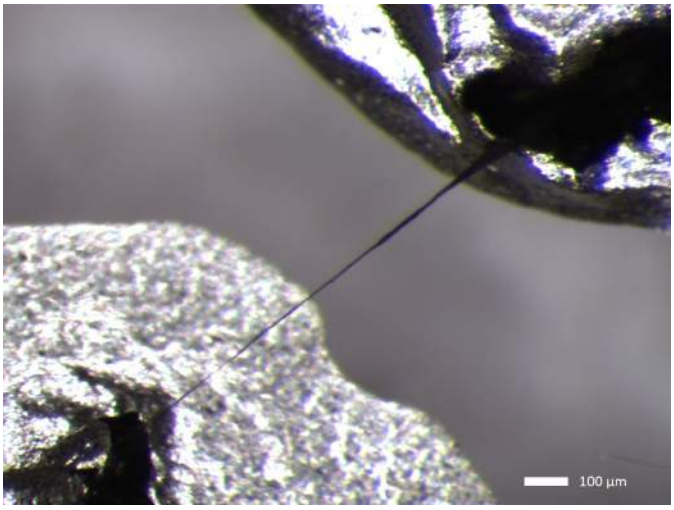

Figure 6.11: Figure of the setup for measuring the resistance of the CNT wire.

CNTs in ethanol did not form a homologous dispersion either. It is suspected that the power of the ultrasonic bath could not reach high enough to loosen the CNTs enough.

References

[1] S. Zhang, K. K. K. Koziol, I. A. Kinloch and A. H. Windle. Macroscopic fibers of well-aligned carbon nanotubes by wet spinning. *Small*, 4(8):1217-1222, 2008

Design of the spinning machine

During this thesis a spinning machine was developed as well. Although fully spinnable forests could not yet be obtained, it is expected that this spinning machine might become useful once forests could be spun. The machine is designed to pull, twist and wind the yarn with one single motor.
The system contains four pulleys which around the CNT yarn can be drawn. The first pulley is to align the CNTs with the longitudinal axis of the yarn. The remaining three pulley are there to dip the yarn into a volatile liquid. Due to Van der Waals forces the yarn will contract when a liquid is immersed. The liquid, which can be ethanol, will evaporate again so no remainders will be present in the dried yarn. Even though the ethanol will evaporate the yarn will keep its dense form. Finally, after immersion with the liquid the yarn will be guided, via the hole of the twisting arm, through one of the small rings at the end of the spinning arms. This twist that is applied will depend on the rotational speed of the motor as well. If the spinning arm rotates one turn and the motor has also turned, the twist applied is 360 degrees per circumference of the spindle. Figure 6.13 shows a rendered image of the spinning machine.

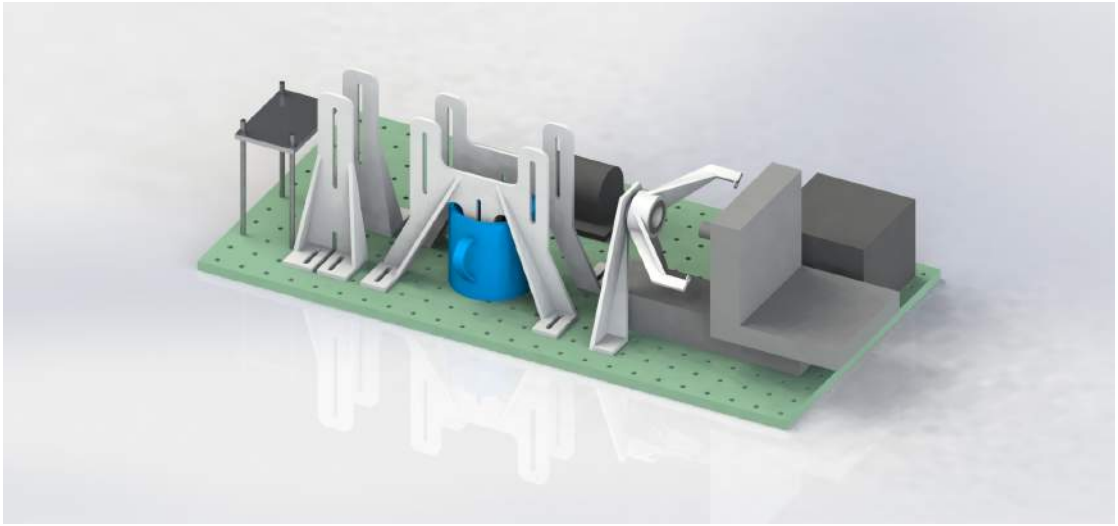

Figure 6.13: Rendered image of the design of the spinning machine.

Chapter 7

Conclusion

Conclusion

During this study the goal was to improve employability of CNTs in potential applications. This was to be accomplished by obtaining a better understanding of growth and spinnability of CNT forests. The central question became: how can a reproducible and spinnable forest reliably grown?

To obtain a systematic approach which gives clear directions for the growth of a long vertically aligned CNT array this study was divided in two parts. First the CNT growth is investigated and clear guidelines for the synthesis of a CNT forest are proposed. The second part contains the investigation of the spinnability of a CNT forest, which can provide the right directions for adjusting the synthesis to obtain spinnable forests.

It was found that several disturbances, or errors, could affect CNT growth. These disturbances were investigated and their influences were reported. To obtain a clear overview they are divided into three categories: system errors, condition errors and operation errors. They are listed below:

- If problems with CNT growth by CVD arise, the system errors could be checked first. It is relatively easy to verify the presence of these errors. They consist of leakages, limited purity of gases, inadequate growth recipe and turbulence in the system.
- CNT growth results are affected the most severely by the condition errors. The condition inside the oven should be suitable for CNT growth. To obtain this the humidity should be reduced and the oven should be free of contaminants. Both can be accomplished by heating the oven to about 750 °C before the samples are loaded and growth is initiated. Furthermore it has been found that the walls of the oven remained substantially cleaner when the oven was brought to temperature prior to growth.
- During operation care should be taken to keep the variation in gas flows and annealing time as low as possible. It has been found that an annealing time of only 5 minutes can make the difference between a few hundred micrometer tall CNT forest and no forest at all. Also, the location of the samples in the oven are found to be important. For the best results the samples are best to be placed at the end of the oven, where the gases are heated and settled.

By taking these errors into account and preventing them carefully, reproducible forests could be obtained. Forests could be grown with high growth rates up to 60 μm per minute. Forests were grown on catalyst layers of 1, 2 and 5 nm. From TEM pictures it was noted that on 1 nm catalyst material (iron) CNTs with diameters of about 8 nm grew. They were mostly triple walled and their lengths could easily reach 500 μm. On 2 nm iron CNTs grew with a diameter of 12 nm thick, while the amount of walls varried between 6 and 8. On these substrates forests of 500 μm and longer were grown as well.

On 5 nm iron however, CNTs were found to be more defective and with a substantial larger diameter of 20 nm. They had about 20 to 30 walls.

From the second part of the thesis about spinnability it can be concluded that a spinnable CNT forest is hard to obtain if not the right growth parameters are known. For a CNT forest to be spinnable it seems to be required to have enough interconnecting CNT bundles and it should be free of amorphous carbon. By carefully changing the composition of the gas mixture during growth to 400 sccm argon, 600 sccm hydrogen and 300 sccm ethylene a forest could be grown that was aligned, while simultaneously containing interconnecting bundles. The drawback was a gray brittle layer of amorphous carbon at the top of the forest. It is presumed that this is the reason for a low level of spinnability. From the resulting forest a wire could be pulled of about 5 mm.

Future work and Recommendations

For future work it is recommended that the morphological and physical requirements of spinnable forests are investigated more in depth. Although multiple groups have succeeded in growing spinnable forests, it remains unclear how a growth recipe that produces such a forest can be devised.
These requirements can be systematically investigated by tuning the flow rates of argon, hydrogen and ethylene. Furthermore, since a gray amorphous carbon top layer is obtained during CNT growth of this study it would be worthwhile to study the effect of adding a controlled amount of water during growth. Once these requirements are found and CNT yarns can be produced at an industrial scale, a future where CNT yarns are used as electrical wires can be envisaged.